

GODDARD/GRANT

IN-46

64481-CR

R 134

Earth Resources Laboratory
Department of Earth, Atmospheric, and Planetary Sciences
Massachusetts Institute of Technology
Cambridge, MA 02139

ANNUAL REPORT TO: National Aeronautics and Space Administration (Crustal Dynamics)

TITLE: The Interpretation of Crustal Dynamics Data in Terms of Plate
Interactions and Active Tectonics of the "Anatolian Plate" and
Surrounding Regions in the Middle East

NASA GRANT: NAG5-753

PRINCIPAL INVESTIGATOR: M. Nafi Toksoz, (617) 253-7852

PERIOD: 15 March 1986 - 14 March 1987

DATE: 10 April 1987

(NASA-CR-180501) THE INTERPRETATION OF
CRUSTAL DYNAMICS DATA IN TERMS OF PLATE
INTERACTIONS AND ACTIVE TECTONICS OF THE
ANATOLIAN PLATE AND SURROUNDING REGIONS IN
THE MIDDLE EAST Annual (Massachusetts Inst. G3/46

N87-20662

Unclas
45186

THE INTERPRETATION OF CRUSTAL DYNAMICS DATA IN TERMS OF PLATE
INTERACTIONS AND ACTIVE TECTONICS OF THE "ANATOLIAN PLATE"
AND SURROUNDING REGIONS IN THE MIDDLE EAST

INTRODUCTION

Our primary effort during the past year has been directed along two separate lines: 1) expanding our finite element models to include the entire Anatolian plate, the Aegean Sea and the Northeastern Mediterranean Sea, and 2) investigating the relationship between fault geometry and earthquake activity for the North Anatolian and similar strike-slip faults (e.g., San Andreas Fault). Both of these efforts are designed to provide an improved basis for interpreting the Crustal Dynamics measurements NASA has planned for this region. The initial phases of both investigations have been completed and the results are being prepared for publication. These investigations are described briefly in this report.

FINITE ELEMENT MODELS FOR PLATE INTERACTIONS IN THE EASTERN
MEDITERRANEAN

McKenzie (1972) provided a regional interpretation of the recent tectonic history of the eastern Mediterranean in terms of the interactions of the Arabian, African and Eurasian plates. An important source of information for this model as well as the more recent modifications in this basic model (e.g., see Sengor, 1985) are the fault plane solutions for instrumentally recorded earthquakes. Because of the ambiguities inherent in interpreting fault plane solutions, the uncertain role of aseismic deformation and the complex nature of plate interactions in this region of plate convergence, considerable uncertainty persists as to the directions and rates of present-day relative plate motions. The SLR measurements in and surrounding the Anatolian plate being made by the NASA/WEGENER project should provide the first direct measurements of relative plate motions and intraplate deformation for this region and thereby place important constraints on allowable models.

In anticipation of these new measurements we have compiled all relevant seismic data (Figure 1) and developed finite element models of plate interactions (Arabian, African, Eurasian, and Turkish-Aegean plates) for the eastern Mediterranean in order to investigate the kinematics and dynamics of this complexly deforming region. An important objective of this study has been to analyze the relationship between continental collision in eastern Turkey and Iran, westward escape of the Anatolian plate, and north-south extension in western Turkey and the Aegean. These models indicate that collision of the Arabian and African plates with Eurasia and associated westward escape of the Anatolian plate can not account for the observed (i.e., from earthquake focal mechanisms) north-south extension in western Turkey and the Aegean. An additional mechanism causing southward migration of the Hellenic trench at a rate of about 1.5 cm/yr relative to Eurasia is required to explain the observed extension. This result has important implications for the nature of plate tectonic driving forces in this and similar regions (i.e., regions of contemporary back-arc spreading).

The basic plate tectonic framework for the eastern Mediterranean used in our finite element studies is shown in Figure 2 (for a detailed description of the finite element calculations see Kasapoglu and Toksoz, 1983). Figure 3 shows four representative examples of the many different boundary conditions (i.e., relative plate motions) for this basic framework which were investigated in this study. Figures 4 through 7 show principle stresses and displacements (Eurasian

plate fixed) for models M1 through M4 respectively. Examination of Figure 4 indicates that collision of the African and Arabian plates with Eurasia and the resulting westward escape of Anatolia is not capable of accounting for either the observed right-lateral strike-slip motion on the western end of the North Anatolian fault or north-south extension in western Turkey and the Aegean. An additional driving force causing southward migration of the Hellenic trench is needed to reproduce these observations. Our preferred model based on the available geologic, geophysical and seismic observations is shown in the bottom right of Figure 3 (M4) and the rates of intraplate deformation and fault slip implied by this model are given in Figure 8.

The need for two independent forces to drive the observed deformation in the eastern Mediterranean has been well established by our numerical experiments. However, important questions remain to be investigated. What is the physical mechanism responsible for the southward migration of the Hellenic trench? What effect does gravity have on the deformation process? Can better constraints be placed on rates of fault slip and intraplate deformation utilizing relevant geophysical and geological data? Our ongoing research effort involving refinement of our modeling experiments and compilation and incorporation of the available geophysical and geological observations (see below) is aimed at addressing these questions. Of course, the most immediately relevant constraints are those that will result from the SLR measurements being made throughout this region. We anticipate that our ongoing effort to utilize geophysical and geological information together with NASA's SLR measurements to constrain quantitative models of lithospheric plate interaction will continue to provide important information on the kinematics and dynamics of this region of active convergence.

STRIKE-SLIP FAULT GEOMETRY AND EARTHQUAKE ACTIVITY IN TURKEY

This work is given in detail in the attached appendices and is therefore described only briefly below.

A comprehensive examination has been made of strike-slip fault geometry and the known historical and instrumental earthquakes along the North Anatolian fault zone in Turkey. Fault geometry is found to be a critical factor in controlling fault segmentation and hence the distribution of large strike-slip earthquakes. This investigation is providing information on the earthquake potential of various segments of the Anatolian fault and has implications for evaluating seismic hazards along other strike-slip faults such as the San Andreas fault in California. In addition, the information on fault geometry and slip is directly relevant to our ongoing numerical studies (i.e., stress orientation and fault slip rates).

REFERENCES

- Kasapoglu, E., and M.N. Toksoz, Tectonic consequences of the collision of the Arabian and Eurasian plates: Finite element models, *Tectonophysics*, 100, 71-96, 1983.
- McKenzie, D., Active tectonics of the Mediterranean region, *Geophys. J. R. Astr. Soc.*, 30, 109-185, 1972.
- Sengor, A.M.C., Structural classification of the tectonic history of Turkey, in, Ketin Symposium, edited by T. Ercan and A.M. Gaylayan, *Spec. Pub. Geol. Soc. Turkey*, 37-62, 1985.

PUBLICATIONS SUPPORTED IN PART BY THE NASA CRUSTAL DYNAMICS PROJECT

Kasapoglu, K.E. and M.N. Toksoz, Finite element modelling of tectonic processes associated with plate interactions in the Eastern Mediterranean, *Tectonophysics*, in preparation, 1987.

Barka, A.A., M.N. Toksoz, K. Kadinsky-Cade and L. Gulen, The segmentation, seismicity and earthquake potential of the eastern part of the North Anatolian fault zone, *J. Geophys. Res.*, submitted, 1987.

Barka, A.A., K. Kadinsky-Cade, and M.N. Toksoz, North Anatolian fault geometry and earthquake activity(abst.), *Seismological Research Letters*, 58, pg. 31, 1987.

Barka, A.A. and K. Kadinsky-Cade, Strike-slip fault geometry and earthquake activity in Turkey, *Tectonics*, submitted, 1987.

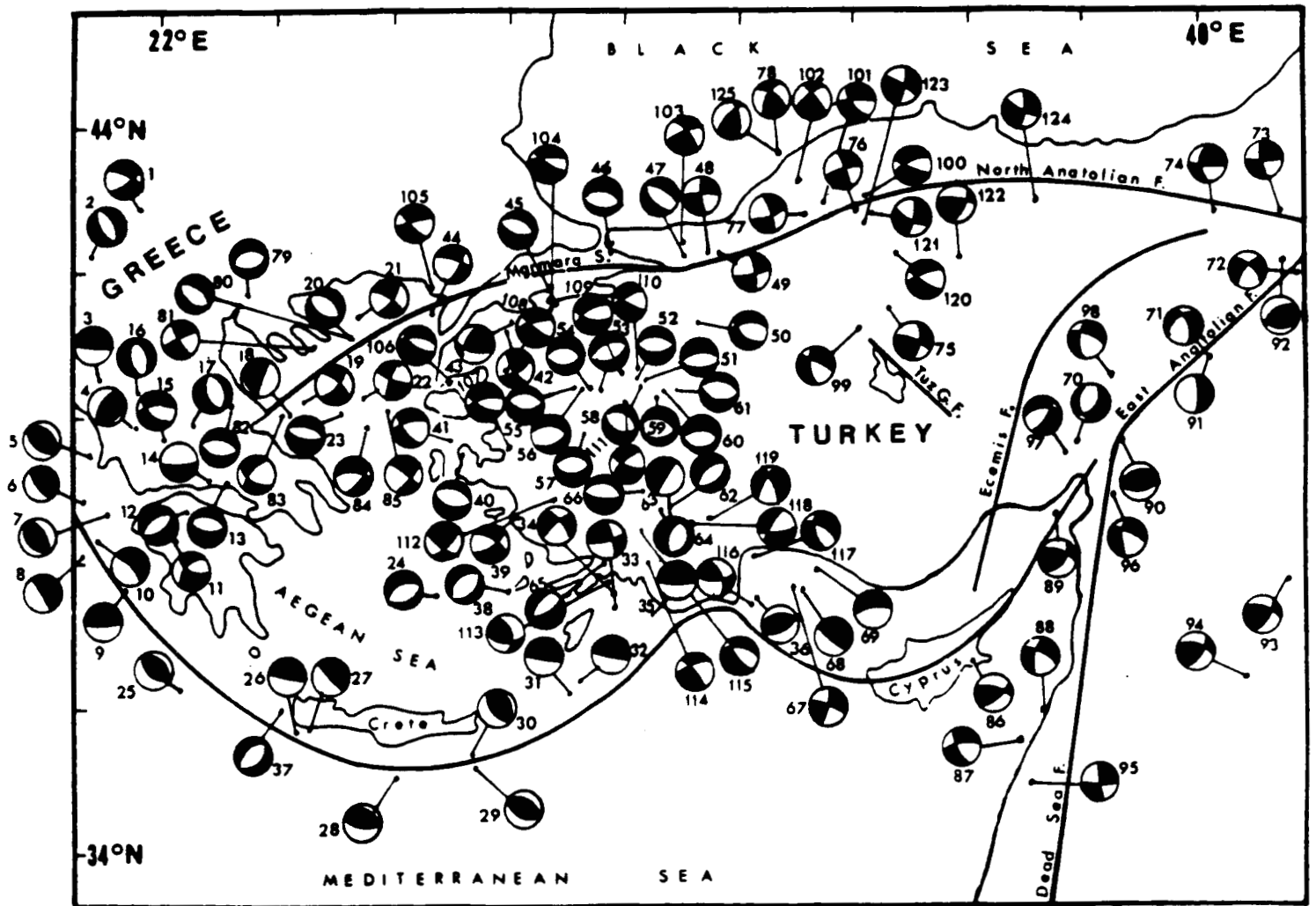


Figure 1: Fault plane solutions for earthquakes in the eastern Mediterranean (see Kasapoglu and Toksoz, 1983 for sources).

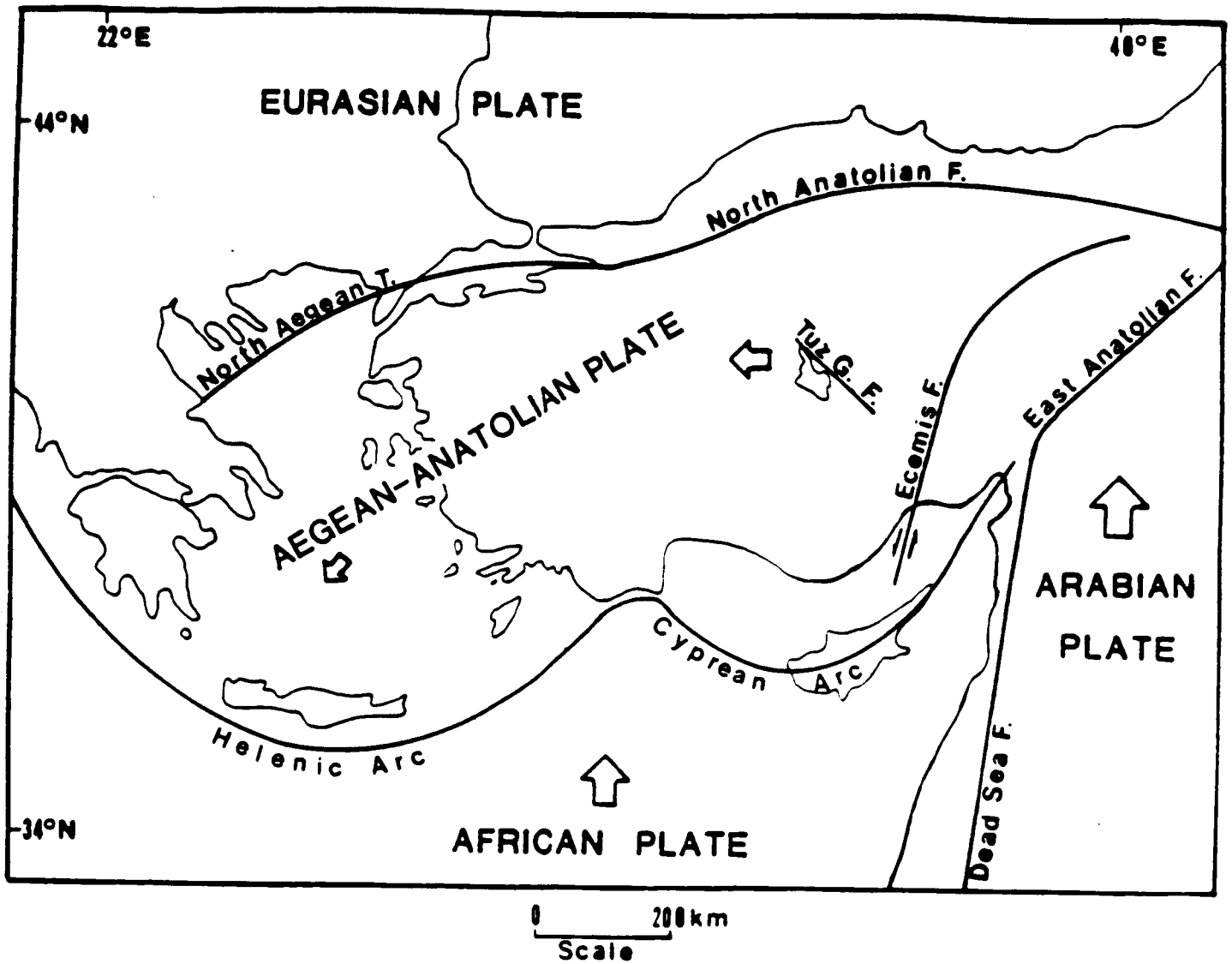


Figure 2: Plate tectonic framework for the eastern Mediterranean used in finite element calculations.

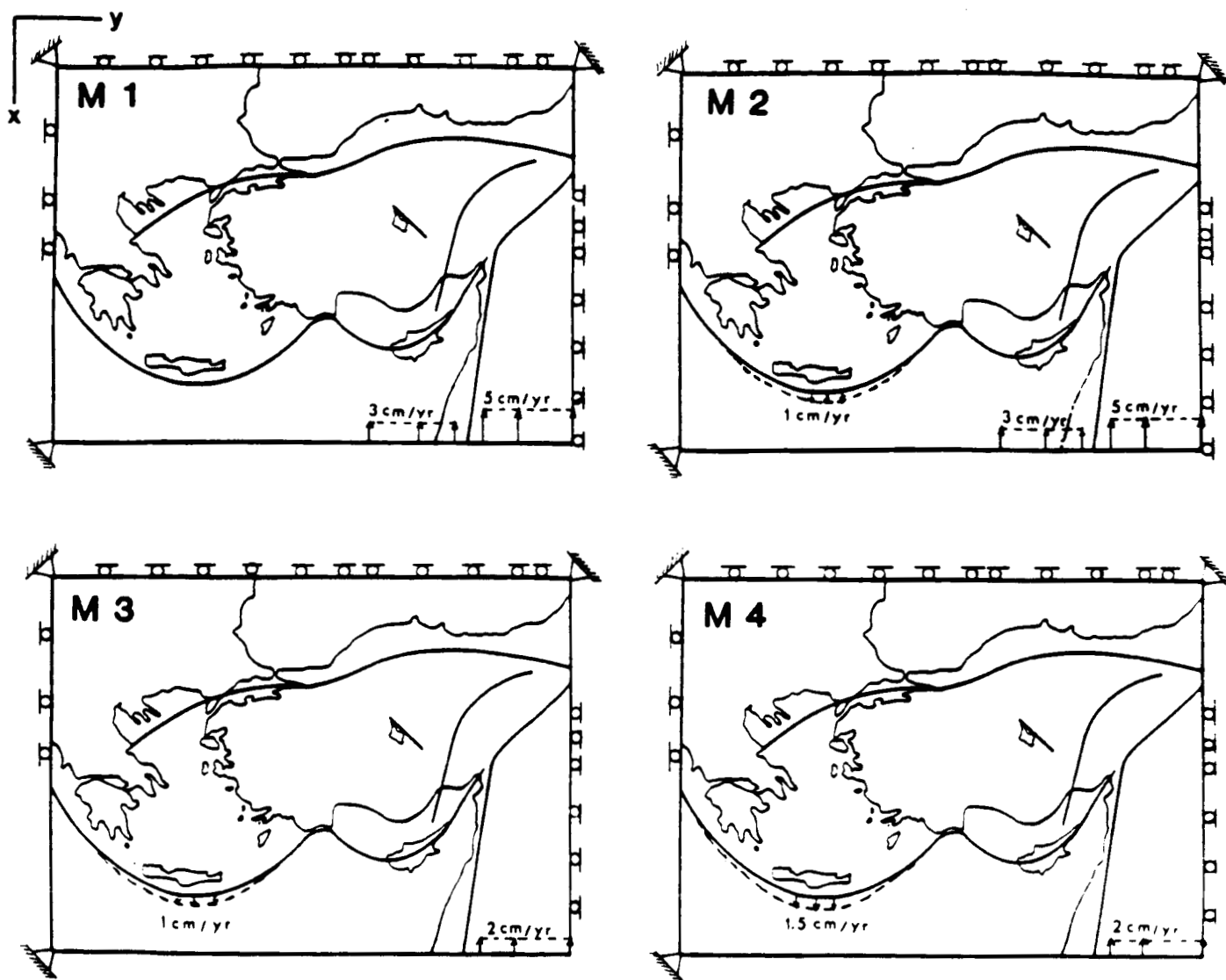


Figure 3: Four representative models used in our finite element experiments to investigate plate interactions.

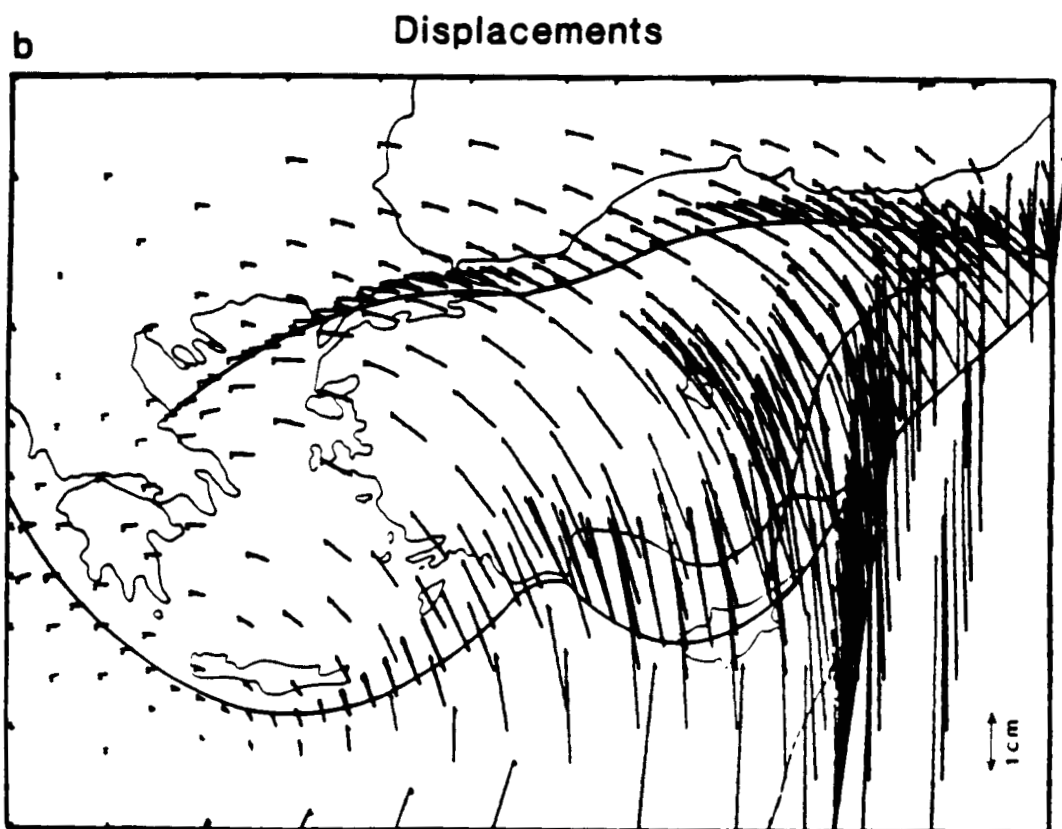
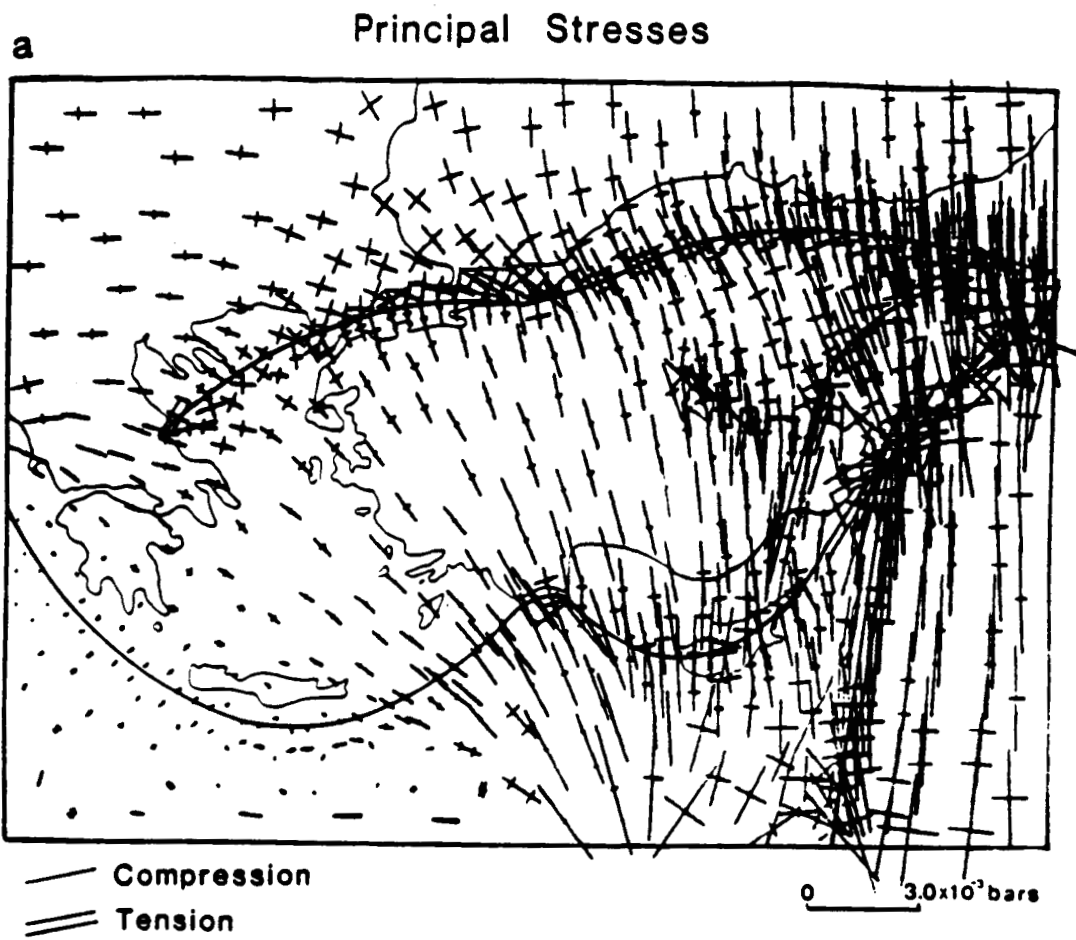


Figure 4: Principal stresses and displacements for model M1 (see Figure 3).

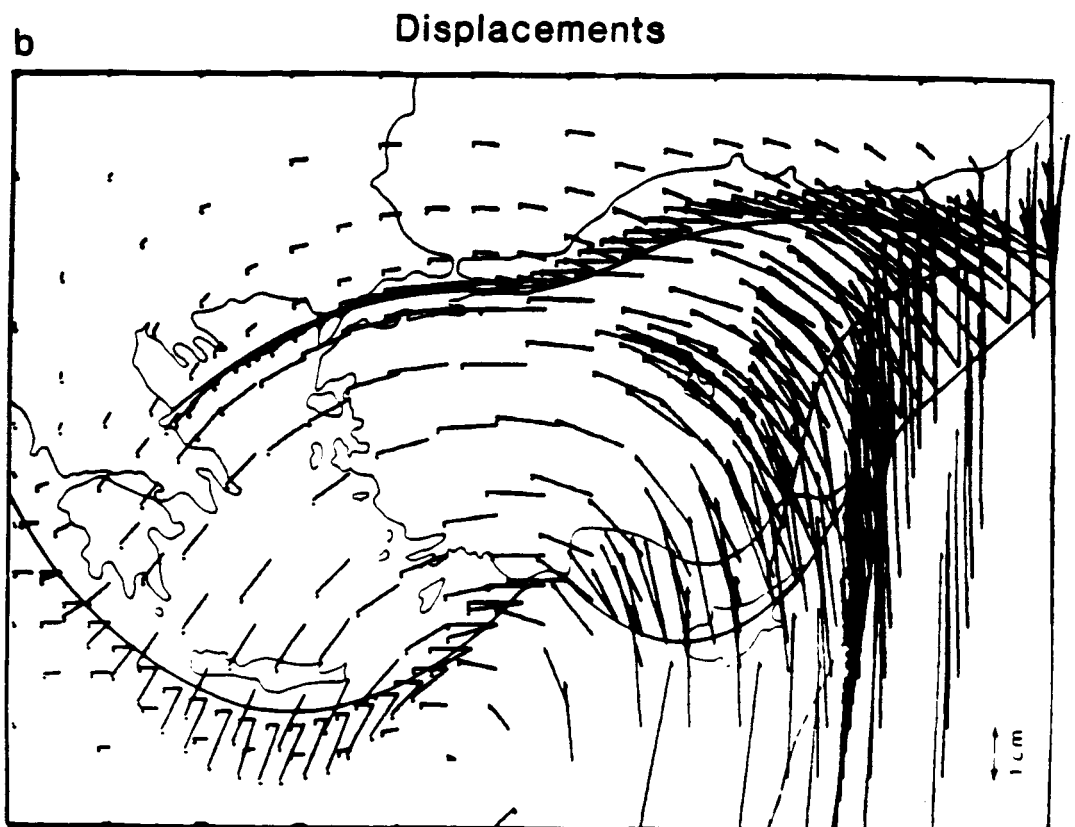
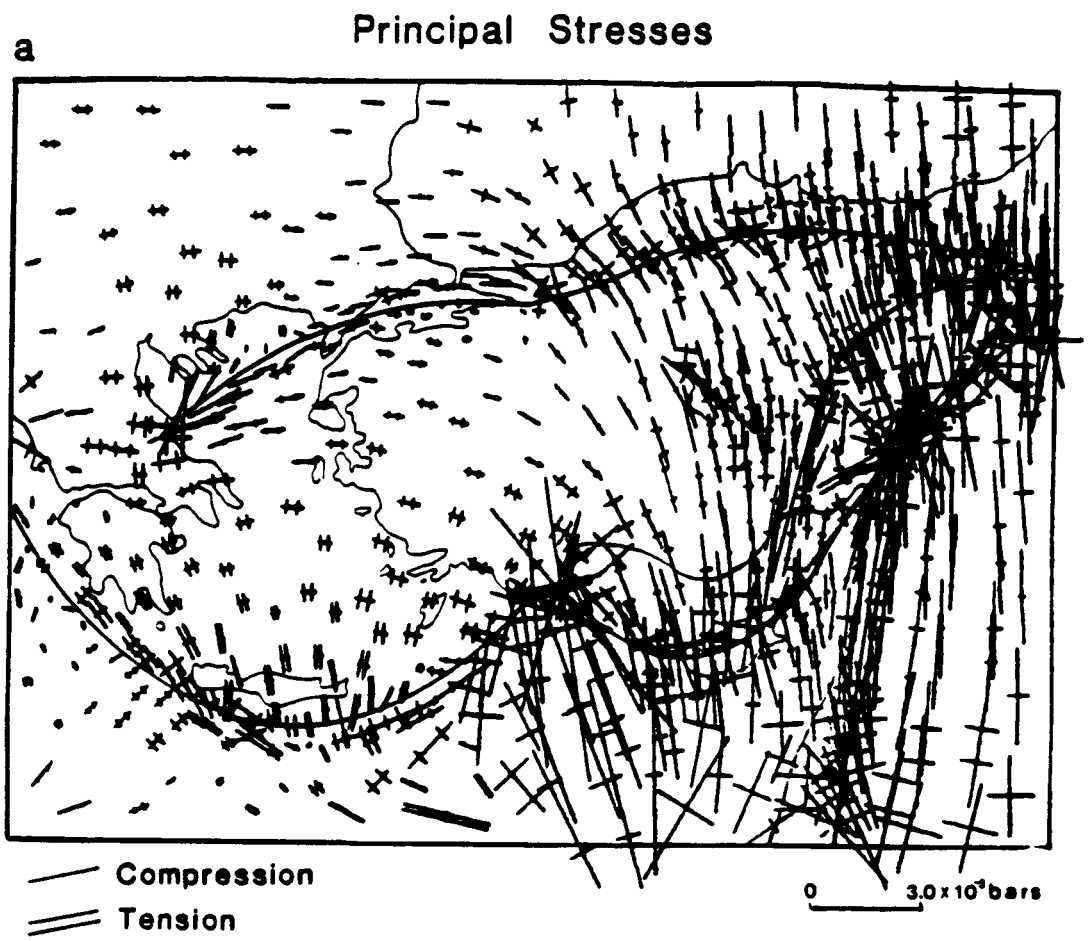


Figure 5: As Figure 4 for model M2.

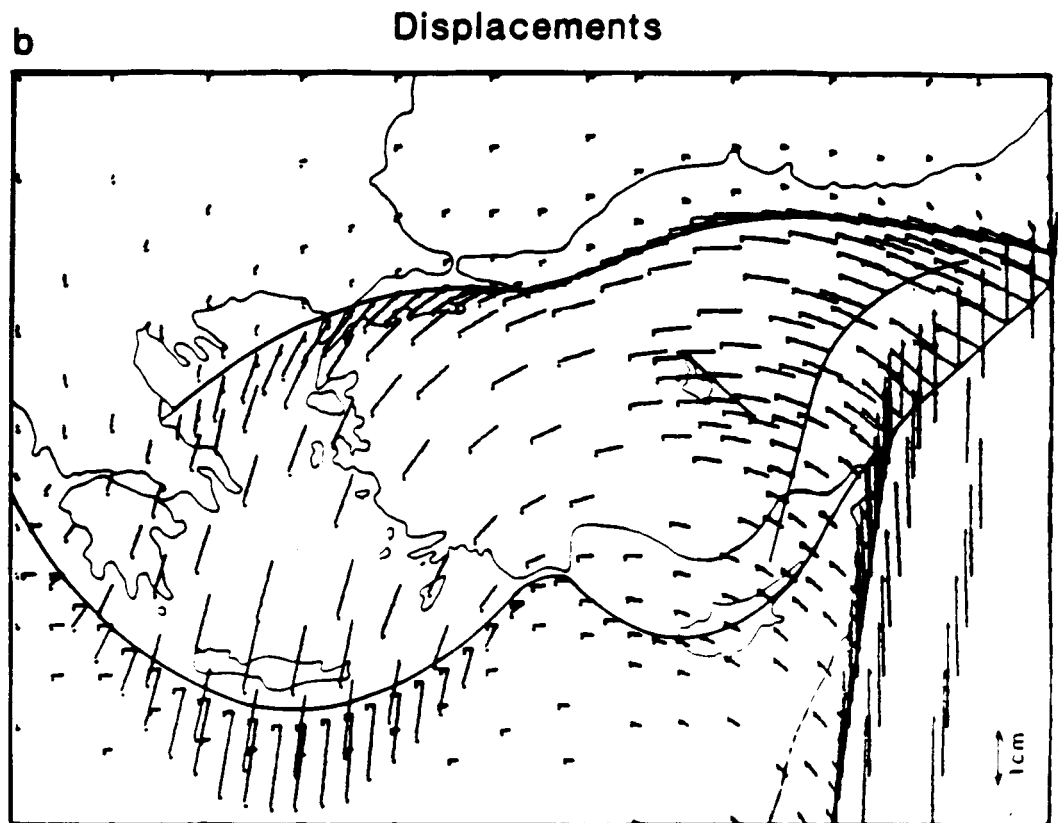
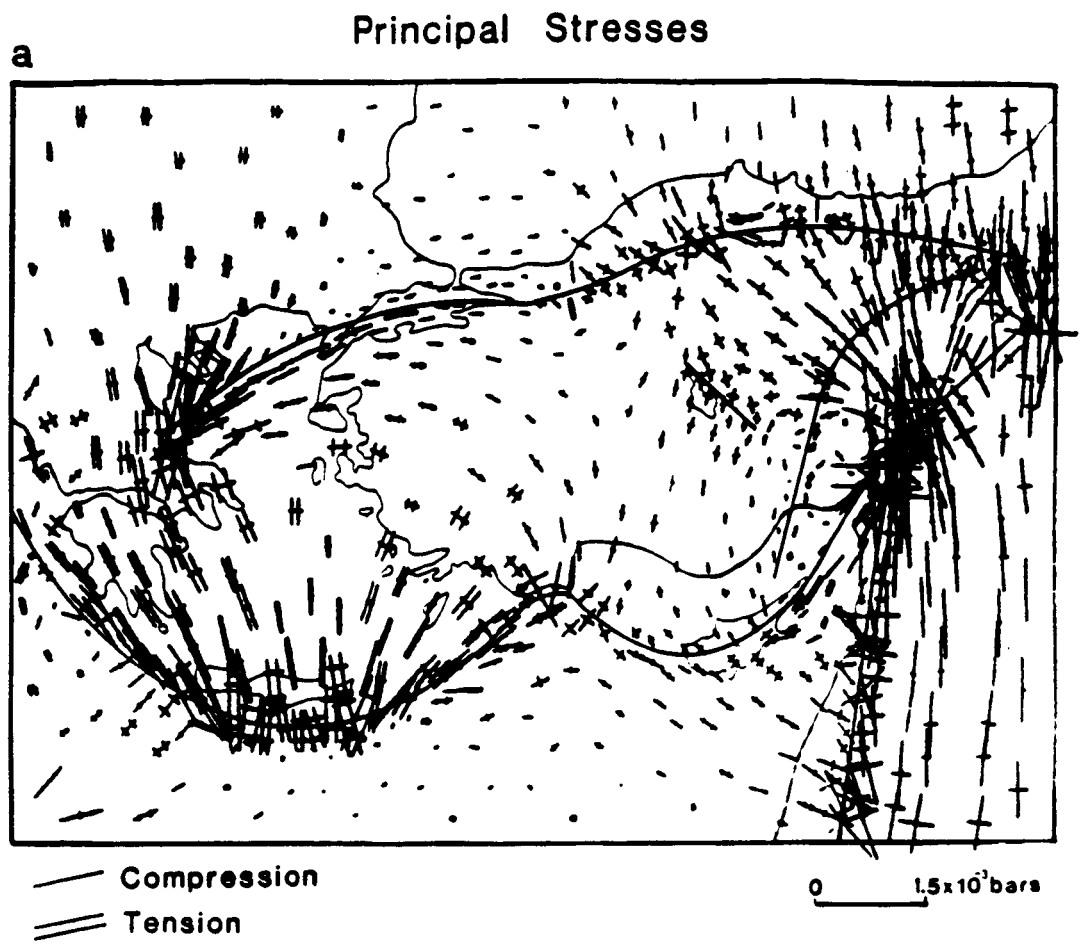


Figure 6: As Figure 4 for model M3.

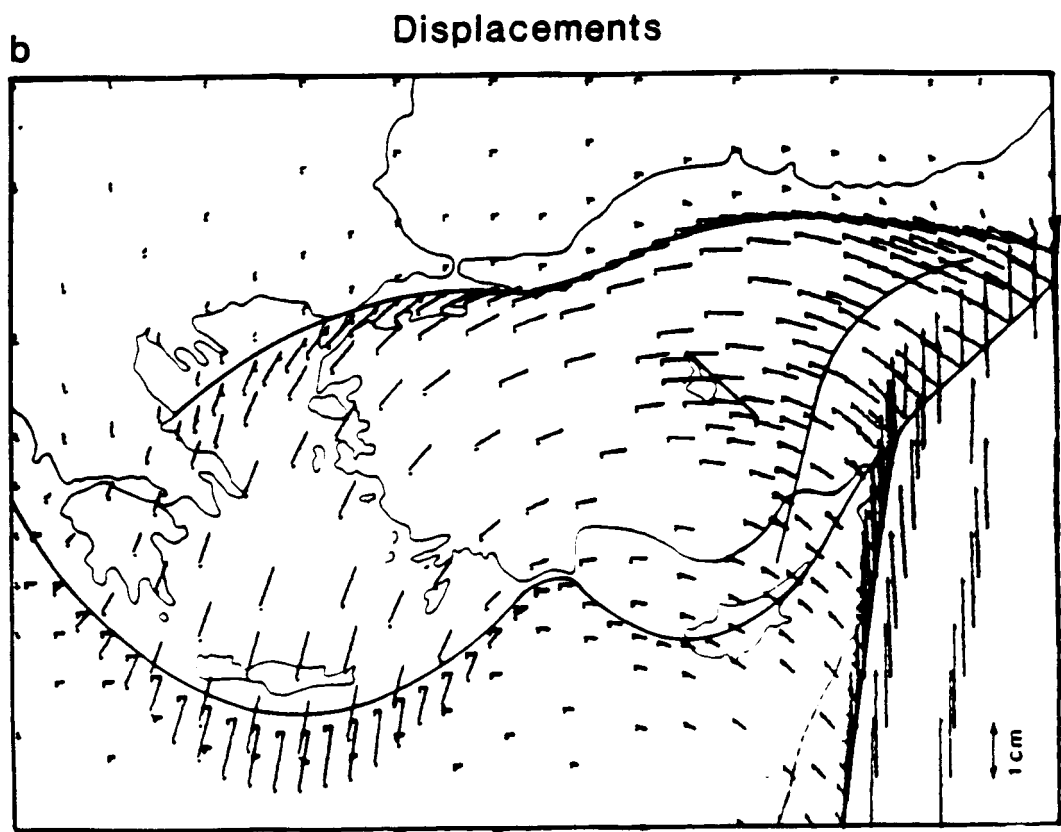
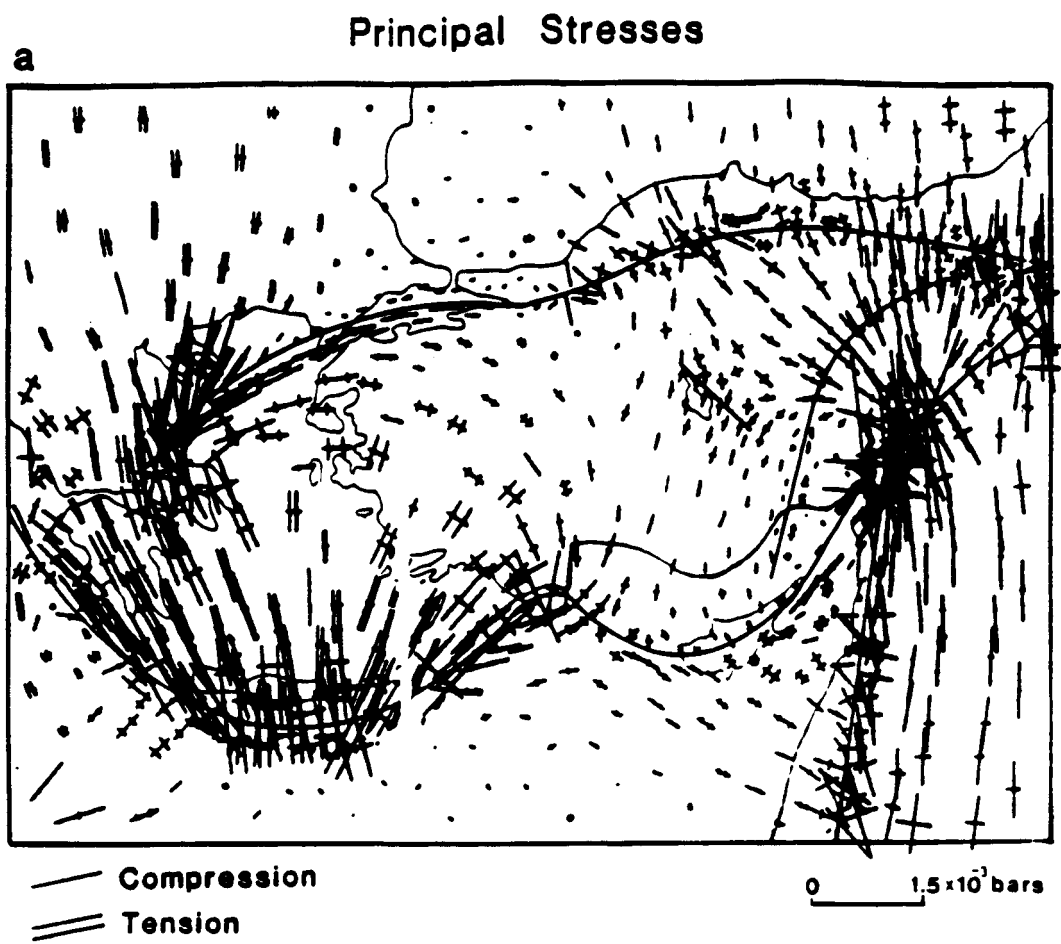


Figure 7: As Figure 4 for model M4.

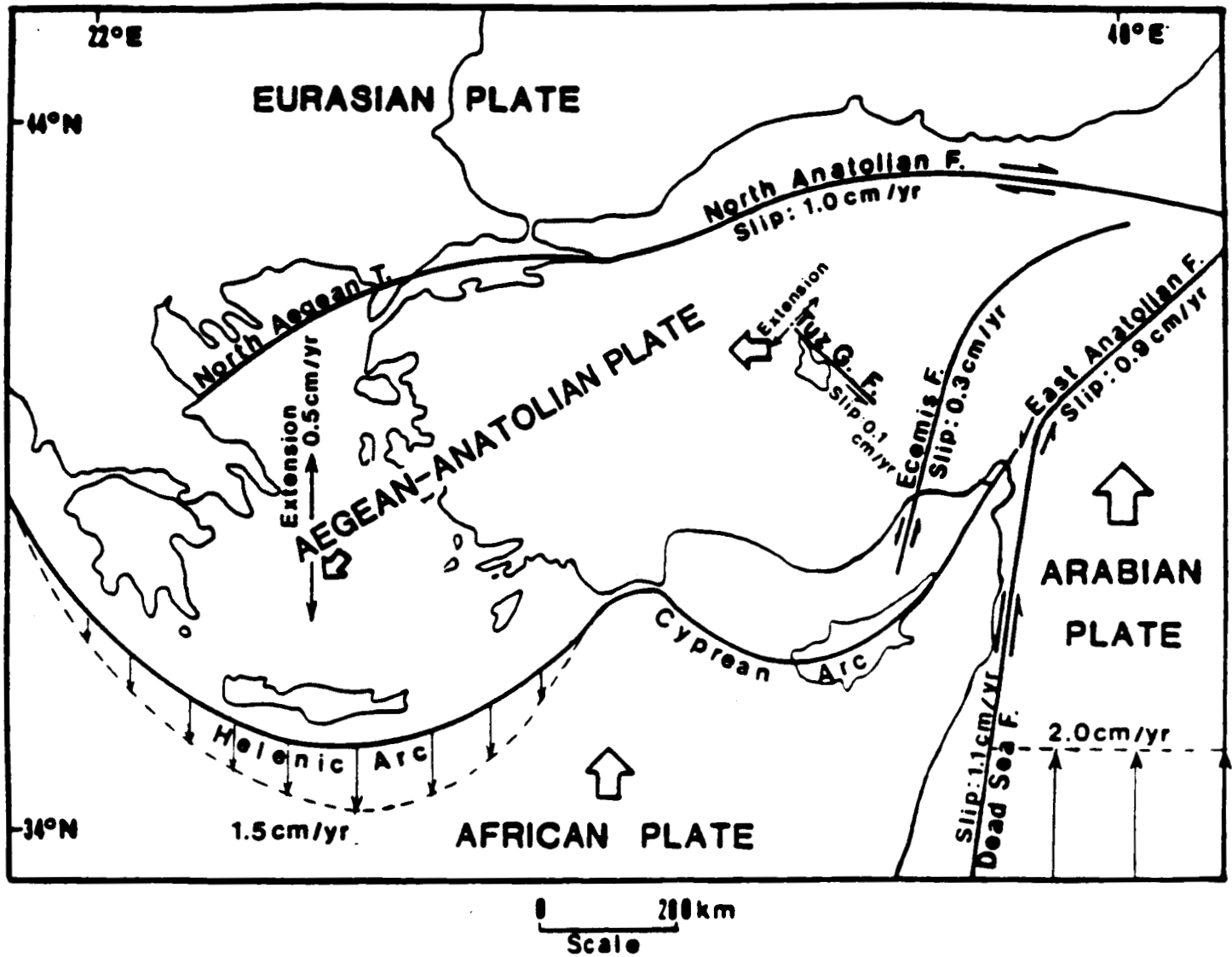


Figure 8: Rates of intraplate deformation and fault slip from model M4.

• APPENDIX I
(Submitted to J. Geophys. Res.)

THE SEGMENTATION, SEISMICITY AND EARTHQUAKE POTENTIAL OF
THE EASTERN PART OF THE NORTH ANATOLIAN FAULT ZONE

A. Barka

M.N. Toksöz

K. Kadinsky-Cade

L. Gülen

Earth Resources Laboratory
Massachusetts Institute of Technology
42 Carleton Street
Cambridge, MA 02142

April, 1987

ABSTRACT

Historical and instrumental earthquakes of the North Anatolian fault zone in the vicinity of the Erzincan basin have been examined in relation to fault segmentation. Results of this study suggest that each segment has its own characteristic earthquakes. The epicenter of the 1939 great Erzincan earthquake ($M=8$) occurred near a 20° restraining bend located about 40 km from the eastern end of the 360 km long segment that ruptured during that earthquake. This segment was terminated at each end by releasing stepovers. Aftershocks mostly occurred in the releasing stepover/releasing bend area located at the eastern end of this segment. Historical records suggest that the 1939 event is characteristic of great earthquakes that occur approximately every 300 years on this segment. Recurrence times of large earthquakes ($I = VIII - IX$) is about 100 to 150 years in the Erzincan region. The segment to the east of the Erzincan segment is identified as a potential seismic gap. It is approximately 100 km long, and extends from the Erzincan releasing stepover to a restraining stepover-bend combination near Yedisu. This segment last ruptured in 1784. It is the only segment of the 900 km long main section of the North Anatolian fault that did not experience a large earthquake during the well-known 1939-1967 sequence of $M_s = 7-8$ earthquakes that ruptured the fault zone between Varto and the western end of the Mudurnu valley.

INTRODUCTION

It has recently been acknowledged that fault geometry plays a critical role in the earthquake rupture process (e.g., Segall and Pollard, 1980; Bakun *et al.*, 1980; Lindh and Boore, 1981; King and Nabelek, 1985; Sibson, 1986; Schwartz and Coppersmith 1986; Barka and Kadinsky-Cade, 1987). The term "fault geometry" includes stepovers, bends, and their many combinations. Each geometric pattern appears to have a characteristic dynamic rupture mechanism. Through fault geometry one can define fault segments, each having its own characteristic earthquakes.

In this paper we identify an approximately 100 km long fault segment in the eastern part of the North Anatolian fault zone which has not ruptured in the last 200 years. This segment is defined by geometric discontinuities. Through the analysis of geometric discontinuities along this and neighboring segments we examine the effect of fault geometry on the location of large earthquake epicenters, foreshocks, aftershocks and interpreted sites of strain accumulation.

The largest known earthquake to have occurred on the North Anatolian fault (NAF) is the 1939 Erzincan earthquake ($M_s = 8.0$). This earthquake caused great damage and killed 32,700 people. It ruptured a section of the NAF that extends from the Erzincan basin to the Amasya province, with surface breaks covering a distance of 360 km. The right-lateral displacement reached 3.7 m in places (Pamir and Ketin, 1941; Ketin, 1948, 1969; Ambraseys, 1970). Both historically and during modern times, the Erzincan area has been one of the most active seismic regions in Turkey (Sieberg, 1932; Ergin *et al.*, 1967; Soysal *et al.*, 1981; Tables 1 and 2).

Figure 1 shows major tectonic elements of Turkey in an area where the northward motion of the Arabian plate causes active convergence. As a result, the Anatolian block escapes westward and the northeast Anatolian block eastward (Ketin, 1948, McKenzie 1972; Kasapoglu and Toksöz, 1983; Gülen, 1984; Dewey *et al.*, 1986). The Anatolian block is bounded by the right-lateral North Anatolian fault to the north, and by its conjugate, the East Anatolian fault, to the south. These two fault zones intersect at the Karliova Triple junction. (Ketin, 1966; Allen, 1969; McKenzie, 1972; Dewey, 1976; Tchalenko, 1977; Sengör, 1979; Toksöz *et al.*, 1979, Jackson & MacKenzie, 1984; Sengör *et al.*, 1986; Dewey *et al.*, 1986). The eastern part of the Anatolian block is divided into two smaller blocks (A_1 and A_2) by the left-lateral strike-slip Ovacik fault. This fault intersects the NAF zone at the southeast end of the Erzincan basin. The eastward escape of the NE Anatolian block is complicated by an extensive internal deformation and by the existence of a number of sub-blocks. A dominant tectonic feature in this region is the NAF, which forms a boundary between the two blocks escaping in opposite directions. The NAF intersects the Northeastern Anatolian fault (NEAF, forming the northern boundary of the NE Anatolian block) northwest of Erzincan (Figures 1 and 2). Figure 2 shows major blocks and boundary faults between the Erzincan and Karliova triple junctions.

Between 1939 and 1967 most of the North Anatolian Fault west of Erzincan ruptured through a westward migrating series of major earthquakes, as shown in Figure 1. Earthquakes along the NAF east of Erzincan followed a more complicated pattern, as can be seen in Figure 2.

Fault Segments

Based on the geometric discontinuities of the main fault traces we have identified fault segments. The North Anatolian fault zone consists of several

segments as shown in Figure 2 (Barka and Kadinsky-Cade, 1987; Barka and Gülen, 1987).

Segment 1: This segment extends from Varto to the Yedisu restraining stepover, where it bends around to the southwest, changing direction by 18° in a convergent sense. Segment 1 has a clear physiographic expression, particularly along the Elmalı Valley (Allen, 1969). During the last 50 years this segment has ruptured in two separate earthquake sequences. The first sequence includes the 1946 Varto and 1949 Elmalı earthquakes ($M=6.0$ and $M=7.0$ respectively), and the second includes the 1966 $M=7.0$ Varto earthquake and its aftershocks. ($M=5.3-6.2$; see also Table 2).

Segment 2: This segment strikes $N 70^\circ W$ and is approximately 100 km long. Segment 2 extends from the Yedisu plain in the east to the Erzincan alluvial plain (western end). The physiographic fault expression is very clear where the fault runs along the Euphrates valley and through the village of Caykumu. The physiographic expression disappears, however, as soon as the segment enters the Erzincan alluvial plain, although the segment may continue further west under the plain. The 1784 earthquake, which last ruptured this entire segment, created surface breaks along a 90 km distance, and caused 1m of vertical displacement (Ambraseys, 1975). The 1967 $M=6$ Pülümür earthquake was also located along this segment. Surface breaks for the 1967 event were, however, only 4 km long; this earthquake was accompanied by 20 cm of right-lateral surface displacement (Ambraseys, 1975).

Segment 3: This segment trends $N 55^\circ W$ and is 40 km long. The northwestern half of segment 3 has a clear physiographic expression. It is characterized by a dominant right-lateral displacement, and is accompanied by contemporaneous thrust faults. The latter are sub-parallel to this part of the segment and indicate

the presence of positive flower structures. The southeastern half of this segment has a discontinuous en-echelon fault structure with contemporaneous volcanics. The Erzincan pull-apart constitutes the region between segments 2 and 3.

Segment 4: This is a major segment striking N 75° W, with a dominantly strike-slip morphology and a length of 320 km. Segment 4 is composed of many sub-segments along its 320 km length. The extended surface breaks of the 1939 Great Erzincan earthquake have revealed that this part of the fault zone could also be considered as a single long segment. The only major discontinuity along this segment is the Susehri releasing stepover which is located approximately 75 km west of the Erzincan basin. Segments 3 and 4 form a 20° restraining bend northwest of Erzincan (Figure 2). In the vicinity of the area where segments 3 and 4 intersect (the bend area), thrusts subparallel to the fault zone are common structures. In particular, the western side of the bend is highly elevated.

Northeast Anatolian Fault - This fault zone consists of several segments with a combined length of approximately 350 km. The southwesternmost segment (Segment A) is located to the north of the Erzincan region (Figure 2). Approximately 70 km long, it strikes NE-SW. Although very little is known about this fault segment, it is assumed to have an oblique movement, consisting mostly of left-lateral slip with a subordinate thrust component. (Tatar, 1978). The study of earthquake records (Soysal *et al.*, 1981; Sipahioglu, 1983; Riad and Meyers, 1985) indicates that it might be less active than the segments of the North Anatolian Fault zone. Apart from the 1939 Tercan earthquake (M=5.9) and several aftershocks of the 1939 great Erzincan earthquake, the only known historical event associated with this segment is the 1254 I=IX earthquake. This event caused surface breaks to occur over a 50 km length on segment A (Ambraseys, 1975).

Ovacik fault - This is another left-lateral fault. It is located near Ovacik, and extends up to the southeast end of the Erzincan basin. This fault is about 120 km long and trends NE-SW. Near Ovacik, where the fault cuts Quaternary alluvial fans, physiographic expressions are very clear (Arpat and Saroglu, 1975). The Ovacik fault has also been participating in the opening of the Erzincan basin. The only earthquake known to have occurred on the Ovacik segment is the 01/28/1960 $M=5.9$ event (macroseismic location; Ergin *et al.*, 1967). There are no historical events that can be specifically associated with this segment.

It should be noted that the area between segments 2 and 4, including the Ovacik fault and segment A of the NEAF zone, is located within the serpentinite-rich ophiolites and ophiolitic melange associated with the Anatolid/Taurid-Pontid suture zone.

Seismicity

Historical Earthquake Records

The history of damaging earthquakes in the Erzincan region was recognized and well documented even before the great earthquake of 1939 (Ali Kemal, 1932). Sieberg (1932) listed some of the Erzincan earthquakes and stated that between 1045 and 1784, at least 17 catastrophic earthquakes had occurred in the Erzincan region. In Table 1 we have tabulated the significant earthquakes affecting the Erzincan region since 1000 A.D., based on sources referenced in the table.

Figure 3a is an intensity-time plot of known earthquakes which have affected the Erzincan region. From this figure, earthquakes can be categorized according to three "characteristic" sizes: (a) small and moderate, with Modified Mercalli intensity $I \leq VIII$, (b) large earthquakes with $VIII \leq I \leq IX$ and (c) great

earthquakes for which $I \geq X$. According to Figure 3a, at least 3 great earthquakes have occurred during the last 1000 years, including the one in 1939. Ambraseys (1970) reported that the 1045 earthquake produced a surface break of a length comparable to the one which occurred in 1939; and that the 1458 earthquake caused the death of about 32,000 people, comparable to the casualties of the 1939 earthquake. The 1668 earthquake is controversial. With the exception of Ambraseys (1975), most of the existing references describe it as an earthquake of intensity about VIII-IX. Ambraseys (1975) reports that the 1668 earthquake produced a 380 km surface break and that the lateral displacement was as much as 4 m, which is again comparable to that of 1939. At least 10 large earthquakes ($VIII \leq I \leq IX$) have occurred in the Erzincan region since 1000 A.D., causing considerable damage and large numbers of casualties.

Figure 3b shows the number of earthquakes that occurred between 1000 and 1900 in the Erzincan region, versus intensity. The dashed line is drawn only through the $I \geq VIII$ points, because the historical record may be incomplete for smaller events. According to this plot, the recurrence interval for the great earthquakes in category (c) (intensity X or greater) is about 400-450 years if the 1668 event is excluded. With the 1668 earthquake, the recurrence interval becomes about 300 years. These recurrence intervals, combined with the amount of displacement created during the great earthquakes (3-4m), give a slip-rate of approximately 1 cm/yr. This is comparable to the creep rate observed at Ismetpasa, on the central part of the NAF, from geodetic measurements (Eren *et al.*, 1984) and creepmeter data (Toksöz, 1984, USGS report). Note that the 1 cm/year slip rate estimated here for the NAF zone near Erzincan does not include a possible additional creep component. This slip-rate is at least two times higher than that obtained from geological results along the NAF (0.4-0.5 cm/yr, Seymen, 1975. Barka and Hancock, 1984). This reveals that

the motion may be progressively accelerating or episodic. Note also that segments 1-3 form a boundary between opposite-moving blocks (the Anatolian and Northeast Anatolian blocks). Thus a higher slip rate is expected in this area than along the main section of the NAF to the west. From Figure 3b the recurrence interval for large earthquakes ($VIII \leq I \leq IX$) is approximately 100-150 years.

Instrumental Earthquake Records

Figure 4 shows the distribution of epicenters for earthquakes with $M_s > 4.9$, that have occurred between Erzincan and Varto since 1900. These events are listed in Table 2. The following points should be made concerning the listed earthquakes:

- a) There is a quiescent period between 1900 and 1930 in the Erzincan region.
- b) The epicenter of the 1930 earthquake ($M=5.4$) was located near the Ovacik fault. Some damage was reported in Erzincan and Kemah (Tabban, 1980; see Figure 2).
- c) Although Pamir and Ketin (1941) showed ESE-WNW trending isoseismals covering the area between Tercan and Baskoy, the epicenter of the 1939/11/21 Tercan earthquake may have been on the NEAF zone. This is not only suggested by some catalogs, but also by the amount of damage that occurred in and near Karakulak (e.g., 130 buildings collapsed), and in some other destroyed villages which are all situated next to the fault zone (Pamir and Ketin, 1941; Ergin *et al.*, 1967; Tabban, 1980).
- d) The December 27, 1939 Erzincan earthquake ($M=8$) is one of the largest earthquakes to have occurred in this area. We will summarize known information concerning foreshocks, main shock, aftershocks, and surface breaks in the

Erzincan region. Pamir and Ketin (1941) reported that two foreshocks were felt within the week preceding the main shock in the Erzincan region. The epicenter of the main shock was within the Erzincan region in the range 39.5° - 39.9° N, 38.5° - 39.7° E (e.g. Tillotson, 1940; Pamir and Ketin, 1941; Ergin *et al.*, 1987; Karnik, 1969; Dewey, 1976). The main surface breaks were associated with segments 3 and 4. Within the basin some discontinuous extension cracks striking WNW-ESE were also observed, and in the salt playa east of Erzincan the fissures were 80-100 cm wide (Pamir and Ketin, 1941). The villages along the northern margin of the Erzincan basin were completely destroyed by either the main shock or the aftershocks. The eastern end of the surface breaks coincided with the eastern end of the Erzincan basin (Pamir and Ketin, 1941; Ketin 1969). Numerous aftershocks occurred in the Erzincan region as well as in many other places (e.g. Nature, 1940 a, b, c): According to Nature (1940c), on February 3, 1940, two villages were destroyed in the Erzincan region (close to the NEAF zone, segment A) by a shock which also killed 45 people and injured many more. Pamir and Ketin (1941) also state that between February 3 and 20, 1940, many earthquakes were felt in the region. However, available earthquake catalogs do not contain many of these earthquake records. Aftershocks 11, 14, 15, 17, and 18 (listed in Table 2) were felt strongly in the Erzincan region and caused some damage in the villages. In particular, aftershock 15 caused 40 buildings to collapse, and aftershock 18 was responsible for 15 deaths and 100 injuries (Tabban, 1980). Most of the aftershocks were located in or near the Erzincan basin.

e) Although some catalogs indicate that the August 17, 1949 earthquake ($M=6.7-7$) was close to the eastern end of segment 2, this earthquake was on the easternmost segment of the NAF zone, called the *Karlıova-Elmalı* segment (Lahn, 1952) (Segment 1 in Figure 2).

f) The epicenter of the 1960/01/26 (M=5.9) earthquake was located near the northeastern part of the Ovacik fault (see Figure 5 and Table 2) (Ergin *et al.*, 1987; Tabban, 1980).

g) The relocated epicenter of the 1967/07/26 M=5.6-6.2 earthquake (Dewey, 1976) was located on the eastern half of segment 2, although the macroseismic epicenter was in Pülümür.

Discussion and Conclusions

It is possible to make a correlation between the pattern of seismic activity and the geometry and distribution of active fault segments in the Erzincan region. Both historical data and the 1939 earthquake have shown that great earthquakes in this region can be associated with segments 3 and 4. The epicenter of the 1939 earthquake occurred near the 20° restraining bend between segments 3 and 4 of the NAF. (Barka and Hancock, 1982; Barka and Kadinsky-Cade, 1987). Furthermore, observations of compressional deformation and uplifting within the young deposits along segments 3 and 4 can be interpreted as surface expressions of high strain accumulation in the area, which eventually results in the occurrence of very large earthquakes. Since the recurrence interval for great earthquakes is about 300-400 years, the last earthquake having occurred in 1939, at present the probability of an earthquake of comparable magnitude is small.

In the Erzincan region, many of the small small to moderate aftershocks (category a in Figure 3a) can be related to the releasing stepover area in the eastern half of the Erzincan basin, between segments 2 - 3 and the Ovacik fault (Barka and Gülen, 1987). Moreover the fault plane solution of the 1983/11/18 earthquake (M4.8), located near the city of Erzincan, shows normal faulting

(Figure 5); this clearly supports the idea of a tensile stress regime produced by the pull-apart extension in the Erzincan basin. Some of the small to moderate earthquakes in the area may also be associated with the Ovacik fault, with segment A of the NEAF zone, or with internal block deformation, as in the case of the Kigi-Karlioiva area in block A_1 (Figure 4). There have been no large earthquakes (category b) for at least 200 years in the vicinity of Erzincan, excluding the segment 1 earthquake near Varto. The last large earthquake occurred in 1784 and was located on segment 2, according to Ambraseys (1975) (Figure 6a), who also reported 90 km surface faulting along a 115° trend. This information is perfectly consistent with segment 2. Although the damage and casualties were less severe than in 1939 (Sieberg 1932), the 1784 earthquake proved quite hazardous for the Erzincan region, killing 5,000-15,000 people (see Table 1). The recurrence interval for category b events is about 100-150 years, and earthquakes most likely correspond to segment 2, the Ovacik fault or segment A of the NEAF zone. Of these, segment 2 has the highest potential for generating large earthquakes in the near future, because (a) segments 1-3 of the NAF zone form a boundary between the eastward-moving NE Anatolian block and the main westward-moving Anatolian block, so that the rate of movement is naturally expected to be higher than along other parts of the NAF zone; and (b) during the 20th century segment 2 is the only segment along the NAF zone which has not experienced a large earthquake between Varto and the western end of the Mudurnü valley (900 km) (see also Ambraseys and Zatopek 1969). Note that segment 1 has already broken twice in the last 40 years (Figure 6c,d). The largest event which has occurred on segment 2 during the instrumental period (since 1900) is the 1967 Pülümür earthquake ($M_s = 5.6 - 6.2$), (Figure 6d). Ambraseys (1975) has reported that this earthquake produced a short rupture, 4 km long, with 20 cm maximum dextral slip, at the eastern half of segment 2. However, if we consider the approximately 100 km length of segment 2, the 1967

event is not large enough to fill the gap (Figure 7). Therefore segment 2 appears to have the highest potential for a large earthquake in the Erzincan region in the near future. The segment 2 gap, which is separate from the gap mentioned by Toksöz *et al.*, (1979; see Figure 7), was first mentioned by Ambraseys and Zatopek (1969).

Only a few earthquakes (e.g., 1960, $M=5.9$) can be associated with the Ovacik fault since 1900. Although the rate of movement is somewhat smaller along this fault than on the NAF zone, the Ovacik fault segment is another candidate for future large earthquakes. Segment A of the NEAF zone is similar to the Ovacik fault. The 1939/11/21 Tercan earthquake and 1940/02/03 (#12 in Table 2) aftershock of the great 1939/12/28 earthquake might have occurred on segment A. From the historical earthquake records, we are only aware of the 1254 large earthquake, which created 50 km of surface faulting along segment A, trending 60° with 5 m (?) maximum vertical displacement (Ambraseys, 1975).

The unruptured fault segments, including segment 2, the Ovacik fault, and Segment A, occur within the serpentinite-rich ophiolitic complexes in the vicinity of Erzincan. Thus creep is an expected phenomenon which probably takes up some of the motion along the fault segments. Nevertheless this does not exclude the potential for future large earthquakes.

In conclusion, defining segmentation of the fault zones through geometric discontinuities and combining resulting segments with existing earthquake data can provide information about seismic gaps and earthquake rupture processes. A possible explanation for the high concentration of seismic activity in the Erzincan region is the fact that many different fault segments begin, terminate or intersect within that region. The geometric arrangement of fault discontinuities (restraining bends, triple junctions and releasing stepovers) and

the rock type (e.g., serpentinite) contribute to the relative ease or difficulty of movement along fault segments in the region. These factors are responsible for the division of earthquakes into categories a, b or c. Our interpretation of fault geometry and earthquake data in the Erzincan region suggests that a large earthquake similar to the 1784 event is expected to occur soon. This earthquake could cause considerable damage in Erzincan and surrounding areas. Further detailed studies are required in order to better characterize this seismic hazard.

REFERENCES

- Ali, K. Erzincan Earthquakes, Erzincan province year-book, 110-115, 1932.
- Allen, C.R., Active faulting in northern Turkey: Contr. No. 1577. Div. Geol. Sci., Calif. Inst. Tech., 32 p., 1969.
- Alsan, E., Tezucan, L. and Bath, M. *An earthquake catalogue for Turkey for the interval 1913-1970*. Kandilli Observatory Seismology Dept. Report No. 7-75. 166 pp., 1975.
- Ambraseys, N.N. Some characteristic features of the North Anatolian fault zone. *Tectonophysics* 9, 143-185, 1970.
- Ambraseys, N.N. Studies in historical seismicity and tectonics, in: *Geodynamics of Today*, The Royal Soc. London, 7-16, 1975.
- Ambraseys, N.N. and Jackson, J.A. Earthquake hazard and vulnerability in the northeastern Mediterranean: the Corinth earthquake sequence of February-March 1981. *Disasters*, 5, 355-368, 1981.
- Arpat E., and Saroglu, F. Some recent tectonic events in Turkey. *Türk. Jeol. Kur. Bul.*, 18, 91-101, 1975.
- Arpat, E. The 1976 Caldiran earthquake: *Yeryuvarı ve İnsan*, 2, 29-41, 1977.
- Bakun, W.F., Stewart, R.M., Bufe, C.G. and Marks, S.J. Implication of seismicity for failure of a section of San Andreas Fault, *Bull. Seism. Soc. Am.*, 70, 185-202, 1980.
- Barka, A.A. Some Neotectonic features of the Erzincan basin, Earthquake Symposium, Atatürk University, special publication, Erzurum (Turkish with English Abst.) pp. 115-125, 1984.

- Barka, A. and Hancock, P.L. Neotectonic deformation patterns in the convex-northwards arc of the North Anatolian fault, in *The Geological Evolution of the Eastern Mediterranean* (edited by Dixon, J.G. and Robertson, A.H.F.), Special publication Geol. Soc. London, 763-773, 1984.
- Barka, A.A. and Hancock, P.L. Relationship between fault geometry and some earthquake epicenters within the North Anatolian fault zone, *Progress in Earthquake Prediction*, edited by A.M. Isikara and A. Vogel, Friedr. Vieweg and John, F.R.G., 2, pp. 137-142, 1982.
- Barka, A.A. and Kadinsky-Cade, K., Strike-slip fault geometry and earthquake activity in Turkey, *Tectonics*, 1987.
- Barka, A.A. and Gülen, L. Tectonic escape origin and complex evolution of the Erzincan pull-apart basin, Eastern Turkey, *Geol. Soc. Amer. Bull.*, 1987.
- Can, R. Seismo-tectonics of the North-Anatolian fault zone, M. Phil. Thesis University of London, 255 pp., 1974.
- Dewey, J.W. Seismicity of Northern Anatolia, *Bull. Seism. Soc. Am.*, 66, 843-868, 1976.
- Eren, D., Akkas, N. and Erdik, M. Finite element modelling of Eastern Mediterranean regime. Unpublished report Middle East Technical University, Ankara, Turkey, 1984.

- Ergin, K., Güclü, U. and Uz, Z. A catalogue of earthquakes for Turkey and surrounding area. Ist. Tek. Uni. Mad. Fak. yay. 24.189 pp., 1967.
- Erzincan Yilligi. Erzincan earthquakes. Year-book of the Erzincan province, 225 pp., 1967.
- Gülen, L. Sr, Nd, Tb isotope trace elements, Geochemistry of calcaline and alkaline volcanics, Eastern Turkey, Ph.D. Thesis, Massachusetts Institute of Technology. 232 pp., 1984.
- Jackson, J. and McKenzie, D. Active tectonics of the Alpine-Himalayan Belt between western Turkey and Pakistan. *Geophys. Journ. R. Ast. Soc.* 77, 185-265, 1984.
- Karnik, V. *Seismicity of the European area*, D. Reidel Pub. Com., Dordreet, Holland, Part I, 365 pp., 1969.
- Karnik, V. *Seismicity of the European area*, D. Reidel Pub. Com., Dordreet, Holland, Part II, 218 pp., 1971.
- Kasapoglu, E. and Toksöz, M.N. Tectonic consequences of the collision of the Arabian and Eurasian plates: finite element models, *Tectonophysics*, 100, 71-96., 1983.
- Ketin, I. Über die tektonisch-mechanischen Folgerungen aus den grossen anatolischen Erdbeben des letzten Desenniums. *Geol. Rdsch.*, 36, 77-83, 1948.
- Ketin, I. Über die nordanatolische horizontalverschiebung, *Bull. Min. Res. Explor. Inst., Turkey*, 72, 1-28 pp., 1969.
- King, G. and Nabelek, J. Role of fault bends in the initiation and termination of

- earthquake rupture. *Science*, 228, pp. 984-987, 1985.
- Lahn, E. Seismic activity in Turkey from 1947-1949, *Bull. Seism. Soc. Amer.*, 42, pp. 111-114, 1952.
- Lindh, A.G., and Boore, D.M. Control of rupture by fault geometry during the 1966 Parkfield earthquake, *Bull. Seism. Soc. Am.*, 71, pp. 95-118, 1981.
- McKenzie, D. Active tectonics of the Mediterranean Region. *Geophys. J.R. Astr. Soc.*, 30, 109-185, 1972.
- Nature*, The earthquake in Turkey, 145, 62, 1940a.
- Nature*, The earthquake in Turkey, 145, 96, 1940b.
- Nature*, Aftershocks of the earthquake in Turkey, 145, 259, 1940c.
- Nature*, 1940d. Earthquakes in Turkey, 145, 346.
- Pamir, N. and Ketin, I. Das Erdbeben in der Türkei vom 27 und 28 Dezember, 1939. *Geol. Rundsch.* 31, 77-78, 1940.
- Pamir, H.N. and Ketin, I. Das Anatolische Erdbeben Ende 1939, *Geol. Rundsch.*, 32, 278-287, 1941.
- Parajes, E., Akyol, I. H. and Altinli, E. Le tremblement de terre d'Erzincan du 17 Decembre 1939. *Revue Fac. Sci. Univ. Istanbul*, XVI, 177-222, 1941.
- Pinar, N. and Lahn, E. Earthquake catalogue of Turkey, Bayin Bakan. Yapi Imar Isle. Reis yayin. 6. 36. Ankara, 1952.
- Riad, S. and Meyers, H. Earthquake catalog for the Middle East countries 1900-1983. World Data Center A., Report, SE-40. 133, 1985.

Salomon-Calvi, W. Die Fortsetzung der Tonalelinie in Kleinasien. Yük. Zira. Enst. Calis, 9. pp. 11-13, 1936.

Study of earthquakes in Turkey, MTA. Enst. Yay. Sei B. No:5, L-121, 1940.

Schwartz, D.P., and Coppersmith, K.J. Seismic hazards: New trends in analysis using geologic data, in *Active tectonics*, National Acad. Press, Washington, D.C., pp. 215-230, 1986.

Segall, P. and Pollard, D.D. Mechanics of discontinuous faults, *J. Geophys. Res.*, 85, pp. 4337-4350, 1980.

Sengor, A.M.L. and Kidd, W.S.F. Post-collisional tectonics of the Turkish-Iranian Plateau and a comparison with Tibet, *Tectonophysics*, 55, pp. 361-376, 1979.

Sengor, A.M.C., Görür, N. and Saroglu, F. Strike-slip faulting and related basin formation in zones of tectonic escape: Turkey as a case study. I: Biddke, K.T. and Christie-Blick, N. (eds.). *Strike-slip faulting and Basin Formation*, Society of Econ. Paleont. Min., Sp. Pub. pp. 227-264, 1985.

Seymen, I. Tectonic aspects of the North Anatolian fault zone within the Kelkit valley, Ph.D. Thesis, Ist. Tek. Uni. 152 pp., 1975.

Sibson, R.H. Earthquakes and lineament infrastructure, *Phil. Trans. R. Soc. London*, 317, pp. 63-79, 1986.

Sieberg, A. Untersuchungen über Erdbeben und Bruchscholenbau im oestlichen Mittelmeergebiet. *Denk. d. Mediz. Natw. Ges. zu Jena*, Bd. 18. pp. 159-273, Jena, 1932.

- Sipahioglu, S. Seismo-tectonic features of the North Anatolian fault zone, Ph. D. Thesis, Ist. Univ. Fen Fak. Jeofizik Böl., 169 pp., 1982.
- Sipahioglu, S. An evaluation of earthquake activity of the Horasan-Narman region before the 30 October 1983 earthquake. *Yeryuvuri ve Insan* 8, 3. pp. 12-15, 1983.
- Soysal, H., Sipahioglu, S., Kolcak, D. and Altinok, Y. Historical earthquake catalogue of Turkey and its vicinity. Turkish Scienc. Res. Found. TBAG 341, 122 pp., 1981.
- Tabban, A. Geology and earthquake activity of the cities, T.C. Imar. Iskan Bakanligi. Aft. Isleri Genel. Mu. Ankara, 343 pp., 1980.
- Tatar, Y. Tectonic investigations on the North Anatolian fault zone between Erzincan and Refahiye, *Publ. Inst. Earth. Sci., Hacettepe Univ.* 4, 201-136, 1978.
- Tillotson, E. The Earthquake in Turkey, *Nature*, 145, pp. 13-15, 1940.
- Toksöz, M.N., Shakal, A.F. and Michael, S.J. Space-time migration of earthquakes along the North Anatolian fault zone and seismic gaps, *Pageoph.*, 117, pp. 1258-1269, 1979.
- Toksöz, M.N. Seismicity and earthquake prediction studies in Turkey, Unpublished USGS proposal, 1984.

FIGURE CAPTIONS

- Figure 1. Tectonic map of Turkey showing the surface rupture along the North Anatolian and other faults due to major earthquakes since 1900. The Anatolian and NE Anatolian blocks are wedged out to the west and east respectively by the convergence of Arabia and Eurasia as shown in the inset map (lower left). The rectangle in the figure delineates the area of study and is enlarged in Figure 2. (Compiled from Arpat & Saroglu 1972; Arpat 1976; Barka 1984; Sengör et al., 1986).
- Figure 2. Simplified geometry of major blocks and their boundary fault zones between Erzincan and Karlioiva. Thick and dashed zones and dates indicate ruptured fault segments and dates of related earthquakes, respectively. Dotted area is the Erzincan basin. A_1 and A_2 are sub-blocks within the Anatolian block.
- Figure 3.(a) Earthquake activity histogram of the Erzincan region. I, Intensity, T, time. Numbers above the dots are the number of casualties resulting from each particular event. a, b, c are the categories of earthquakes, S-2, S-3, S-4 and S-A are the fault segments. For explanation and references see the text and Tables 1 and 2 respectively. (b) log (number of earthquakes) versus intensity, 1000 - 1900, in the Erzincan region. The dashed line is drawn through the $I \geq VIII$ data points ($\log N = -0.271 I + 2.98$).
- Figure 4. Distribution of earthquake epicenters ($M > 4.9$) in the easternmost part of the NAF zone between Erzincan and Karlioiva for the interval 1900-1983. A = instrumental data only, B = macroseismic information only, C = best of instrumental or macroseismic information, D = instrumental and macroseismic data agree. Details are given in Table 2.
- Figure 5. Fault plane solutions between Erzincan and Karlioiva (McKenzie, 1972). Note that a) the 1983/11/18 earthquake, $M_s = 4.8$, has a normal fault solution which agrees with the opening of the Erzincan basin and b) solutions east of the Karlioiva junction have a clear thrust component.
- Figure 6. Sequence of events which produced surface faulting in the Erzincan-Karlioiva region in the last 200 years. For explanation see text.
- Figure 7. Space-time distribution of surface ruptures of 20th century earthquakes, indicating a clear seismic gap between 39.8 and $40.8^\circ E$, where segment 2 lies. The area to the east of 41.8° has been identified already as another seismic gap (Toksöz et al., 1979).

Table 1. List of historical earthquakes
in the Erzincan Region.

Number	Date	Intensity (I)	Number of casualties
(1)	1045	X-XI	
(2)	1161	VI	
(3)	1165	VII	
(4)	1166	VI	
(5)	1168	VIII	12,000
(6)	1170	VIII-IX	
(7)	1236	VI	
(8)	1251	VIII	
(9)	1254-55	VIII	16,000
(10)	1268	IX	15,000
(11)	1287	VIII	
(12)	1289	VIII	
(13)	1308	VI	
(14)	1356	V	
(15)	1366	VI	
(16)	1374	VII	
(17)	1422	VIII	
(18)	1433	VI	
(19)	1458	X	32,000
(20)	1543	VII	
(21)	1578	VIII	1,500-15,000
(22)	1605	?	
(23)	1667-8	VIII-X	Half of the town was destroyed
(24)	1784	VIII-IX	5,000-15,000
(25)	1887	VI	

* Documented from Sieberg 1932, A. Kemal 1932, Solomon-Calvi 1936-1940, Parejas *et al.*, 1941, Pinar and Lahn 1952, Ergin *et al.*, 1967, Ambraseys 1970, 1975, Karnik 1972, Can 1974, Dewey 1976, Soysal *et al.*, 1981, 1982, Sipahioğlu 1982, 1983.

Table 2. List of instrumental earthquakes with $M_s > 4.9$, for the 1900-1983 interval in the eastern part of the NAF zone.

Number	Dates	Epicenter		M	Reference
		Lat. N	Long. E		
(1)	1907/04/08	*39.30	40.40	4.9	3.2
		Damage at Kigi			2
(2)	1909/-/-	*39.3	40.3	5	4
		Kigi			2
(3)	1909/05/03	*39.	40	5.3	4
		(Tercan?)			2
(4)	1930/04/09	*39.6	39.3	5.	3
(5)	1930/12/10	39.8	39.1	5.6	1
		39.5	39.4	5.4	4
		*39.7	39.2	5.6	3
		Slight damage at Kernak and Erzincan			2
(6)	1934/11/12	39.2	40.5	5.9	1
		*39.	41.	5.8	4
(7)	1935/05/11	*39.3	40.6	6.1	4
(8)	1935/10/13	*39.4	40.2	5.1	1
		39.3	40.5	4.8	4
		39.4	40.5	5.	3
(9)	1939/11/21	*40.	39.7	5.9	1
		39.7	40.4	4.7	(?)4
		39.8	39.7	5.9	3
		43 deaths at Erzincan, heavy damage at Karakulak			2
(10)	1939/12/26	*39.8	39.4	8	1
		39.7	39.5	8	4
		39.8	39.5	7.9	3
(11)	1939/12/29	*39.7	39.7	5	4
(12)	1940/02/03	40.1	39.9	?	5
		45 deaths, Besin and Pulur destroyed			
(13)	1940/02/04	*39.7	39.5	5	3

Number	Dates	Epicenter		M	Reference
		Lat. N	Long. E		
(14)	1940/04/22	39.5	40.	5.2	1
		*39.7	39.7	5.	4
		39.6	39.9	4.9	3
		at Erzincan			2
(15)	1940/05/29	*39.7	39.7	5.	4
		40 buidings collapsed in the villages, vicinity of Erzincan			2
(16)	1940/09/11	*39.9	38.8	5.	4
(17)	1941/11/08	*39.7	39.7	5.3	4
		39.7	39.7	5.	3
		at Erzincan			2
(18)	1941/11/12	39.9	39.4	5.9	1
		*39.7	39.7	5.7	4
		39.7	39.4	5.9	3
		15 deaths, 100 injured at Erzincan			2
(19)	1946/5/31	*39.3	41.1	5.9	1
		40.	41.5	6	4
		39.3	41.2	5.7	3
		839 deaths at Varto and Usturkiran			2
(20)	1946/12/13	*slight damage at Pulumur		5.2	2
(21)	1949/8/17	39.	40.5	6.7	1
		39.4	40.9	6.5	4
		39.6	40.6	7.	3
		*39.4	40.8		6
		300 deaths at Karlioiva			2
(22)	1949/8/17	39.6	40.4	5.2	1
		*39.5	40.6	5.	4
		40.1	40.6	5.3	3
(23)	1949/8/17	*39.6	40.6	5.2	3
(24)	1949/11/01	*39.3	40.3	4.9	3
		slight damage at Kigi			2
(25)	1950/02/04	*39.3	41.	4.9	3
(26)	1950/08/27	*39.4	41.	4.9	3
		two deaths at Varto			2
(27)	1953/12/15	39.7	41.2	5.5	1
		39.1	41.4	5.3	4

Number	Dates	Epicenter		M	Reference
		Lat. N	Long. E		
(28)	1954/03/28	*39.1	41.	5.2	4
(29)	1954/10/24	*40.	40.	5.8	4
(30)	1957/07/07	39.2	40.2	5.5	1
		*39.2	40.3	5.3	4
		39.4	40.5	5.1	3
		7 injured at Kigi			2
(31)	1959/01/14	*39.5	40.4	5.1	3
(32)	1959/09/10	39.7	41.4	5.6	1
		39.6	41.7	5.1	4
		*damage at Varto			2
		(39.3	41.4)		
(33)	1959/10/25	*39.2	41.5	5.	1
		39.3	41.6	4.8	4
(34)	1959/12/25	*39.1(?)	41.6(?)	6.2(?)	4
(35)	1960/01/26	40.1	38.6	5.	1
		*39.5	39.5	5.9	4
		felt at Kemah and Erzincan			2
(36)	1960/06/09	39.9	39.5	5.	1
		*39.5	39.5	4.8	4
(37)	1964/09/4	39.	40.2	5	1
		*39.8	40.3, 40.2	4.6	4
		felt at Cayirli			2
(38)	1964/11/16	39.4	40.3	5.1	1
		*39.8	39.9	4.8	4
		39.5	40.3	4.9	3
		felt at Erzincan			2
(39)	1965/08/31	*39.4	40.7	5	
		39.3	40.8	4.8	4
		39.4	40.8	5.6	3
		25 deaths, 40 injured at Karliova			2
(40)	1966/03/07	*39.2	41.5	5.3	1
		39.1	41.6	6	4
		39.2	41.6	5.6	3
		4 deaths at Varto			2

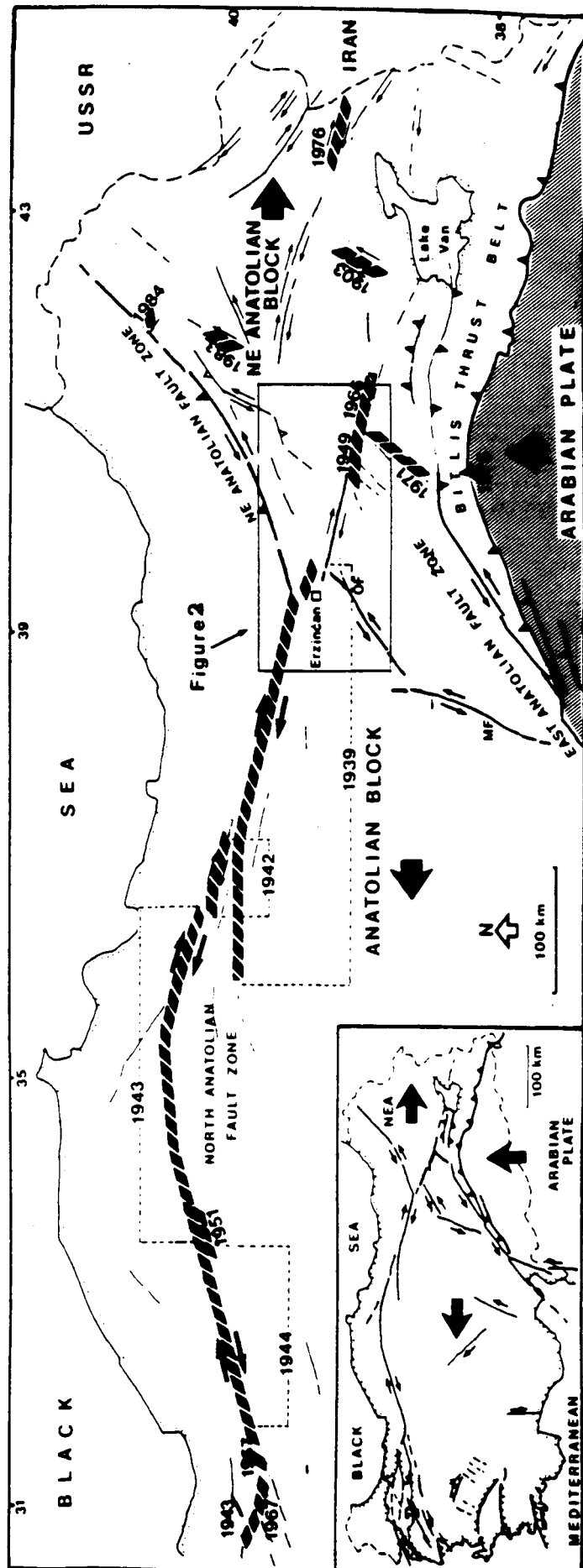
Number	Dates	Epicenter		M	Reference
		Lat. N	Long. E		
(41)	1966/08/19	*39.2	41.5	6.8	1
		39.2	41.6	7.1	4
		39.2	41.6	6.9	3
		2394 deaths at Varto and its vicinity			2
(42)	1966/08/19	*39.3	41.2	5	1
		39.4	41.3	5.3	3
(43)	1966/08/14	*39.3	41.1	5	1
		39.	41.8	5.1	3
(44)	1966/08/20	*39.4	40.9	5.3	1
		39.4	40.9	5.3	1
		39.4	40.9	5.1	4
		39.4	41	6.2	3
		Damage at Karliova			2
(45)	1966/08/20	39.1	39.8	5.5	1
		*39.1	40.7	5.4	4
		39.2	40.7	6.1	3
(46)	1967/01/30	*39.4	41.5	5	3
(47)	1967/07/26	*39.5	40.3	5.6	1
		39.5	40.4	6.2	4
		39.5	40.3	6.2	3
		97 deaths at Pulumur			2
		39.5	40.4	5.6	7
(48)	1968/09/24	4km surface faulting			
		118 azimuth, 20 cm right-lateral displacement			7
		*39.2	40.3	5.1	1
		39.2	40.1	5.1	4
		39.2	40.3	5.1	3
(49)	1968/09/25	2 deaths, 87 injured at Kigi			
		6 km length of surface faulting			
		150 azimuth, 25 cm vertical displacement			2,7
(49)	1968/09/25	*39.3	40.2	5.1	1
		39.2	40.2	4.8	4
(50)	1969/09/10	*39.3	41.4	5.2	1
		39.2	41.4	5	4
		39.3	41.4	5.2	3
(51)	1970/09/03	3 injured at Kemahy			2

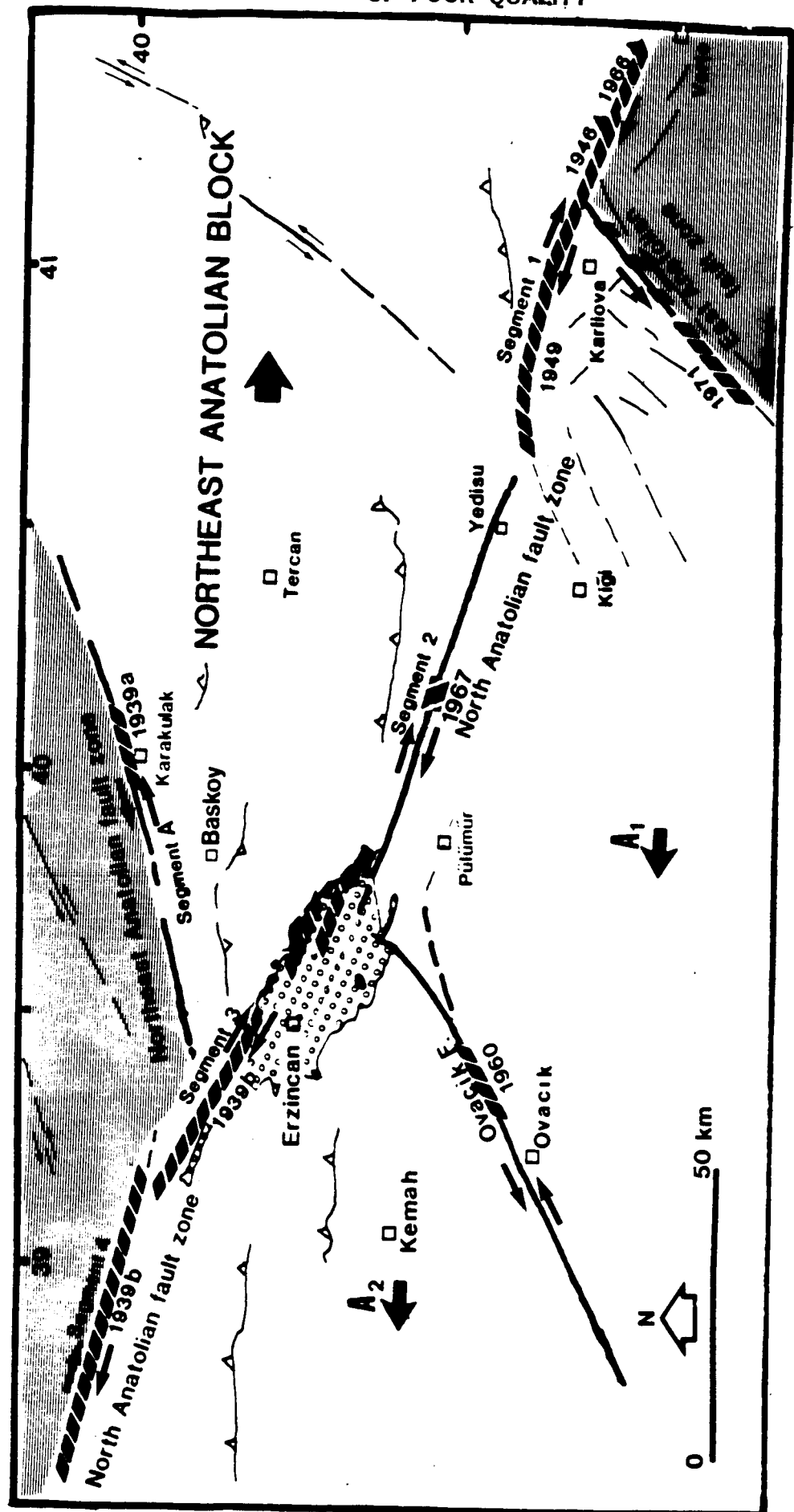
Number	Dates	Epicenter		M	Reference
		Lat. N	Long. E		
(52)	1971/05/22	*39.1	40.6	5.4	3

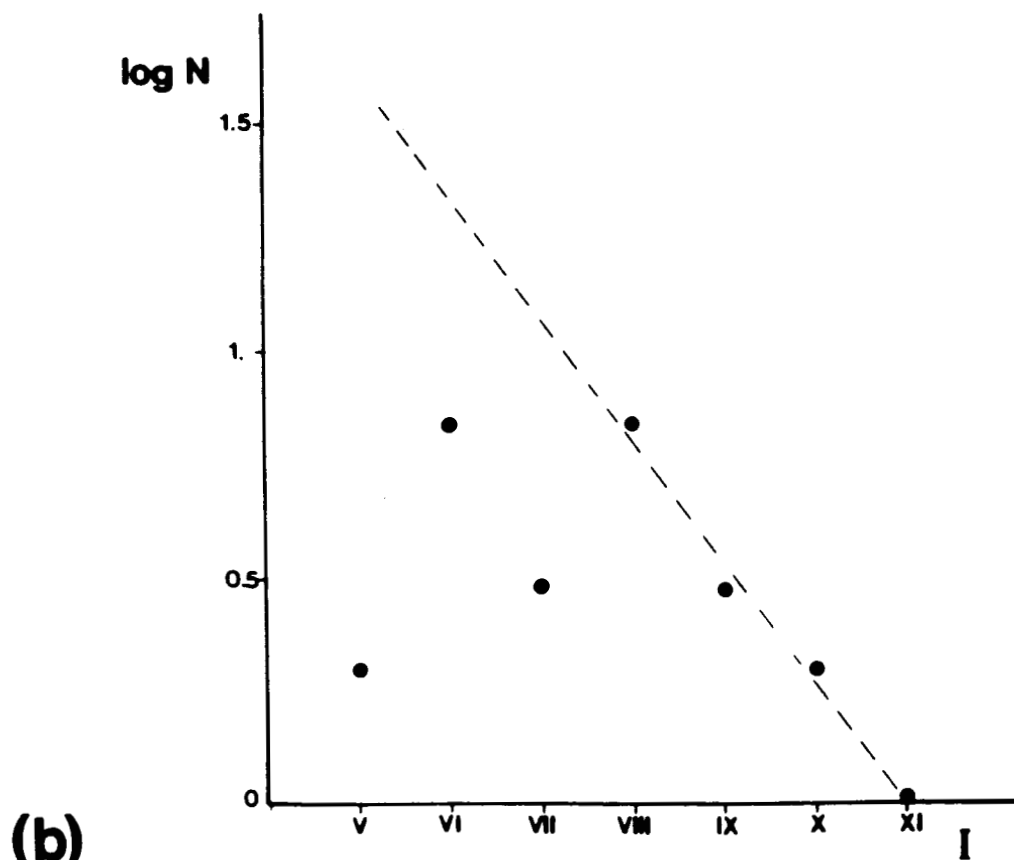
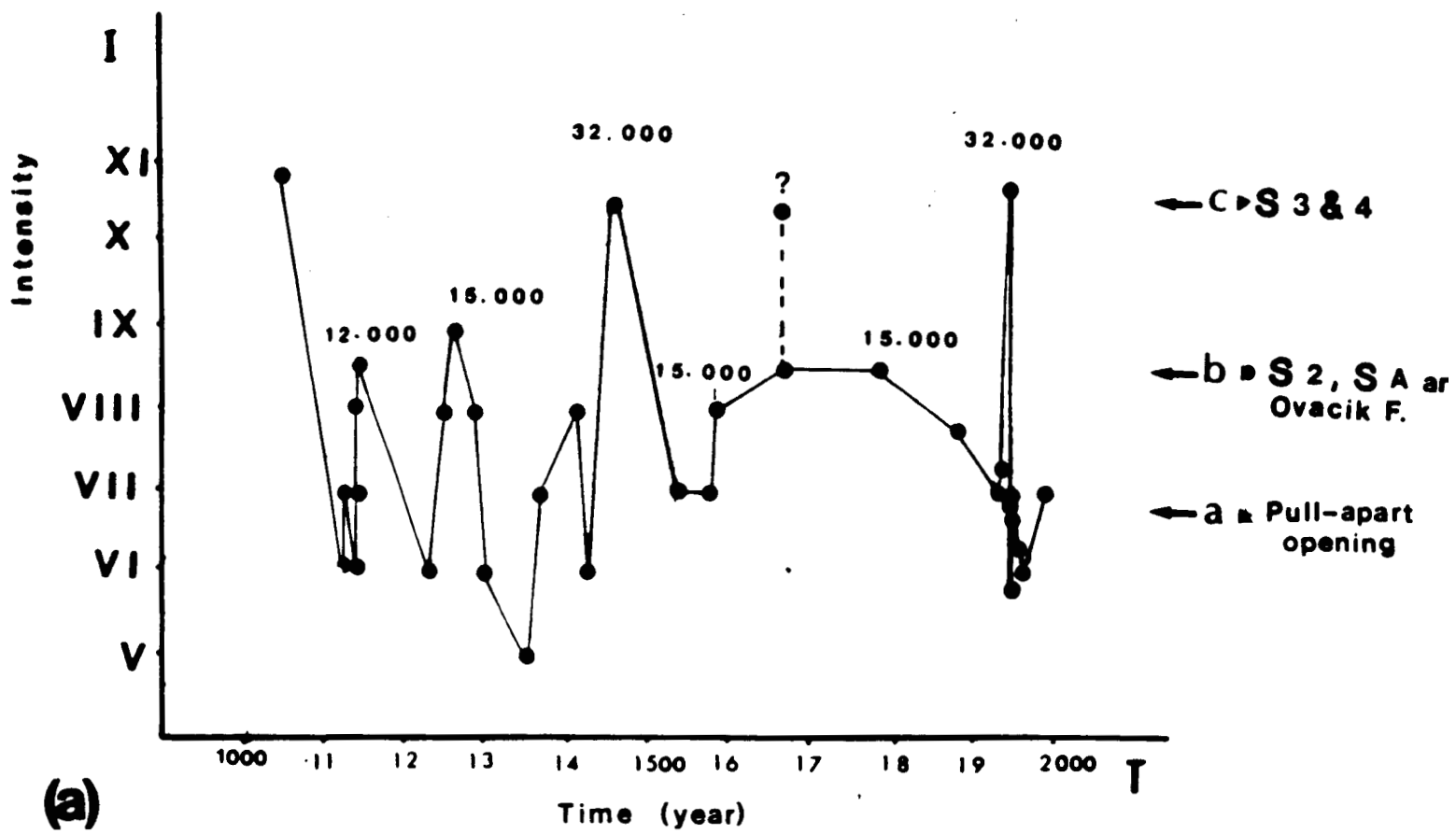
* Indicates preferred epicenter location which is shown in Figure 4.

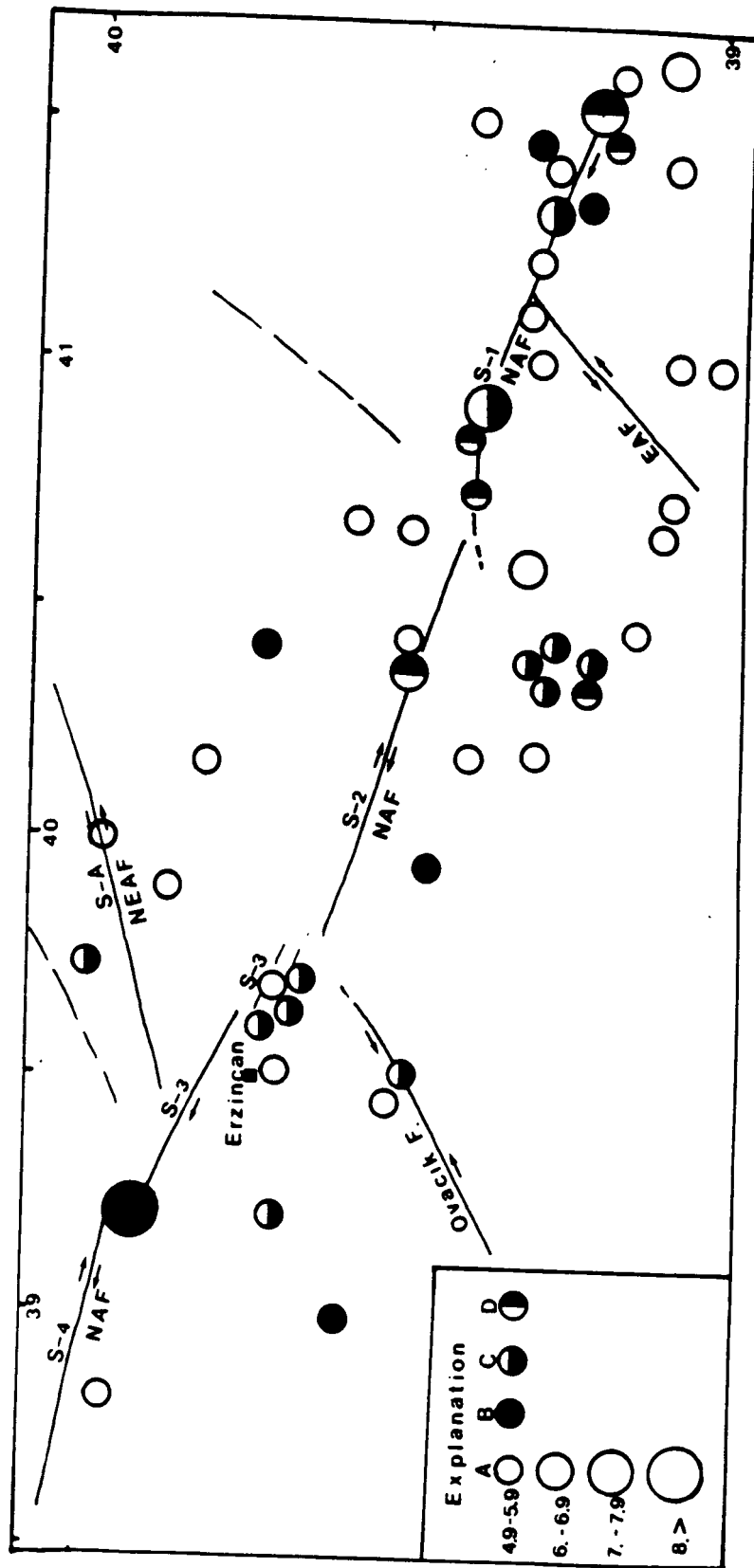
- 1) Dewey, 1976
- 2) Tabban, 1980
- 3) Soysal et al., 1981; Sipahioglu, 1983
- 4) Riad and Meyers, 1985
- 5) Nature, 1940c
- 6) Lahn, 1952
- 7) Ambraseys, 1975

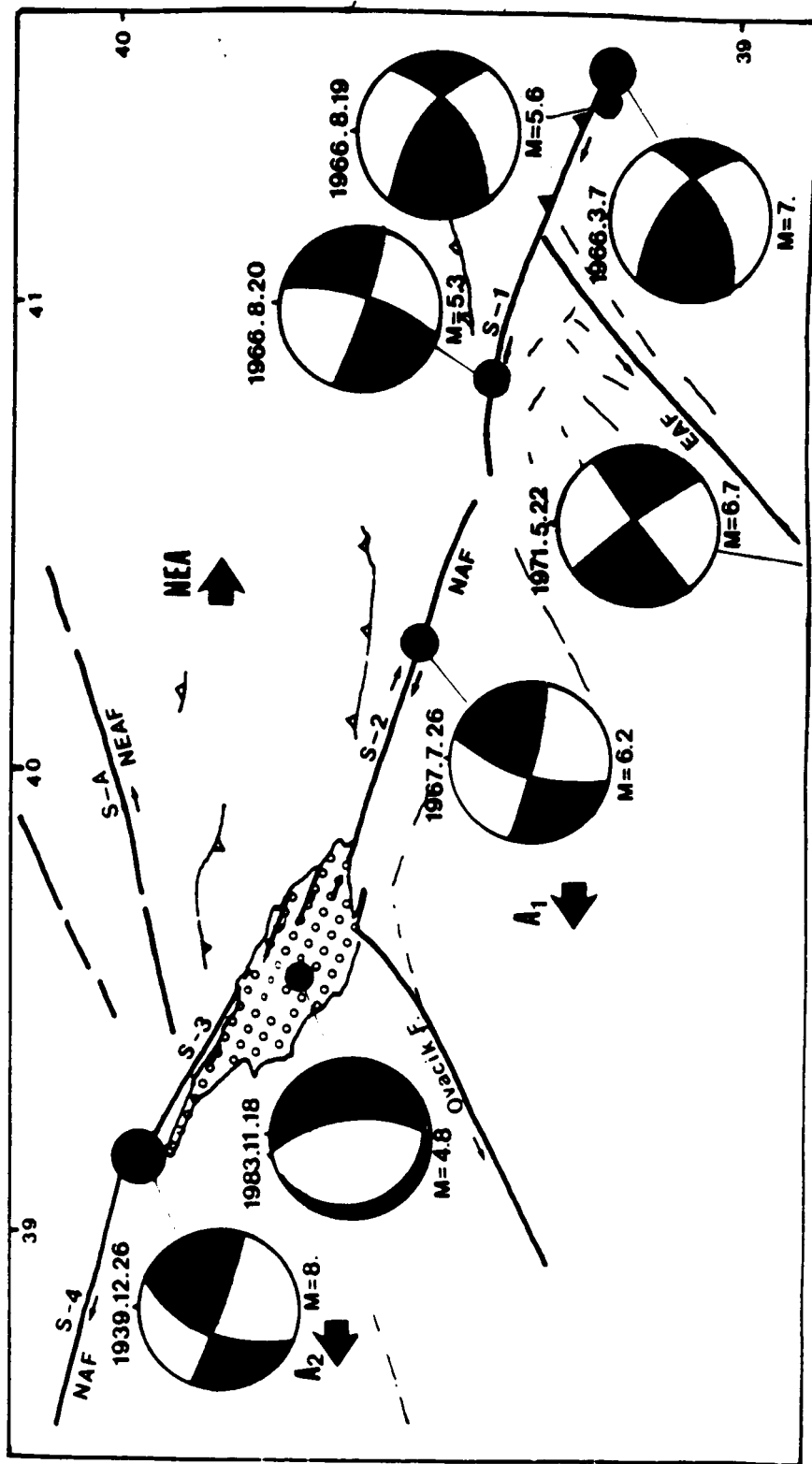
ORIGINAL PAGE IS
OF POOR QUALITY

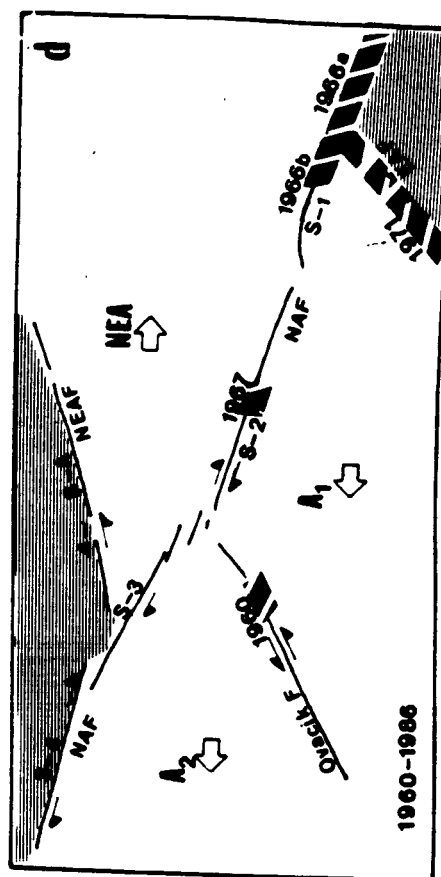
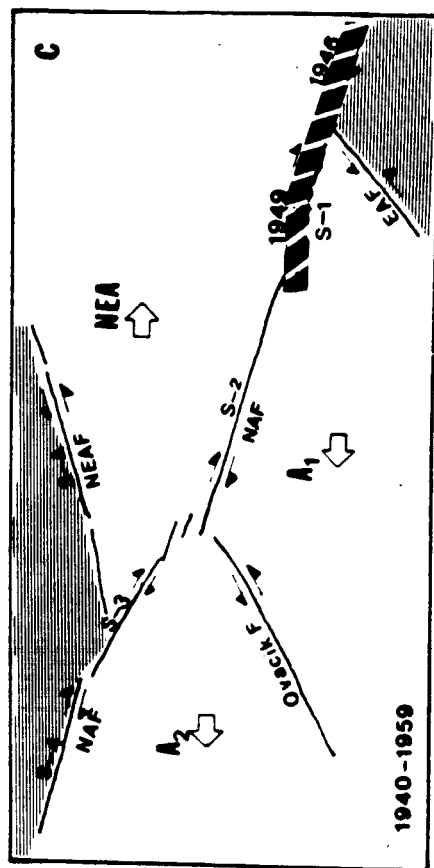
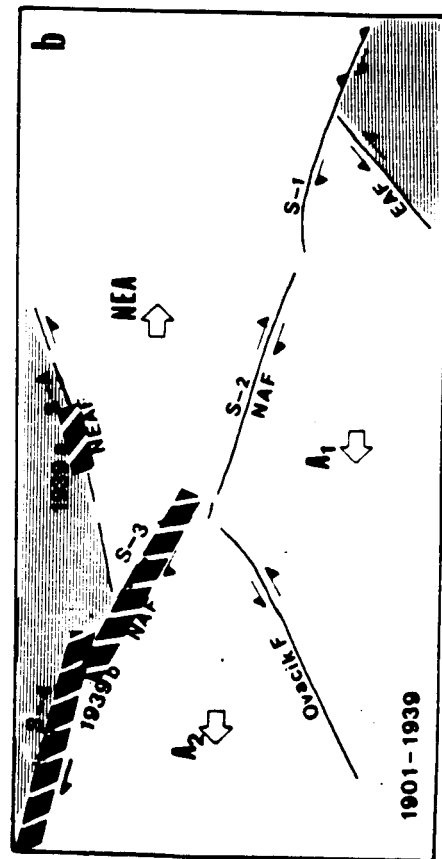
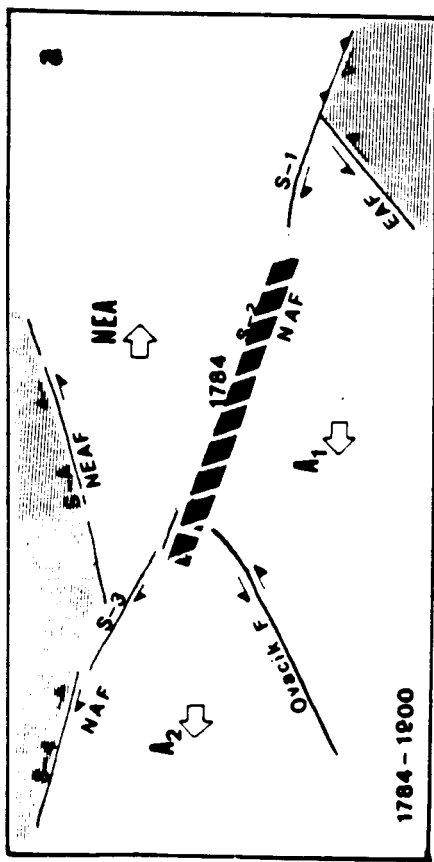


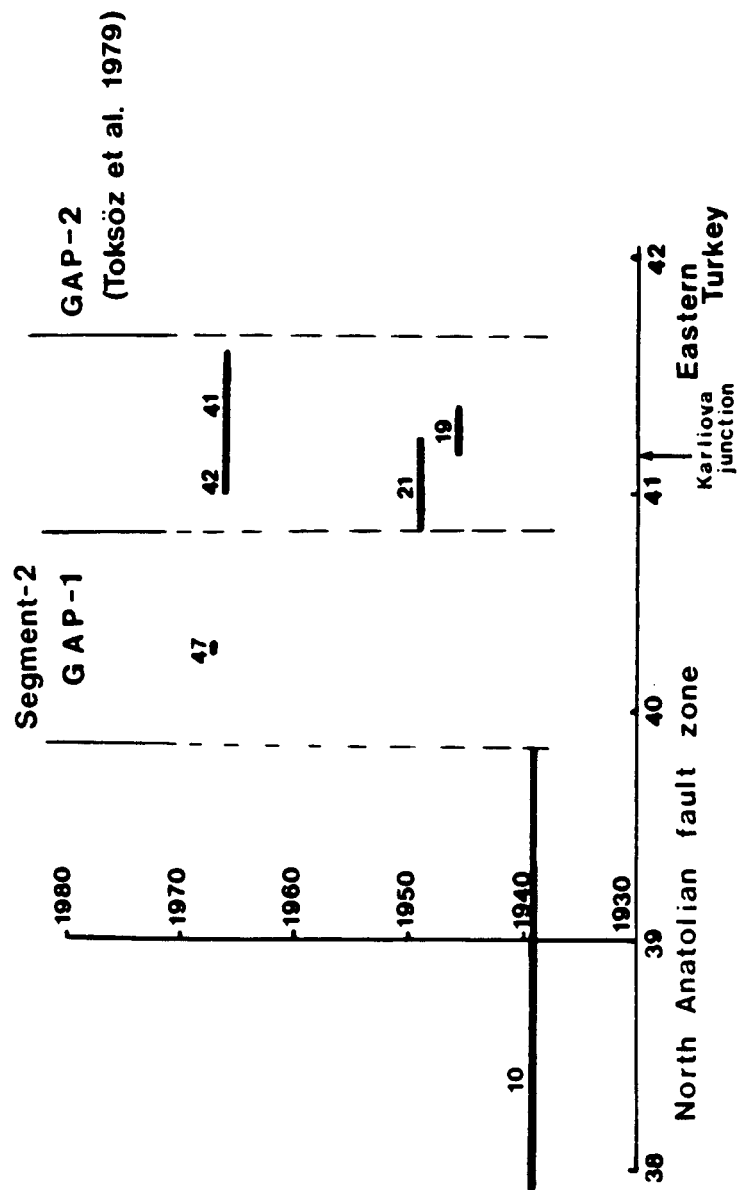












**STRIKE-SLIP FAULT GEOMETRY AND
EARTHQUAKE ACTIVITY IN TURKEY**

by

A. Barka and K. Kadinsky-Cade

**Earth Resources Laboratory
Department of Earth, Atmospheric, and Planetary Sciences
Massachusetts Institute of Technology
Cambridge, MA 02142**

February, 1987

ABSTRACT

A comprehensive examination has been made of strike slip fault geometry in Turkey. The influence of fault geometry on the behavior of large earthquakes has been compared with that for well-studied strike-slip earthquakes in California and Asia. The two main elements comprising the geometric patterns are stepovers and bends. There are many observed combinations of these two elements. Each combination can be associated with a particular fault behavior. The most commonly encountered patterns are (1) the restraining double bend and (2) the restraining bend with adjacent releasing stepover. Fault segmentation is closely related to fault geometry. The geometric patterns are seen to influence the distribution of maximum dislocation and intensity during large earthquakes. Fault geometry is also a critical factor in providing sites for localized strain accumulation, preferred epicenter locations and aftershock sites. The most important fault geometry parameters are: stepover width (less than about 10 km for a through-going rupture), bend angle α (less than about 30° for a through-going rupture), the length L_2 of the restraining fault segment and the angle β between the direction of block motion and the strike of the main fault. In the case of single and double restraining bends it is observed that $\log(\alpha L_2)$ is roughly proportional to earthquake magnitude, and that the epicenter rarely occurs on the restraining segment L_2 . Aftershocks and swarms of smaller earthquakes cluster in releasing bend and releasing stepover areas. In a few cases foreshocks can be associated with releasing features located adjacent to or within restraining areas.

INTRODUCTION

There has been a lot of recent interest in relationships between fault geometry, fault segmentation and earthquake activity (e.g., Allen, 1968; Bakun *et al.* 1980; Barka and Hancock, 1982; Koide, 1983; Bilham and Williams, 1985; King and Nabelek, 1985; Slemmons and Depolo, 1986; Schwartz and Coppersmith, 1986; Sibson, 1986; King, 1986). Strike-slip faults lend themselves particularly well to the study of these relationships because variations in strike-slip fault geometry are easy to observe at the surface. Furthermore, because depths of shallow earthquakes are usually not as well constrained as their epicentral locations (except when the events are directly overlain by a seismic network), it is usually difficult to associate earthquake locations with geometric features at specified depths as would be required by the study of dip-slip fault geometry. In this study we examine the above relationships in detail by focusing on strike-slip fault geometry and earthquakes in Turkey. There is a wealth of data available for Turkish faults that has not been examined in a comprehensive way from this perspective. This region will be used as a case study. Results will be applicable to strike-slip faults in other parts of the world.

The procedure employed in this study is as follows. First, we identify major geometric discontinuities in the fault zones and relate many of those discontinuities and resulting fault segmentation to $M \geq 6.5$ earthquakes that have already occurred. Second, we apply results from the first step to areas that have not experienced a large earthquake recently, in order to predict characteristics of future large events.

The philosophy behind this study is a test of the hypothesis that fault geometry strongly affects (1) fault segmentation, (2) the location of epicenters for large earthquakes, (3) the rupture propagation direction for these earthquakes, (4) the size of the large earthquakes, and (5) the distribution of the

highest intensity and/or fault dislocations that are observed during the earthquakes. Clearly, geometrical constraints are not the only factors affecting earthquake phenomena (other constraints may be provided by variations in fluid pressure, friction, etc.; see e.g., Sibson, 1986). Observations in Turkey and elsewhere, however, suggest that a definite cause and effect relationship exists between fault geometry and earthquake processes.

TECTONIC FRAMEWORK AND GEOMETRIC PATTERN DEFINITIONS

Major tectonic elements of Turkey and adjacent areas are illustrated in Figure 1. Rapid northward motion of the Arabian Plate relative to Eurasia (5 cm/yr; Solomon *et al.*, 1975) causes lateral escape of the Anatolian block to the West (e.g. Ketin 1948, McKenzie, 1972) and a complex internal deformation of northeastern Turkey.

The North Anatolian fault zone is a 1200 km long seismically active right-lateral strike-slip fault that takes up the relative motion between the Anatolian Block and Black Sea plate. This fault zone extends from the Karliova triple junction (39.3°N, 41.1°E; "K" in Figure 1) to the Aegean Sea. It is divided into segments which range in length from 30 to 350 km. Adjacent segments are separated from each other by stepovers, bends, or combinations of these discontinuities (Figure 2). It is generally thought that the age of the North Anatolian fault zone is late Miocene to Pliocene (13-5 Ma; see e.g., Ketin, 1969; Barka and Hancock, 1984; Sengör *et al.*, 1985). Estimates of the total relative displacement along the fault range from 25 to 120 km (e.g., Bergougnan, 1976; Seymen, 1975; Barka and Hancock, 1984; Sengör *et al.*, 1985). Between 1939 and 1967 most of the North Anatolian fault ruptured in a westward-migrating series of 6 large earthquakes (magnitude 7-8), producing continuous surface breaks from Erzincan to the west end of the Mudurnu Valley (39.5°E -31° E; see Ketin,

1948, 1969; Ambraseys, 1970, 1975). Focal mechanisms for moderate and large earthquakes along this portion of the fault zone are mostly pure right-lateral strike-slip solutions (Canitez and Ucer, 1967; McKenzie, 1972). Rates of slip along the North Anatolian fault zone are estimated at 0.5-1.5 cm/year from geological data (Tokay, 1973; Seymen, 1975; Barka and Hancock, 1985), and 1-8 cm/yr from seismological results (Brune, 1968; McKenzie, 1972; Canitez, 1973; Toksöz *et al.*, 1979).

Relative motion between the Anatolian Block and the Arabian plate is taken up by the left-lateral East Anatolian fault zone. This fault zone extends from the Karliova triple junction (39.3°N, 41.1°E) at least as far as a point southeast of Kahraman Maras (37.5°N, 36.8°E; "M" in Figure 1). The East Anatolian fault zone is also segmented, with five major segments ranging from 50 to 100 km. The age of the fault is younger than Miocene and the total amount of displacement along the fault has been 22 km (Arpat and Saroglu, 1972, 1975). This implies a geological slip rate along the East Anatolian fault of about 0.4 cm/yr. (see also Dewey *et al.*, 1986). Only one $M > 6.5$ earthquake has occurred during this century along the East Anatolian fault zone (1971 $M=6.7$ Bingöl earthquake, near the northeast end of the fault zone). The focal mechanism for that event was pure left-lateral strike-slip (McKenzie, 1972).

The Eastern Turkey block, a wedge-shaped region located to the east of 39°E, is bounded by the Northeast Anatolian fault to the north and by the North Anatolian fault zone and its eastward extension to the south (see Figure 1). East of 41.5°E this southern boundary is not well-defined by surface morphology or seismological observations (Tchalenko, 1977). The Eastern Turkey block differs from the Anatolian block to the west in that strain is released by internal fault zones (mozaic structure) in the former, whereas in the latter most of the strain

is released along major boundary faults. Internal deformation in the Eastern Turkey block occurs along the following structures: (a) NNE-SSW and/or NE-SW trending left-lateral strike-slip faults, (b) NW-SE trending right-lateral strike-slip faults, (c) E-W trending thrusts and folds, and (d) N-S trending extension cracks (Arpat, 1977; Saroglu and Yilmaz, 1985).

This phase of deformation in the East Turkey block began in Late Miocene time (Sengör *et al.*, 1985). Large earthquakes within the last century in this region have occurred mostly along the strike-slip faults (e.g., Toksöz *et al.*, 1977; Toksöz *et al.*, 1983; Eyidoğan *et al.*, 1986).

REGIONAL DISCUSSION

Four areas will be reviewed in detail in this section using the geometric definitions that are described in Figure 2. The areas are shown in figures 3, 4, 7 and 8 (see Figure 1 for location of these areas). The procedure followed here will be to describe characteristics of individual fault segments which are identified in these figures.

I. NORTH ANATOLIAN FAULT ZONE (Figure 3)

- (1) This segment is roughly 50 km long, and extends from the Karliova triple junction to the stepover separating segments (1) and (2) (see Figure 3A). It has a clear physiographic expression (Allen, 1969), and includes a 16° smooth bend near its west end. The 8/17/49 earthquake ($M=6.7-7$) is associated with this fault segment based on damage reports (Lahn, 1952), on a relocated epicenter (Dewey, 1976) that is only 10 km from the western end of the fault (with epicentral error 10-20 km) and on general agreement between earthquake magnitude and fault length (see, e.g., $\log L = 0.78 M - 3.62$ for the North Anatolian fault system from

Toksöz *et al.*, 1979). The 1946 and 1966 earthquakes ($M = 6$, $M=7$) occurred to the east of the intersection of the North and East Anatolian faults, and are not associated with segment (1).

- (2) This segment is 100 km long, and extends from the restraining stepover that separates it from segment (1) to the Erzincan releasing stepover (segment (3); see Figure 3B). According to Ambraseys (1975) the last large earthquake on this fault segment occurred in 1784. The surface rupture during that earthquake was 90 km long. An $M_s=5.9$ earthquake occurred near the middle of segment (2) in 1967 (Dewey, 1976). It was characterized by pure strike-slip faulting, and produced a surface break approximately 4 km long with a horizontal slip of 20 cm (McKenzie, 1972; Ambraseys, 1975). This is the only segment along the North Anatolian fault zone between Varto (east of segment 1, Figure 3A) and the western end of the Mudurnu valley (western end of segment 10, Figure 4A) that has not experienced a large earthquake during this century. Segment (2) thus appears to be a seismic gap (for further discussion see Barka *et al.*, 1987).
- (3) The Erzincan pull-apart system is 25 km long, and is characterized by a series of en-echelon strike-slip faults and contemporaneous volcanism (Barka and Gülen, 1987). An $M_s=4.8$ earthquake occurred within the pull-apart system on November 18, 1983; its fault plane solution was characterized by ENE-WSW extension (*International Seismological Centre Bulletin*, 1983).
- (4) and (5) Segment (4) is 40 km long, and has clear physiographic features at the surface. It is separated from segment (5) by a 20° sharp bend in the fault zone (Tatar, 1978; Barka and Hancock, 1982). Segment (5) is

320 km long and has only one major discontinuity, a releasing stepover 75 km west of the bend area (Susehri basin; Hempton and Dunn, 1984). The 1939 great Erzincan earthquake ($M=8.0$) produced surface breaks along segments (4) and (5), and some in segment (3) (Pamir and Ketin, 1941). Segment (5) also includes a smooth bend (about 15°) south of Niksar (inset C of Figure 3), and is separated from segment (6) by the Niksar pull-apart basin (e.g., Hampton and Dunn, 1984). The relocated epicenter of the 1939 earthquake (Dewey, 1976) lies near segment (4) only 20 km from the 20° sharp restraining bend separating segments (4) and (5). The error on this relocated epicenter is fairly small (only ± 10 -20 km; Dewey, 1976). According to Riad and Meyers (1985), five of the six reported $M>5$ aftershocks of the 1939 event appear to have occurred in the segment (3)-(4) region, near the pull-apart zone. According to the same catalog, there is some indication, that some aftershocks also occurred near the Niksar releasing stepover separating segments (5) and (6), although epicenters for these aftershocks are not well constrained (see also Barka *et al.*, 1987).

- (6) This segment is 50 km long, and extends from Niksar to the Erbaa basin. It contains a 14° sharp restraining bend north of Erbaa. Pull-apart basins separate segments (5) from (6) and (6) from (7) (south of Niksar and between Erbaa and Tasova; see Figure 3C). Dewey's relocated epicenter for the 1942 earthquake is not well constrained. Isoseismals for this event (Blumenthal, 1943; Pamir and Akyol, 1943) outline a zone of maximum intensity ($I=IX$) along the fault segment that is about 5 km long and centered on the 14° sharp bend north of Erbaa. The rupture zone for this event extended along the full length of segment (6) (Dewey, 1976; Gündoğdu, 1984).

(7) This segment is 250 km long, and extends from northeast of Tasova to north of Kursunlu (Figure 3C, 3D). It has two bends: a smooth bend (about 25°) in the eastern part between Tasova and Kargi, and a sharp bend at 34°E , north of Tosya (about 15°). Three releasing stepovers can be found along the smooth bend. From west to east these are located at Kargi (41.1°N , 34.4°E), with fault separation 1 km; one at 41.1°N , 35.2°E , with fault separation 1.5 km, and at 40.9°N , 36.0°E with separation 1 km. Only the second stepover exhibits a pull-apart morphology (Ladik Lake). Several minor releasing stepovers are located about 25 km west of the sharp bend, in the area just north of Kursunlu-Ilgaz. The westernmost stepover is about 1.5 km wide, and defines the termination of segment 7. The relocated epicenter of the 1943 earthquake ($M = 7.3$) is not well constrained ($\pm 20\text{--}30$ km; Dewey, 1976), but was definitely located near the western end of segment (7) (near Tosya). The area of maximum damage during this event was also Tosya near the 15° restraining sharp bend (Figure 3D). The 1943 earthquake caused surface breaks along the full length of segment (7) (Ketin, 1948, 1969; Ambraseys, 1970). Aftershocks of the 1943 earthquake (Karnik, 1969; magnitudes 4.5–5.0) appear to have occurred near the western end of the fault, although these events have not been relocated.

(8) This segment is about 180 km long, and extends from the area north of Kursunlu (Bayramoren) to Abant Lake (Figures 3D, 4A). The surface rupture of the 1944 earthquake ($M=7.3$) covered this whole segment (Ketin, 1948, 1969; Ambraseys, 1970). The relocated epicenter of the 1944 event (Dewey, 1976) occurred at the east end of segment (8), north of Cerkes. Aftershocks of the 1944 earthquake with magnitude

$M > 5$ were mostly concentrated near the ends of segment 8 (Ambraseys and Zatopek 1969, Dewey 1976) and caused additional damage at Düzce and Gerede, and in the Mudurnu Valley (Ambraseys and Zatopek, 1969; Dewey, 1976; Riad and Meyers, 1985). The area of the 1.5 km releasing stepover that separates segments (7) and (8) just northwest of Kurusunlu has been the site of continuous earthquake activity (small and moderate-sized events), both before and after the 1943 earthquake sequence. A survey conducted by one of the authors of this paper (A. Barka) in the towns of Cerkes, Kursunlu, Ilgaz and Tosya (Figure 3D) indicates that the 1943 earthquake only damaged the region east of Kursunlu, whereas damage from the 1944 earthquake was restricted to areas west of Kursunlu. The town of Kursunlu and surrounding villages were most affected not by the 1943 and 1944 events, but by a $M=6.8$ earthquake that occurred in 1951 along a strike-slip fault parallel to the main trace (Pinar, 1953). This earthquake also caused reactivation of the eastern part of the 1944 rupture zone (Pinar, 1953). Segment 8 is very straight, except for a 7° restraining bend that is located 10 km east of Ismetpasa (40.8° N, 32.6° E; Tokay, 1982). Fault creep activity at Ismetpasa, first recognized by Ambraseys (1970), is about 1 cm/year (Aytun, 1982). Aftershocks of the 1944 earthquake with magnitude $M > 5$ were mostly concentrated near the ends of segment 8 (Riad and Meyer, 1985).

II. MARMARA SEA REGION (FIGURE 4)

A. Onshore areas

(9), (10) and (11) At this point the North Anatolian Fault zone changes character. It is no longer composed of a single main strand as it is to the east, but now divides into several branches (see Figure 4A). Segments 9 and 10 are 45 and 70 km long respectively, and are separated by a restraining double bend. The 1957 earthquake caused surface breaks to occur along most of segment 9. During the 1967 earthquake the westernmost 20 km of segment 9 reruptured in addition to segment 10. Surface displacement on the reruptured fault segment was smaller, however, than that on segment 10 (Ambraseys and Zatopek, 1969). The relocated epicenters for the 1957 and 1967 earthquakes ($M = 7.0$ and 6.8) are both very near the zone of overlap between segments 9 and 10 (Dewey, 1976). The epicentral locations and surface breaks for these events (although the surface breaks are much better documented for the 1967 shock than for the 1957 case; see Ambraseys and Zatopek, 1969; Ambraseys, 1970) suggest that both earthquakes ruptured away from the zone of overlap: 1967 to the west and 1957 to the east. The eastern end of segment 9 corresponds to a directional change in the fault, which is 11° between segments 8 and 9. Observations of slip produced by the 1967 earthquake (Ambraseys and Zatopek, 1969; Ambraseys, 1970) show that in general the ratio of strike-slip to dip-slip motion along the main fault trace decreases towards the west and northwest as the strike of the fault changes. The largest aftershock (1967/7/30; $M=5.6$) of the 1967 earthquake occurred at the west end of segment 10, south of Adapazari. It had a normal faulting focal

mechanism, with extension in a NE-SW direction (McKenzie, 1972). This type of mechanism and the reduced strike-slip to dip-slip ratio at the west end of the fault appear to be caused by the change in trend of the fault segment from NE-SW to WNW-ESE. The appearance of normal faulting west of 30.5°E has been noted by McKenzie (1972, 1978), Evans *et al.*, (1984) and Jackson and McKenzie (1984) as well. The exact location of the 1943/6/20 earthquake ($M = 6.5$, Figure 4A) is not well known. It caused most damage in the towns of Adapazari and Hendek, and its relocated epicenter (Dewey, 1976) lies between those towns as well. It could be related to segment 11, which is active according to field observations by one of the authors (A. Barka), or to the western half of segment 10.

(12) This segment has not experienced any large earthquakes during this century, but it is very distinct morphologically. The NE end of segment 12 splay off clearly from segment 10. About 10 km west of the splay area the fault zone widens and turns into many short subparallel segments as it changes direction towards the SW by 17° . This area of directional change is characterized by an ophiolitic melange (Saroglu and Barka, 1983). In contrast, the main part of segment 12, to the SW of this directional change, is narrower and more distinct. Segment (12) terminates at a releasing stepover near Geyve, that has a pull-apart morphology.

(13) The NW side of the Geyve pull-apart is the NE end of segment 13. This segment passes south of Iznik (Figure 4B), and skirts the southern shore of Lake Iznik. It is not clear whether the fault zone continues west as far as Gemlik or changes direction at Sölöz (Figure 4B). This segment has not experienced a known large earthquake in at least 1000 years

(Sieberg, 1932; Sipahioglu, 1983).

(14) Segment 14 is interpreted as consisting of two parallel ENE-WSW trending segments (Figure 4B), about 4-7 km apart, and about 20 and 35 km long respectively. The onshore portion of the shorter segment is clearly visible at the surface. The offshore portions of both segments are inferred from unpublished seismic reflection data and bathymetry (Personal communication; M.T.A., 1984) and by comparison with a similar geometric fault pattern near Izmit (segments 16a, 16b to be discussed later).

(15) and (16) Segment 15 extends from Sapanca Lake through Gölcük, where it changes direction and continues to the SW (see Figure 4B). This directional change is 20°. Segment 16a is separated from segment 15 by a releasing stepover that is about 4-5 km wide (Izmit Bay). Segment 16b is separated from segment 16a by another releasing stepover, also about 7 km wide. In these three segments the NE-SW trending fault branches are dominated by right-lateral strike-slip motion, whereas the eastern half of segment 15, which trends E-W, has a combination of normal slip and strike-slip motion. This difference is clearly reflected in the morphology of the area. Although historical earthquakes have damaged Izmit and Karamürsel frequently (Sipahioglu, 1983), this region has not experienced a large earthquake during the 20th century. Toksöz *et al.*, (1979) consider this area to be a seismic gap. The most recent notable earthquakes to have affected the segment 15-16 area occurred in 1878 (Izmit-Sapanca Lake region; estimated maximum magnitude 6.7 according to Karnik, 1971) and in 1894 (intensity IX, damaging the area between Izmit and Istanbul; see Eginitis, 1894, 1895). Until now the area extending from Sapanca lake thorough the

Gulf of Izmit has been considered to be a single through-going graben characterized by North-South extension (Sengör *et al.*, 1985; Crampin and Evans, 1986). Aerial photographs and detailed field work by one of the authors (A. Barka) suggest, however, that the three segments (15, 16a, 16b) described here are a preferable interpretation.

- (17) The two NE-SW trending strike-slip faults forming segment 17a (Figure 4B) bound the Yenisehir Basin, which is considered here to be a pull-apart basin from examination of aerial photographs. Segment 17b trends E-W and is dominated by normal faulting, and 17c is a NE-SW trending segment dominated by right-lateral strike-slip motion. The last large earthquakes to occur on these segments were two intensity IX events in 1855 (Sandison, 1855, Sieberg, 1932; Ergin *et al.*, 1967; Soysal *et al.*, 1981; Karnik, 1971). The first event (Feb. 28, 1855) caused damage near segment 17c, whereas the second event (April 11, 1855) produced extensive damage mostly to the north of Bursa, near segment 17b (Sandison, 1855). In segments 17a, 17b and 17c NE-SW trending faults are associated with predominantly strike-slip motion, whereas E-W trending faults exhibit a predominantly normal slip motion that is clearly identifiable in the surface morphology of the region. The extensive damage to the north of Bursa during the April 11, 1855 event is compatible with the north dipping geometry of the E-W trending segment 17b which is clearly reflected by the fault morphology. Segment 17d is composed of poorly-defined NW-SE trending surface breaks characterized by NE-SW extension. The 1964 $M=6.6$ earthquake had a NW-SE trending pure dip-slip mechanism with NE-SW extension (McKenzie, 1972, 1978). Surface ruptures for this earthquake, as mapped by Erentöz and Kurtman (1964) and by Ketin (1966), confirm the exten-

sional nature of this segment. Dewey's (1976) relocated epicenter for the 1964 event is well constrained and lies only about 15 km north of the mapped surface breaks.

(18) This segment is composed of two strands. The first strand has an onshore portion that is morphologically distinct. The offshore portion of both strands is inferred from the shape of Bandirma Bay, from bathymetric observations and by comparison with the interpreted geometry of segments 14 and 16 (Figure 4B). This segment has not experienced an earthquake with intensity larger than VII in the last 1400 years; the area was last seriously damaged by an earthquake in 543 (Sieberg, 1932; Soysal *et al.*, 1981).

(19) This segment has not experienced any known earthquakes historically, but that may be due to the fact that the area is sparsely populated. Segment 19 is very clear in aerial photographs. It can also be seen on LANDSAT images (McKenzie, 1978). Segment (19) has a sharp restraining bend in its central part (17-18°) and a classic pull-apart basin (containing the village Asagiinova, which means "descending into a plain") at location x in Figure 4c.

(20) This segment is composed of two parallel faults with a central bend (15-20°), and has been studied by Herekeci (personal communication, 1983). No earthquakes have been reported historically for this segment. The southwest extension of segments (18) - (20) has not been studied so far. Further work is necessary to determine whether this fault zone extends as far as the Aegean Sea.

(21) The Yenice-Gönen segment experienced a magnitude 7.2 right-lateral strike-slip earthquake in 1953 (McKenzie, 1972, Dewey, 1976). The

mapped surface break for this event was 50 km long (Ketin and Roesli, 1953). No previous historical activity has been recorded for this segment. The morphological expression of segment 21 is not as clear as that of segment 19. Segment 21 includes a restraining double bend with a bend angle of 17° .

- (22) This segment has a 14° restraining bend in the central part and a 5 km restraining stepover at its eastern end which creates the Ganos mountains ("GM" in Figure 4D). The 1912 $M = 7.3$ earthquake produced surface rupture along most of segment 22 (Macovei 1912, Karnik 1971, Tabban and Ates 1976). The eastern and western end of the segment joins the western Marmara basin and Saros basin (Lyberis 1984; Le Pichon *et al.*, 1984) which are both interpreted here as pull-apart basins.

B. Offshore areas

The Marmara Sea is composed of a series of basins and ridges that are discontinuous in nature. Our interpretation of the distribution of active fault segments beneath the Marmara Sea is shown in Figure 5. This interpretation is much less well constrained than that in the onshore areas. It is put forward here in an attempt to provide a comprehensive model of active fault trends in northwestern Turkey. The deepest part of the sea is the northern half. Basins A, B and C are approximately 1100, 1355 and 1225 meters deep respectively. The depths of intervening ridges are 700 m between A and B, and 450 m between B and C (Pfannenstiel, 1944). The northern half of the Marmara Sea is interpreted as a large pull-apart basin between segments 16 and 22 (Figure 4). This basin is subdivided into smaller basins (A, B, C) separated by strike-slip fault segments trending NE-SW. The southern half of the Marmara Sea is shallower than 100 m,

but can also be divided into ridges and basins which are visible on reflection profiles (Marathon, 1974). A reexamination of these profiles suggests that the size of these structures and the amount of offset along bounding faults are smaller in the southern half of the Marmara Sea than in the northern half. The interpretation shown in Figure 5 results from an extrapolation of onshore fault geometry, from bathymetry and from examination of seismic reflection profiles.

This interpretation is different from previous ones in the area. It is based on the onshore results described above. In Figure 6 four other interpretations are shown. In Figure 6B, Pinar (1943) correctly identifies faults south of the Marmara sea (including segment 21, that would later rupture in 1953), but simply draws a line through the Marmara Sea basins, interpreting their origin as tectonic. In Figure 6C, Pfannenstiel (1944) describes the northern ridges and basins as normal fault-bounded horsts and grabens, and suggests that the basins are connected by NE-SW trending faults. In Figure 6D, Sengör (1986) includes basins C and A (as labeled in Figure 5), and connects them with a suspected fault. In Figure 6E, Crampin and Evans (1986) consider the Marmara Sea to be one long E-W trending graben. Figure 6A is our interpretation for comparison. This model is by no means finalized. Future work needs to be done in the offshore areas.

Historical earthquake activity in the Marmara Sea region indicates that the fault system in the northern half of the sea is more active than in the southern half. Istanbul, on the North Shore, has been repeatedly affected by damaging ($I > VIII$) earthquakes throughout the historical record (about 2000 years, see e.g. Ambraseys, 1971; Soysal *et al.*, 1981), whereas Bandırma, Bursa and Iznik, along the south shore, have been damaged much less frequently (Sipahioglu, 1983). The area of maximum damage cause by the 1894 Istanbul earthquake ($I = IX$; see Eginitis, 1894, 1895), coincides with two major strike-slip fault segments, 16a and 16b. The size of the earthquake and the combined

length of the fault segments are quite comparable. The only focal mechanism available from the northern half of the Marmara Sea is that of the 1963 earthquake located near basin C (see Figure 5), which is characterized by NNE-SSW extension (McKenzie, 1972).

Microseismicity in the Marmara Sea region (both onshore and offshore), recorded during the past 10 years, exhibits a swarm-like character (Ucer *et al.*, 1985) with swarms concentrated mostly near our inferred pull-apart basins, and also near normal faults that have a strike-slip component (e.g., segments 17b and 15).

III. EAST ANATOLIAN FAULT ZONE (Figure 7)

This fault zone is about 450 km long, and extends from the Karliova triple junction at the northeast end to Turkoglu at the southwest end where it intersects with the Dead Sea transform (see Figure 7). The East Anatolian fault has not been very active during this century, as will be seen below. We feel that it is important to review the fault geometry anyway, because the fault zone has experienced intensity \geq VIII earthquakes historically. Most of these events occurred within the first 1000 years A.D. (Ambraseys, 1970). Some earthquakes caused damage in towns along the fault zone after 1000 A.D. (Soysal *et al.*, 1981). These were mostly concentrated near the NE and SW ends of the fault zone, but cannot be tied to specific segments. Nevertheless the presence of historical earthquake activity and the clear physiographic expression of the East Anatolian fault zone are good reasons for a detailed examination of fault geometry in this area. The fault zone can be divided into 7 segments, which are generally shorter than those on the North Anatolian fault.

- (1) This segment extends from the Karliova triple junction to Bingöl (Figure 7).

It is about 60 km long and is composed of many closely-spaced parallel

strike-slip fault strands. A detailed map of these fault traces is provided by Arpat and Saroglu (1972). The 1971 Bingöl earthquake ($M = 6.7$) produced surface breaks along the southwestern half of segment 1 (Seymen and Aydin, 1972; Arpat and Saroglu, 1972). The relocated epicenter for the 1971 earthquake is at the southwestern end of the surface breaks (Dewey, 1978). Two historical earthquakes of a similar size have been documented for the area of this segment (1789 and 1875; exact location not known; see Soysal *et al.*, 1981).

- (2) This area is not really a segment, but can be better described as a deformed region that separates segments (1) and (3). It is a restraining area characterized by compressional features (east-west trending folds and thrusts; Arpat and Saroglu, 1972), which are also expressed topographically. This area has been subjected to an unusually large concentration of moderate-sized earthquakes over the last century (see, e.g., Tabban, 1980; Ercan, 1982; Riad and Meyers, 1985).
- (3) This segment is about 100 km long. There is a directional change of at least 19° between segments (1) and (3). Between Gökdere and Genc the northeastern end of the fault segment is oriented E-W and is characterized mostly by thrust faulting that is a continuation of the Mus-Van thrust system (that runs into the western end of Lake Van at the bottom of the inset map in Figure 8). The 19° change mentioned above excludes this portion of segment (3). The main part of segment (3), to the southwest, is fairly straight. Hazar Lake, located near the middle of the segment, has been described as a pull-apart basin (Hempton, 1984; Hempton and Dunne, 1984). The separation between the parallel fault segments at this location is less than 2 km. The southwestern end of segment (3) is located north of Keferdiz. The last destructive

earthquake along segment 3 occurred in 995 AD (Ambraseys, 1970). This earthquake damaged towns all along segment 3, and had a particularly destructive effect on the area between Palu and Gökdere (bend area), where streams were diverted (Ambraseys, 1970). Within this century a number of moderate-sized earthquakes have affected segment (3), particularly since about 1948 (e.g., Tabban, 1980).

- (4) This segment is about 50 km long, and is centered north of Pötürge (Figure 7B). The northeast end of the segment, near Keferdiz, is a 17° restraining bend. The historical site of Claudius (coinciding approximately with Keferdiz) experienced at least four damaging earthquakes in the period 10-1000AD (Ambraseys, 1970), but the exact location of these events relative to segment (4) is unknown. Since that time segment (4) has been relatively quiet.
- (5) This segment is about 90 km long. It is separated at its northeast end from segment 4 by a small releasing stepover, and at its southwest end from segment (6) by a small restraining stepover. The central part of segment (5), near Celikhan, is characterized by a number of anomalous features. These include a 7.5 km wide restraining stepover east of Celikhan, a restraining bend and an east-west trending splay off the main fault (the Sürgü fault, interpreted here as a P-shear fault. The restraining area which includes the restraining bend and stepover, is characterized by E-W trending folds and thrusts. These folds and thrusts can be traced eastward to the main Bitlis frontal thrust system (see Figure 1). A moderate sized earthquake (6/14/64, $M = 5.9$, Jackson and McKenzie, 1984) was relocated by Dewey (1976) within the restraining area. Its focal mechanism was characterized by east-west extension. A pair of moderate-sized earthquakes occurred recently in

this area (May 5, 1986, $M_s = 5.9$; June 8, 1986, $M_s = 5.6$). The first event was located on the Sürgü fault splay (see, e.g., Erdik, 1986). Its focal mechanism indicates NE-SW compression, resulting in a combination of thrusting and left-lateral strike-slip faulting on a north-dipping fault (based on Harvard moment tensor solution in U.S. Geological Survey Earthquake Data Report). The second event had a pure strike-slip mechanism (from Harvard moment tensor solution in U.S. Geological Survey Earthquake Data Report) that was consistent with left-lateral slip on the East Anatolian fault near the Surgü fault splay.

- (6) This segment is about 50 km long, and represents a 13 km wide releasing stepover. It has a R-shear characteristics. Fault segment (6) makes an angle of about 18° with the main trace. The segment is divided into two main strands, which are separated from each other by a series of lakes, near Gölbaşı, suggesting a pull-apart geometry. There are no damaging earthquakes on segment (6) in the historical record.
- (7) We are defining segment (7) to extend over a minimum distance of 55 km, from Tetirlik to the Türkoglu triple junction. This segment has been mapped by Yalcin (1978). The East Anatolian fault continues towards the southwest beyond its intersection with the Dead Sea fault. When it reaches the NE end of the Adana basin, the East Anatolian fault changes direction towards the SW, where it becomes the Yumurtalik fault (Figure 1; Ketin, 1948; McKenzie, 1978; Sengör *et al.*, 1985). Segment (7) contains a small double bend (Figure 7D: (a), (b)). The portion of segment (7) that lies between (a) and (b) makes an angle of 18° with the fault trace on either side, is characterized by P-shear, and acts as a 1.5 km wide restraining area. Several moderate-sized earthquakes have occurred in the segment 7 area during this century, as

defined by damage at or near the nearby town of K. Maras; (Tabban, 1980; Ercan, 1982). The last seriously damaging earthquakes near Maras-Ceyhan occurred in 1114-1115 (Sieberg, 1932; Salomon-Calvi, 1941; Soysal *et al.*, 1981), but descriptions of damage are not detailed enough to assign these events to a specific fault segment.

The East Anatolian fault zone is different in some respects from the North Anatolian fault zone. The two main differences are: (1) the maximum segment length on the East Anatolian fault is less than 100 km (by comparison with more than 300 km on the North Anatolian fault); and (2) the East Anatolian fault zone contains more restraining stepovers and bends than the NAF zone. As a result we might expect the two fault zones to behave differently. However, although the total displacement along the two fault zones has been comparable over the last 5 MY, we cannot determine the following from available data. (1) How long will the decreased rate of earthquake activity that has characterized the EAF zone since 1000 A.D. continue? (2) Does strain accumulate continuously along the fault zone or episodically (i.e., what stress drops and recurrence times can we expect for this zone)?

IV. NORTHEASTERN TURKEY BLOCK (Figure 8)

We shall restrict our attention in this area to strike-slip faults, although not all of these strike-slip fault segments have experienced large earthquakes during this century.

Horasan-Narman fault zone (Figure 8A)

This strike-slip fault zone is about 50 km long, and is characterized by left-lateral strike-slip motion. At the surface the fault zone is divided into many short parallel segments, forming a shear zone that is about 5 km wide. This shear zone is comprised of an ophiolitic melange (Barka *et al.*, 1983; Saroglu

and Barka, 1983). An abrupt change in strike (about 15° - 18°) occurs NNW of Horasan. On 10/30/83 a magnitude 6.9 earthquake occurred along this fault zone, north of the bend. Both surface breaks and the highest intensities produced by this event were located within 20 km and northeast of the bend (Barka *et al.*, 1983). More than 3000 aftershocks were recorded during a portable network survey in the epicentral area (Toksöz *et al.*, 1983; Eyidoğan *et al.*, 1986). The aftershocks were clustered near the zone of highest intensity during the first month, and then migrated away from the bend. Most of the aftershock migration was to the northeast along the fault zone, although some aftershocks were recorded southwest of the bend and on either side of the main fault zone. Although the 1983 earthquake had a focal mechanism that was predominantly left-lateral strike-slip with a small thrust component (Eyidoğan *et al.*, 1986), the continuation of the fault zone southwest of the bend could be expected to rupture (in the future) with a higher component of thrusting.

Caldiran fault (Figure 8B)

This fault is approximately 50 km long, and contains a 17° - 19° bend near Caldiran. The 1976 Caldiran earthquake ($M = 7.3$) ruptured the fault bilaterally starting from the bend, according to seismic waveform modeling (surface and body waves; see King and Nabelek, 1985).

Balıkgözü fault (Figure 9C)

This fault zone is about 80 km long in Turkey, and extends into Iran where it is called the Northwest Fault System (Tchalenko, 1977). The Turkish section has been mapped in detail by Arpat (1977). It consists of many small subparallel segments, some of which may combine at depth. The northwestern section is divided into 2 branches with an angular separation of about 35° . This geometry creates a releasing area, a "negative flower structure" (Harding, 1985), charac-

terized by an abundance of N-S trending normal faults and the presence of a lake. Southeast of that area the two branches converge, and the motion on the fault has a larger strike-slip component. A short segment near Dogubeyazit is separated from the main fault strand. It is bounded by a releasing stepover at one end and a restraining stepover at the other end. According to Ambraseys and Melville (1982) an earthquake of intensity IX (known as the "Ararat earthquake") occurred on the Turkish part of the Balıkgölü fault in 1840.

Tutak and Karayazi faults (Figure 8D)

The Tutak fault is about 95 km long and has been mapped by Saroglu and Güner (1979). It includes a 19° bend near Mizrak. Northwest of that bend the fault segment is parallel to the Karayazi fault (mapped by Kocyigit, 1985) and the area between the parallel segments is a 16 km wide restraining stepover. Southeast of the bend the Tutak fault is not represented by a continuous surface trace. In the middle of that southeast segment in particular, the fault is broken up into short discontinuous pieces. Saroglu and Güner (1979) assume that the Tutak fault is active, based on a fault morphology which is very similar to that of the Caldiran fault and on the existence of many relics of destroyed sites. However, details of these historical events are not well known. Both the Tutak and Karayazi faults are clearly visible in aerial photographs.

Erzurum fault zone (Figure 8E)

This is a 5-10 km wide left-lateral shear zone. Its southern end truncates a series of ENE-WSW trending thrust faults. Near its northern end the Erzurum fault zone changes direction abruptly (a 30° restraining bend). Immediately northeast of that bend the fault zone still has a predominantly strike-slip character, distinctly different from the southwest trending thrust faults south of Erzurum. The town of Erzurum has experienced several earthquakes histori-

cally. Records of activity go back as far as 1200 AD, with a notable event occurring in 1482 (30,000 people killed) and 1859 (heavy damage in the vicinity of Erzurum) and many moderate-sized earthquakes listed for the 18th and 19th centuries (Sipahioglu, 1983). We do not have enough information to associate the historical earthquakes with particular fault segments. However, both the left-lateral strike-slip fault and southern thrust appear to be active, as evidenced by displaced streams and other morphological features (Barka *et al.*, 1983; Saroglu, 1985; Kocyigit *et al.*, 1985).

DISCUSSION AND INTERPRETATION

The relationship between fault segment geometry and strike-slip earthquake rupture zones is described in a series of schematic diagrams shown in Figures 9 and 10. Figure 9 contains examples of fault segments that have already ruptured. Most of the examples in that figure are from Turkey, and have been described in detail in the regional discussion. Some examples are taken from the Western U.S., Japan and China for comparison. Figure 10 shows fault segments that have not yet ruptured. The examples in Figure 10 have geometries similar to those observed in the already ruptured cases, and might therefore be expected to have predictable rupture characteristics. This figure is intended to be used as a guide, and not for prediction purposes. Further detailed study of the examples is necessary. Individual examples in Figures 9 and 10 are mostly self-explanatory. They can be grouped, however, to match up with the categories shown in Figure 2. The following description of segment characteristics covers stepovers, bends, double bends and combinations, as defined in Figure 2. Most of the examples shown in Figures 9 and 10 belong to the combinations category which includes double bends, as summarized in Table 1. Geological effects such as rock type and preexisting structures influence the rupture characteristics of strike-slip earthquakes in addition to fault geometry.

Some of the geological effects will be discussed briefly at the end of this section.

Characteristics of Stepoverters

It appears that the segmentation of the fault zones and the extent of fault rupture are controlled mostly by the distribution of stepovers, and sometimes by bends. The type and width of each stepover are clearly important factors in determining whether a segment ends at that location.

Two types of stepover are assumed to exist in cross-section. The first type involves a "flower-like structure" (Bakun *et al.*, 1980; Segall and Pollard, 1980; Harding, 1985; Naylor *et al.*, 1986). In this case the stepover does not extend through the whole crust. The segments separated by the stepover are connected at depth (see Figure 2, Da and Db). Many sag ponds and pressure ridges may overly these flower structures. The maximum width of this type of stepover can reach 10 km. This width may be controlled by the thickness and rheology of the brittle-ductile zone at the top of the upper crust (see King, 1986). A single earthquake rupture may propagate through this type of stepover. The second type of stepover extends through the whole crust, thus really separating two different fault segments (Figure 2, Dc). This type may be characteristic of a more brittle upper crust. It can be as narrow as 1 km. The character of the earthquakes may be variable, both from one segment to the next across a stepover, and in the stepover region itself (characteristic size, focal mechanism, etc.). This second type of stepover is more likely to control fault segmentation than the first type. From surface observations alone we cannot distinguish between the two stepover types.

Both releasing and restraining stepovers can cause segmentation, but for different physical reasons. Although an extensional component along a strike-slip fault should facilitate rupture propagation, releasing stepovers have been observed to block or delay rupture in some cases. Three examples of this are

the Nixsar pull-apart basin (1939 earthquake; segment 5 of the NAF, Fig. 9b, c) the Salton Sea (1979 Imperial Valley earthquake, Fig. 9q) and the Cholame Valley (1968 Parkfield earthquake, Fig. 9l). In the two California cases aftershocks were clustered in the pull-apart area (aftershock locations in the 1939 Turkish case are not as well determined). The releasing stepover areas may absorb some of the rupture propagation energy along extensional faults, such that less energy is transferred to the next segment. Sibson (1986) suggested that fluid pressure in the releasing stepover areas may play a barrier-type role.

Restraining stepovers may act as resistant areas through which little or no motion is transferred to the next segment. This appears to be the case for some of the larger (wider than 1 km) stepovers that do not extend all the way through the crust (segments join at depth) and for stepovers that do extend all the way through the crust (those with width less than a few km). Although either releasing or restraining stepovers can cause segmentation, the stepover width required to stop the propagation of an earthquake rupture may be larger for releasing than for restraining stepovers.

Restraining stepovers can be sites of enhanced strain accumulation. If a stepover is narrow, a single earthquake can rupture both segments and the stepover in between. A good example of this is the Borrego Mountain earthquake (Figure 9u). On the other hand, if the stepover is wide, separate earthquakes may occur. For example in the Songpan, China earthquake sequence (Fig. 9v, Jones *et al.*, 1984) three separate mainshocks ($M = 7.2$, 6.7, and 7.2) occurred within a week: the first and third events on strike-slip fault segments, and the second event on the 12 km wide intervening stepover (a reverse fault).

Characteristics of Bends

From the observations made in this study, the maximum angle of bend between two strike slip fault segments is $\sim 30^\circ$. This angle coincides with the

angles that P and R shear directions make with the direction of simple shear in strain slip diagrams (e.g., Tchalenko and Ambraseys, 1970; Wilcox *et al.*, 1973; Bartlett *et al.*, 1981; Hancock, 1985; Naylor *et al.*, 1986). The bends can be either restraining or releasing (Figure 2). Whether a bend occurs within a single segment or separates two different segments depends not only on the bend angle α between the two segments, but also on the orientation β of the direction of block motion relative to the segments (see also Bilham and Hurst, 1986). These relationships are shown in Figure 11. Variations in the relative size and orientation of β relative to α lead to the following situations (Figure 11 single bend case):

- a) $\beta > \alpha$. In this case both L_1 and L_2 have a thrust component, but there is a larger thrust component on L_2 than on L_1 . In this case we expect two separate earthquakes. Rupture could be stopped or initiated by the bend area. Due to the smaller thrust component on L_1 , this is the segment that would probably rupture first. Two examples of this situation can be seen in Turkey. In the case of the 1983 Horasan-Narman earthquake (see Figures 8a and 9i), the epicenter was located near the bend. The surface breaks and most of the aftershocks for this event were located along L_1 . L_2 has not ruptured yet. In the case of the 1944 Gerede-Cerkes and 1957 Abant earthquakes (Figures 4a and 9d, e), both epicenters were located away from the common bend area, but ruptures both propagated towards and stopped at the bend.
- b) $\alpha \geq \beta$ and $\beta > 0$. In this case we expect a single earthquake to rupture both segments. The epicenter may occur at or near the bend, and rupture may propagate bilaterally away from the bend. Examples of this situation are provided by the earthquakes in Figure 12. The amount of coseismic slip that occurs on either side of the bend may not be the

same. For example in the Caldiran 1976 earthquake (Figure 8b, 9g) the coseismic slip on the fault segment west of the bend (restraining segment) was higher than on the eastern side (Saroglu and Erdogan, 1983).

- c) $\beta \leq 0$ and $\alpha \geq |\beta|$. In this case we can have either pure strike-slip movement on L_2 and an extension component on L_1 , or both segments may have an extension component. Either way, L_1 has a larger extension component than L_2 . L_2 probably ruptures before L_1 , but we expect more continuous background seismicity on L_1 than on L_2 . An example of this situation is provided by the 1855 Bursa earthquakes (Figures 4c and 9h). The first event occurred on L_2 . L_1 ruptured six weeks later. It is likely that the epicenter for the L_2 rupture is located near the bend, but we do not have good constraints on epicentral locations.
- d) Block rotation. In this case the slip vector is parallel to both L_1 and L_2 . This can happen over long distances. For example a counter-clockwise rotation of the Anatolian block along the North Anatolian fault can be interpreted from focal mechanisms along the length of the fault (e.g., McKenzie, 1972; Jackson and McKenzie, 1984). The block rotation case is characterized by smooth bends over long distances (e.g., the 1976 Guatemala earthquake; Kanamori and Stewart, 1978). These bends do not cause segmentation even though α and β are related as in case (b) above, perhaps because the bends are not sharp enough to cause a high stress concentration.

Characteristics of bend-steppover combinations

(1) Double bends

One of the most commonly observed combination forms is the double bend situation (Table 1, Figure 2-Cd). By double bend we mean two separated en echelon fault segments (L_1 and L_3) connected by an intervening segment L_2 . Dominant motion along L_1 and L_3 is strike-slip. Thus the bend angle α between L_1 and L_2 or between L_2 and L_3 is again less than 30° , as in the single bend case. The two bend angles, α_{12} and α_{23} , can be different (see Figure 11, double bend case). The angle β of the direction of block motion must be considered here as well. The double bends observed in this study all fall into the $\alpha \geq \beta, \beta > 0$ category. The $\alpha > 30^\circ$ case corresponds to releasing or restraining stepovers. In that case the width d of the stepover is important.

(2) Other combinations

The second most commonly observed type of bend-steppover combination is the restraining bend with adjacent releasing stepover (see Table 1 and Figure 2-Ce). In this case it appears that the earthquake rupture generally stops at the releasing stepover, even though the stepover width can be quite small (e.g., 1 km). To understand why the rupture is arrested at the stepover location it is necessary to have three-dimensional information on the stepover geometry (as illustrated in the cross-sectional views of Figure 2D).

Two other bend-steppovers combination patterns (Figures 2 Cf, 2Cg, 2Cj) are quite similar to the commonly observed Figure 2Ce type. However, these three patterns are not observed as often, and well-documented ruptures in category 2Cf have not yet occurred. Note the difference between 2Cf and 2Cj: in 2Cf the stepover is on the restraining side of the bend, whereas in 2Cj the stepover is on the releasing side of the bend. Most of the other bend-steppover combinations in

Figure 2 include stepovers in the bend area(cases Ca,Cb, Ch, Ci).

Effects of segmentation on the dynamics of earthquake rupture.

Certain specific factors are influential in determining whether geometric discontinuities cause segmentation within a fault zone. These factors include the bend angle (α), the direction of block motion (β), the length of the restraining fault branch (L_2) for the single or double bend cases (see Figure 11), and the stepover width (d). Usually these factors are not isolated, but contribute to the behavior of the fault zone in various combined forms. It is therefore difficult to make generalizations covering all of the categories in Figure 2. Certain fault segment behavioral patterns have emerged from the observations, however, and will be described below.

(1) Restraining segment geometry versus magnitude

We have compared the single restraining bend-single rupture case ($\alpha \geq \beta, \beta > 0$) and the double restraining bend situation, as shown at the top of Figure 13 (numerical values included in Table 2). In both cases the geometry of the bend area can be correlated with earthquake magnitude. Specifically $\log(\alpha L_2)$ is linearly related to magnitude, as can be seen in Figure 13a.

The points plotted in Figure 13a correspond to earthquakes in Figure 9 (a, b, c, d, e, f, g, k, l, m, n, o, p, q, r and s), with the following exceptions. In the case of the 1857 earthquake, the values are as in Figure 9, but it should be noted that the restraining bend angle is 34° (the larger angle). Although this is larger than the 30° considered to be the maximum angle, β is interpreted as being smaller than α by at least $5-6^\circ$. For the 1943 Tosya earthquake case, L_2 is taken to be 25 km rather than 65 km because a series of releasing stepovers can be found 25 km from the bend. Although the earthquake ruptured through these stepovers, it seems that the portion of the fault beyond the stepovers did

not play a restraining role (the same situation characterizes the 1939 earthquake). In the 1966 Parkfield case we plotted the $M_L = 5.1$ foreshock that occurred at the restraining bend rather than the mainshock, which occurred south of the bend and may have been triggered by the foreshock (Lindh and Boore, 1981). We also included the 1973 Luhuo, China earthquake (Zhou *et al.*, 1983), a single restraining bend earthquake.

We interpret the relationship shown in Figure 13a in the following way. As α increases, the effective normal stress on L_2 increases (see e.g., Bott, 1959; Donath, 1981; Angelier, 1984; and Mohr's circle representation in Figure 7.35 of Hobbs *et al.*, 1976). This normal stress increase is accompanied by a shear stress increase. L_2 can thus be associated with earthquakes of greater stress drop for a given fault area (see Scholz *et al.*, 1972; Scholz, 1977), i.e., greater displacement and therefore greater moment and magnitude. The angle α does not increase indefinitely. Beyond $\alpha = 30^\circ$, as we saw earlier, single throughgoing earthquakes do not occur easily in the bend area. This limit is in general agreement with laboratory results (see Nur *et al.*, 1986, Naylor *et al.*, 1986).

Note that the area of the L_2 branch can also increase if the dip of that branch decreases from vertical (e.g. Rickard 1972). This would be caused for example by an increase in α , due to an increase in the thrusting component on that fault branch. Thus an increase in α can cause not only an increase in displacement, as seen above, but also an increase in area. Both of these effects would contribute to a larger moment, or earthquake magnitude.

Previous studies have related earthquake magnitude to $\log L$, where L is the overall fault length (see, e.g., Slemmons, 1977; Toksöz *et al.*, 1979). In Figure 13b we compare $\log L$ with M_s for the same data as shown in Figure 13a. The only point from Figure 13a that has not been plotted in Figure 13b is the Parkfield foreshock, for which we do not know L . The points in Figure 13b show

more scatter than those in 13a. This scatter can be seen more quantitatively by performing a linear regression (see Table 2; correlation coefficients of 0.70 and 0.87 respectively). In Figure 13c, a comparison of $\log(\alpha L_2)$ and $\log L$ still shows scatter. This scatter is reduced in Figure 13d by adding a fault displacement factor u . The parameter $\log(uL)$ can be related to $\log(\text{moment})$ or to magnitude. Thus the correlation shown in Figure 13d agrees with that of 13a. From Figure 13a we conclude that, for the fault geometries considered here, we can estimate an earthquake magnitude by simply measuring α and L_2 . From Figure 13d, we can determine possible combinations of u and L by knowing α and L_2 . If, in addition, we know L (for example if fault segmentation is defined by additional geometric discontinuities, we can estimate u as well. Note that Figure 13 only refers to one type of geometry and resulting fault behavior. Other geometric patterns have to be treated individually.

There are observations in a few cases to suggest that the area of maximum observed intensity and/or maximum fault displacement (total surface displacement, including strike-slip and thrust components) coincides with the L_2 branch. A good maximum intensity example is the 1943 Tosya earthquake (segment 7 of the NAF), which damaged the towns of Tosya and Ilgaz much more than any other town along segment 7. The L_2 branch for this earthquake coincides with the highest topography within a 200 km radius. In the 1967 Mudurnu Valley earthquake (segment 10 of the NAF) the highest intensities occurred in the L_2 and L_3 area (according to isoseismal contours from Ohashi and Ohta, 1983). Maximum measured fault displacement at the surface occurred on the L_2 branch, although it was almost as high on L_3 (Ambraseys, 1970). In the 1976 Caldiran earthquake maximum measured displacement occurred on L_2 (e.g., Toksöz *et al.*, 1977; Saroglu and Erdogan, 1983).

Maximum fault displacement is not always coincident with L_2 , however. The 1857 California earthquake had a larger horizontal displacement on the L_3

branch (Carrizo Plain area) than L_2 (Sieh, 1978), but vertical displacements need to be considered as well. In the case of the 1906 California earthquake there was a higher displacement on L_3 than on L_2 (Lawson *et al.*, 1908; Sieh, 1978). There may have been an additional complication there in that the L_2 branch was a region of overlap between the 1906 and 1838 earthquakes (Loudenback, 1947).

In the 1966 Parkfield situation it would appear from field observations that most surface displacement occurred on L_1 (" L_0 " in Figure 9l; see Lindh and Boore, 1981). However the Parkfield case can be interpreted as follows. An $M_L = 5.1$ foreshock occurred in the restraining bend area 17 minutes before the mainshock (McEvilly *et al.*, 1967). The magnitude and location of this foreshock suggest that it was caused by strain accumulation along the restraining L_2 segment (it agrees with the data plotted in Figure 13a). The mainshock would then have been triggered by the foreshock and would have ruptured the L_1 segment of the fault. It appears therefore that the mainshock cannot be directly related to the restraining bend, because L_1 is too long relative to L_2 . Instead it is triggered by an earthquake at the restraining bend.

More complete three-dimensional data from California suggest that the maximum dislocation on the fault occurs on the L_2 branch. During the 1979 Imperial Valley earthquake, simultaneous inversion of local strong ground motions and teleseismic body waves (Hartzell and Heaton, 1983) shows that the maximum dislocation occurred between Interstate 8 and the El Centro Array (see also modeling of geodetic and seismological data by Slade *et al.*, 1984). This corresponds to the L_2 segment of the double bend in Figure 9q. During the 1984 Morgan Hill earthquake, the maximum dislocation occurred under Anderson Reservoir (Hartzell and Heaton, 1986), which corresponds again to segment L_2 (Figure 9s).

(2) Restraining segment geometry versus epicenter location

An interesting question to ask at this point is where the mainshock epicenters are located relative to discontinuities in the fault geometry. We have considered two cases. First, most of our data pertain to single rupture earthquakes on segments containing restraining stepovers, restraining bends or restraining double bends. We shall examine epicenter locations for single rupture cases in which the epicenter is well constrained, both in Turkey and elsewhere. Second, we shall consider multiple shock cases, in which separate earthquakes occur on each portion of the fault segment, separated by geometric discontinuities.

There are two examples of well-constrained epicenters for single rupture earthquakes in Turkey. The 1976 Caldiran earthquake epicenter was located very close to the bend between L_1 and L_2 , and the earthquake ruptured bilaterally (Figure 9g), from inversion of teleseismic body waves (King and Nabelek, 1985). The 1939 Erzincan earthquake had an epicenter near the bend (the accuracy of the location is not ideal, but adequate here because the fault was very long; see Figure 9b), and ruptured bilaterally. Other Turkish earthquakes (1942, 1943, 1967 Fig. 9c, d, e) had epicenters close to restraining bends, but the resolution of these locations relative to the length of the surface fault trace is not sufficient for a detailed comparison of epicenter with fault geometry. In both of the better constrained cases the epicenter was located near the bend, and rupture took place away from the bend.

Additional information can be obtained from earthquakes outside Turkey. The 1968 Parkfield earthquake (Fig. 9l, e.g., Brown *et al.*, 1967; Bakun and Lindh, 1985) and the 1975 Tangshan earthquake (Fig. 9k, King and Nabelek, 1985) had epicenters near a bend in the fault. The Parkfield earthquake ruptured away from the restraining segment (King and Nabelek, 1985; Figure 9l). The

Tangshan, China earthquake had a clear bilateral rupture (King and Nabelek, 1985; Figure 9k). In neither case was the epicenter within the restraining L_2 segment. The 1988 Borrego Mountain earthquake had an epicenter outside the restraining stepover (Figure 9u). The 1979 Imperial Valley, 1979 Coyote Lake and 1984 Morgan Hill earthquakes all had epicenters located away from the restraining L_2 segment (see Figures 9q, 9r and 9s). The pattern that emerges in the single earthquake rupture case is as follows. The epicenter occurs either at the bend or on the L_1 or L_3 segment (as defined in Figures 11 and 13). It does not occur within the restraining area (either segment L_2 in Figures 11 and 13 or the restraining stepover area).

Some of the restraining double bend segments in our study have a greater angle of bend on one side than on the other. This applies, for example, to the 1857 and 1906 California earthquakes (Fig. 9n, o; see Reid, 1908 and Sieh, 1978). If the whole fault segment in this situation is subject to the same stress level, it is easier for rupture to initiate on the segment (L_1 or L_3) that is closest to the bend of greater angle (L_3 at the bottom of Figure 11). This assumption is based on the fact that the segment (L_1 or L_3) closest to the bend of greater angle has a larger extensional component of slip than the other segments. We do not have well-determined epicenter locations for documentation of this situation.

In the multiple earthquake situation it is possible to get an epicenter within the restraining area. Two examples of this are the 1976 Songpan, China earthquakes (Jones *et al.*, 1984; see Figure 9v) and the earthquake sequence on the Main Recent Fault, in Iran (Tchalenko and Brand, 1974; see Figure 9t). In both of these cases the fault geometry may not have satisfied the requirements of a single strike-slip rupture. In the first case the stepover width was too high (12 km). Pure thrusting characterized the earthquake within the restraining segment. In the second case L_2 was excessively long (or $\log(\alpha L_2)$ was too high, so that it may have been difficult to accumulate enough strain on L_2 for a single

earthquake rupture. Two possible additional candidates for epicenters along the restraining segment emerge from this study. Both the 1971 Bingöl earthquake (East Anatolian fault; Figure 9x) and the 1983 Horasan-Narman earthquake (Figure 9i) had epicenters close to the bend between L_1 and L_2 , and ruptured away from L_2 . It is possible that a second earthquake would occur within the L_2 restraining segment area. Alternatively, in both these cases, a larger earthquake could have an epicenter coinciding with the previous epicenter, and rupture both segments L_1 and L_2 . Note that in the 1971 earthquake situation the combination of restraining stepover and restraining bend (Figure 9x) decreases the likelihood of having a single rupture on L_1 and L_2 over what it would be for a simple restraining bend.

(3) Releasing stepovers and bends versus aftershock locations and swarm activity

Although epicentral locations of small and moderate earthquakes are often not well determined in Turkey, it can be said that both aftershocks of large earthquakes and earthquake swarm activity tend to occur in releasing bend and releasing stepover areas. This observation confirms previous results in California (e.g., Eaton *et al.*, 1970; Hill, 1977; Weaver and Hill, 1978, 1979; Segall and Pollard, 1980). In the case of aftershocks it has been explained by fluid pore pressure arguments (Sibson, 1986). In Turkey, examples of this phenomenon are the 1939 Erzincan earthquake (where large felt aftershocks occurred in the area of a releasing stepover, Fig. 3 and 9 b,c), the 1967 Mudurnu Valley earthquake (aftershocks along the releasing segment adjacent to a releasing bend), and the Marmara Sea area (Fig. 4 and 10 b,c). In this last case, earthquake swarms (Ucer *et al.*, 1985) coincide with pull-apart basins.

(4) Foreshocks

Most of the earthquakes in this study do not have well-located foreshocks, either because they did not occur or because they were difficult to locate due to their small magnitude. In two cases, however, foreshocks can be related to fault geometry. In the 1968 Parkfield case, a foreshock occurred at the restraining bend (Lindh and Boore, 1981), and triggered a larger shock on an adjacent segment (Figure 9i). In the case of the 1975 Haicheng (earthquake $M_s = 7.3$), foreshocks were observed at a releasing stepover within a restraining bend along the mainshock fault segment (geometry shown in Figure 2- Ck; see Jones *et al.*, 1982). This second situation may be fairly common, because a secondary releasing feature within a restraining area provides a weak point that is likely to rupture first. It should be noted that releasing features adjacent to or within restraining areas occur in some of the unruptured fault segments shown in Figure 10. These include 10a, b, f and h. The 1930 Salmas earthquake (Figure 9w) had a damaging foreshock 15 hours before the mainshock (Tchalenko and Berberian, 1974). Although this foreshock has not been accurately located, the fault segment that ruptured during the mainshock also contained a releasing stepover adjacent to a restraining stepover. The distribution of damaged villages during the foreshock is not inconsistent with a location in the releasing stepover area (see Tchalenko and Berberian, 1974).

(5) Geological factors associated with fault discontinuities

Although it is beyond the scope of this paper to document all of the geological effects that are responsible for the observed fault discontinuities, some of the more important effects will be reviewed here. First it should be noted that complex fracture patterns are characteristic of simple shear laboratory experiments (e.g., Tchalenko, 1970; Wilcox *et al.*, 1973; Barlett *et al.*, 1981; Naylor *et al.*, 1986). These patterns can be due, for example, to rotation of the material within the fault zone.

En echelon fault patterns can often be explained by the rheology of the top part of the upper crust. First, the occurrence of ductile material such as a thick pile of sediments (Harding, 1985) or clay-rich rocks can cause discontinuities. For example Saroglu and Barka (1983) documented some cases in Turkey in which the effect of serpentinite-rich ophiolitic melange on fault zones was to widen the zones and break them up into many smaller faults with unclear surface expression (compared to the single break areas). Second, a decrease in confining pressure near the earth's surface may in some cases cause a widening of the zone of deformation.

The occurrence of bends can be explained by a number of factors. First, pre-existing zones of weakness can be an important factor at any scale. For example, on a large scale, the eastern half of the North Anatolian fault zone follows the Antolide/Tauride/Pontide suture zone, and the western half follows the Intra Pontide suture zone (both Eocene-Miocene features). Second, changes in stress orientation or magnitude can cause bends. A third factor includes heterogeneities in rock type. The discontinuities may also form progressively as a rupture either follows a boundary (Rogers, 1973) or encounters (at a higher angle) a boundary between dissimilar rock types (Jackson and McKenzie, 1984). In the second case, the rupture could initially change direction due to a refraction effect; subsequently the bend angle could increase due to differential deformation across the boundary.

Geometric fault discontinuities are often associated with clear morphological features. Near restraining segments mountains are often observed. Examples of this are the Ilgaz Mountains on segment 7 of the North Anatolian fault (near Tosya) and the San Gabriel Mountain range (1857 earthquake), Black Mountain (1906 earthquake) or Middle Mountain (1966 Parkfield earthquake) along the San Andreas fault. Releasing features are often associated with low areas as has been seen several times in the detailed Turkish fault descriptions.

Finally, restraining bends are sometimes associated with kink structures or folds with an orientation that is oblique to the fault zone, indicating variations in rheology within the moving blocks or plates. Examples of this are the Palmyra kink (Lebanon-Syria) or the Kirikhan-Gaziantep kink (southern Turkey), both adjacent to the Dead Sea fault.

Geometric discontinuities along strike-slip faults are stable in the short term, but they can be subject to progressive deformation over a longer time period. For example progressive deformation of single or double bends can cause an increase in α which eventually blocks movement on the fault. The fault is then replaced by newer faults. Examples of this can be observed in New Zealand and California. A progressive increase of α to 40° at a restraining double bend along the Alpine fault in New Zealand has caused motion along subparallel faults (Awatere, Clarence, Hope faults; see Rynn and Scholz, 1978). Similarly, near the Black Mountain - San Juan Bautista double bend motion is taken up by the Calaveras and Hayward faults (Sykes and Nishenko, 1984). In southern California many subparallel faults take up motion near bends in the San Andreas fault (e.g., Scholz 1977; Ziong and Yerkes, 1985). One possible interpretation for these subparallel faults is that slip has become difficult along the main fault strand.

CONCLUSIONS

An important contribution of this paper has been to provide a comprehensive description of strike-slip faults in Turkey. This description is based both on a compilation of work by many geologists in separate areas, and by many years of field work conducted by one of the authors (A. Barka). There is room, however, for further detailed field studies in Turkey. Due to this situation and to the lack of certain geophysical constraints, we found it useful to include additional examples from strike-slip faults in other countries.

It is unclear what problems might arise from trying to extrapolate results based on large earthquakes, and on segments many kilometers long, to moderate-size earthquakes. We have restricted our attention to larger events because information on smaller earthquakes is not well constrained in Turkey. We feel that on the scale of the larger events it is probably realistic to extrapolate surface geometric features down through a substantial thickness of the crust.

Fault segmentation is caused by discontinuities such as stepovers and sharp bends. Whether an earthquake starts or stops near a discontinuity depends not only on the nature of the stepover or bend, but on the arrangement of a series of discontinuities in a geometric pattern. These patterns differ from one another mechanically, because they control the sites where strain either accumulates or is easily released.

Both stepovers or bends can act as barriers to rupture propagation. In the restraining stepover or bend case, strike-slip motion is difficult within the stepover area or along the restraining L_2 segment. This difficulty is enhanced if the stepover is wide or the bend angle is high. Similarly releasing stepovers or bends can act as barriers to rupture propagation by absorbing rupture energy.

In the stepover case the critical width for preventing rupture propagation is difficult to determine from surface observations alone because it depends on the three-dimensional behavior of the stepover. A stepover can be as wide as 10 km before it stops rupture if the fault branches that it separates are connected at depth. The maximum bend angle is more easily fixed at about 30° , in agreement with laboratory results. Whether or not rupture is stopped by a bend does not depend only on the bend angle, but also on the direction of block motion relative to the fault orientation, i.e., on the amount of convergence that the fault branches on either side of the bend are subjected to.

The restraining segment in several geometric patterns appears to play an important role in the behavior of large earthquakes. These geometric patterns include single restraining bends, double restraining bends and restraining bends with an adjacent releasing stepover on the restraining side (illustrated in Figure 2-Ce). The restraining segment L_2 may play the role of what has been referred to as an asperity (e.g., Kanamori, 1981; Lay *et al.*, 1982; Aki, 1984). It is the site of main strain accumulation, and appears in some cases to be the site of maximum dislocation and maximum observed surface intensity (although the latter is strongly controlled by local geology as well. In most cases the epicenter appears to be located outside the restraining segment area for through-going earthquakes (those that are not restricted only to that branch). The length L_2 of the restraining segment, when combined with the bend angle α , appears to control earthquake magnitude; $\log (\alpha L_2)$ increases linearly with M . Similarly restraining stepovers can play the role of strain accumulation sites. The magnitude of a resulting earthquake most likely depends on the stepover width, although we do not have enough data in this study to document this effect. Releasing bends and stepovers are the preferred location for aftershocks and for swarms of smaller earthquakes. The extensional component of fault motion is increased there, facilitating rupture.

ACKNOWLEDGEMENTS

The field work on which a large part of this study was based would not have been possible without the M.T.A. Institute's (Ankara, Turkey) support of one of the authors (A. A. Barka). We would like to thank M. Nafi Toksöz for many helpful discussions. This work was supported by U.S. Geological Survey contract number 14-08-0001-G1151.

REFERENCES

- Aki, K., Asperities, barriers, characteristic earthquakes and strong motion prediction, *J. Geophys. Res.*, **89**, 5867-5872, 1984.
- Allen, C.R., The tectonic environments of seismically active and inactive areas along the San Andreas fault system, in Proceedings of the Conference on Geologic Problems of the San Andreas Fault System, edited by W.R. Dickinson and A. Grantz, *Stanford Univ. Publ. Geol. Sci.*, **11**, 70-82, 1968.
- Allen, C.R., Active faulting in northern Turkey: Contr. No. 1577. Div. Geol. Sci., Calif. Inst. Tech., 32 p., 1969.
- Ambraseys, N.N., Some characteristic features of the North Anatolian fault zone. *Tectonophysics* **9**, pp. 143-165, 1970.
- Ambraseys, N.N., Value of historical records of earthquakes, *Nature, Lond.* **232**, 379-397, 1971.
- Ambraseys, N.N., Studies in historical seismicity and tectonics. In: *Geodynamics of Today*, The Royal Soc., London, 9-16, 1975.
- Ambraseys, N.N. and Zatopek, A., The Mudurnu valley, West Anatolia, Turkey, earthquake of 22 July 1967. *Bull. Seis. Soc. Amer.*, **59**, 521-589, 1969.
- Angelier, J., Tectonic analysis of fault slip data sets. *J. Geophys. Res.*, **89**, 5835-5848, 1984.
- Arpat, E., The 1976 Caldiran earthquake: *Yeryuvari ve Insan*, **2**, 29-41, 1977.

- Arpat, E. and Saroglu, F., The East Anatolian Fault System: thoughts on its development. *Bull. Mineral Res., Explor. Inst., Ankara*, 78, 33-39, 1972.
- Arpat E. and Saroglu, F., Some recent tectonic events in Turkey. In Turkish. *Bull. Geol. Soc. Turkey*, 18, pp. 91-101, 1975.
- Ates, R. and Tabban, A., Preliminary report for the Murefte-Sarkay earthquake of 9th August 1912. *Publ. Earthquake. Res. Institute*, Ankara, Turkey (in Turkish), 1976.
- Aytun, A., Creep measurements in the Ismetpasa region of the North Anatolian fault zone, In *Multidisciplinary approach to earthquake prediction*, edited by A. M. Isikara and A. Vogel., pp. 279-295, Friedr. Vieweg & Sohn, 1982.
- Bakun, W.H., Seismic activity on the southern Calaveras fault in Central California. *Bull. Seis. Soc. Am.*, 70, 1181-1198, 1980.
- Bakun, W.H., Stewart, R.M., Bufe, C.G. and Marks, S.M., Implication of seismicity for failure of a section of San Andreas Fault. *Bull. Seism. Soc. Am.* 70, 185-202, 1980.
- Bakun, W.H., Clark, M.M., Cockerharm, R.S., Ellsworth, W.L., Lindh, A.G., Prescott, W.H., Shakal, A.F. and Spudich, P., The 1984 Morgan Hill, California, Earthquake. *Science*, 225, 288-291, 1984.
- Bakun, W.H. and Lindh, A.F., The Parkfield, California, Prediction experiment, *Earth Pred. Res.*, 3, 285-304, 1985.
- Barka, A.A. and Hancock. P.L., Relationship between fault geometry and some earthquake epicenters within the North Anatolian fault zone. In

- Progress in earthquake prediction*, v. 2, edited by A.M. Isikara and A. Vogel, 137-142 pp., Friedr. Vieweg and John, F.R.G., 1982.
- Barka, A.A., Saroglu, F. and Güner, Y., Horasan-Narman earthquake and its relation to the neotectonics of Eastern Turkey. *Yeryuvarı ve İnsan*, 8, 16-21, 1983.
- Barka, A.A. and Hancock, P.L., Neotectonic deformation patterns in the convex-northwards arc of the North Anatolian fault, in *The Geological Evolution of the Eastern Mediterranean*, edited by J.G. Dixon and A.H.F. Robertson, pp. 763-773, Special publication, Geol. Soc. London, 1984.
- Barka, A.A. and Bayraktutan, S., Active fault patterns in the vicinity of the Erzurum basin. Abstract. 39th Ann. Geol. Cong. Geol. Soc. Turkey. p. 11, 1985.
- Barka, A.A., Toksöz, M.N. and Gülen, L., in prep., The structure, seismicity and earthquake potential of the eastern part of the North Anatolian fault zone, 1987.
- Barka, A.A. and Gülen, Tectonic escape origin and complex evolution of the Erzincan pullapart basin, Eastern Turkey submitted to, *Geol. Soc. Am. Bull.*, 1987.
- Barka, A.A., Seismo-tectonic aspects of the North Anatolian fault zone, Ph.D. thesis, University of Bristol, England, 335 pp., 1981.
- Barka, A. and Kato, H., Research on comparison: the North Anatolian fault zone and Medreri Tectonic Line of Japan in relation to earthquake faults, active faults and earthquake prediction. *Rep. Inter. Res. Dev. Coop. ITIT, Japan*. 8212, 96 pp., 1985.

- Barlett, W.L., Friedman, M., and Logan, J.M., Experimental folding and faulting of rocks under confining pressure: Part IX: wrench faults in limestone layers., *Tectonophysics*, 79, 155-277, 1981.
- Bergougnan, H., 1978. Structure de la Chaîne pontique dans le Haut-Kelkit (Nord-Est de l'Anatolie). *Bull. Soc. Géol. Fr.*, 18, 675-686, 1978.
- Bilham, R. and Hurst, K., Relationships between fault zone deformation and segment obliquity on the San Andreas fault, California, *The China-U.S. Symposium on Crustal Deformation and Earthquakes*, Wuhan, 1985, 1986.
- Blumenthal, M.M., Ladik earthquake zone. *Bull. Min. Res. Expl. Inst. Turkey* 1/33, 153-174, 1945a.
- Blumenthal, M. M., Die Kelkit-Dislokation und ihre tektonische Rolle. *MTA Mecmuasi*, 2/34, 372-386, 1945b.
- Bott, M.H.P., The Mechanics of oblique-slip faulting. *Geol. Mag.*, 46, 109-117, 1959.
- Brown, R.D., Jr., Vedder, J.G., Wallace, R.E., Roth, E.F., Yerkes, R.F., Castle, R.O., Waananen, A.O., Page, R.W., and Eaton, J.P., The Parkfield-Cholame, California, earthquakes of June-August 1966-Surface geologic effects, water-resources aspects, and preliminary seismic data: *U.S. Geol. Survey Prof. Paper* 579, 66 pp., 1967.
- Brown, R.D., Jr., Map showing recently active breaks along the San Andreas and related faults between the northern Gabilan Range and Cholame Valley, California, USGS, Misc. Geol. Inves. Map I-575, 1970.
- Brune, J.N. M., Seismic moment, seismicity and rate of slip along major fault

- zones. *J. Geophys. Res.*, **73**, 777-784, 1968.
- Butler, R., Stewart, G.S., and Kanamori, H., The July 27, 1976 Tangshan, China, earthquake - A complex sequence of intraplate events, *Bull. Seismol. Soc. Amer.*, **69**, 207-220, 1979.
- Canitez, N., Studies on recent crustal movements and the North anatolian fault problem, in: Symposium on the North Anatolian fault zone. Spec. Publ. of Min. Res. Expl. Inst. Turkey, 35-58, 1973.
- Clark, M.M., Surface rupture along the Coyote Creek fault in the Borrego Mountain earthquake of April 9, 1968. *USGS Prof. paper 787*, 55-86, 1972.
- Clark, M.M. *et al.*, Preliminary slip-rate table and map of late-Quaternary faults of California. *USGS Open file report*, 84-106. plate 1-5, 1984.
- Crampin, S. and Evans, R., Neotectonics of the Marmara Sea region of Turkey. *Jour. Geol. Soc. London*, **143**, 343-348, 1986.
- Dewey, J.W., Seismicity of Northern Anatolia, *Bull. Seism. Soc. Am.*, **66**, 843-868, 1976.
- Dewey, J.F., Hempton, M.R., Kidd, W.S.F., Saroglu, F. and Sengör, A.M.C., 1986. Shortening of continental lithosphere: the neotectonics of eastern Anatolia - a young collision zone. In: *Collision Tectonics*, edited by Coward, M.P. and Ries, A.C., 19, pp. 1-36, Geol. Soc. Sec. Publ., London, 1986.
- Ding, G., Active faults of China, in *The Active faults of China*, pp. 225-241, Seismological Press, China, 1982.
- Donath, F.A., Experimental study of shear failure in anisotropic rocks. *Geol. Soc. Am. Bull.*, **72**, 985-990, 1961.

- Dozer, D.J. and Kanamori, H., Depth of Seismicity in the Imperial Valley region (1977-1983) and its relationship to heat flow, crustal structure and Oct. 15, 1979 earthquake. *J. Geophys. Res.*, 91, 675-700, 1986.
- Eaton, J.P., O'Neill, M.E. and Murdock, J.N., Aftershocks of the 1968 Parkfield-Cholame, California earthquake: A detailed study. *Bull. Seism. Soc. Am.*, 60, 1151-1197, 1970.
- Eginitis, M.D., Sur le tremblement de terre de Constantinople, du 10 Juillet 1894. *Comp. Rendus*. 52, 480-484, 1894.
- Eginitis, M.D., Le tremblement de terre de Constantinople du 10 Juillet 1894. *Annales de Geographie*, 4, 151-165, 1895.
- Ercan, A., A statistical analysis of the major and micro earthquakes along the East Anatolian fault. In: *Multidisciplinary approach to Earthquake prediction*, edited by A.M. Isikara and A. Vogel, pp. 239-261, Fried. Vieweg & Sohn, 1982.
- Erdik, M., Damage at the Sürücü Dam during May 5, 1986 Malatya earthquake, Turkey. Unpublished report. Middle East Tech. Univ., Turkey, 15 pp., 1986.
- Erentoz, C. and Kurtman, F., Report on 1964 Manyas earthquake. *Bull. Min. Res. Expl. Inst. Turkey*, 63, 1-5, 1964.
- Ergin, K., Güçlü, U. & Uz, Z., A catalogue of earthquakes of Turkey and surrounding area (11 AD to 1964 AD) *Publ. Mining Fac. Global Phys. Inst., Istanbul*, 24, 1-28, 1967.
- Evans, R., Asudeh, I., Crampin, S. and Ucer, S.B., Tectonics of the Marmara Sea region of Turkey: new evidence from micro-earthquake fault plane

- solutions. *Geophys. Jour. R. Astr. Soc.*, **83**, 47-60, 1985.
- Eyidogan, H., Toksöz, M.N., Gülen, L., and Nabelek, J., Aftershock migration following the 1983 Horasan-Narman earthquake, Earth Resources Laboratory unpublished report, Massachusetts Insittute of Technology, Cambridge, 1986.
- Gündoğdu, O., Source characteristics of some major earthquakes in Turkey. Ph.D. Thesis, University of Istanbul, 175 pp., 1985.
- Hamilton, R.M., Aftershocks of the Borrego Mountain earthquake from April 12 to June 12, 1968, The Borrego Montain earthquake of April 9, 1968. U.S.G.S. Prof. Pap. 787, 31-54, 1972.
- Hancock, P.L., Brittle microtectonics; Principles and practice. *Journ. Struct. Geol.*, **7**, 437-357, 1985.
- Harding, T.P., Seismic characteristics and identification of negative flower structures and positive flower structures, and positive structural inversion. *AAPG*, **69**, 582-600, 1985.
- Hartzell, S.H. and Heaton T.H., Inversion of strong ground motion and teleseismic waveform data for the rupture history of the 1979 Imperial Valley, California, earthquake, *Bull. Seis. Soc. Am.*, **73**, 1553-1584, 1983.
- Hartzell, S.H., and Heaton, T., Rupture history of the 1984 Morgan Hill, California, earthquake from the inversion of strong motion records. *Bull. Seis. Soc. Am.*, **76**, 649-674, 1986.
- Hempton, M.R. and Dunne, L.A., Sedimentation in pull-apart basins: Active examples in eastern Turkey, *J. Geol.*, **92**, 513-530, 1984.

- Hill, D.P., A model for earthquake swarms, *J. Geophys. Res.*, **82**, 1347-1352, 1977.
- Hobbs, B.E., Means, W.D. and Williams, P.E., *An Outline of Structural Geology*, 571 pp., John Wiley and Sons, Inc., 1976.
- Jackson, J. and McKenzie, D., Active tectonics of the Alpine-Himalayan Belt between western Turkey and Pakistan. *Geophys. Journ. R. Ast. Soc.* **77**, 1, 185-265, 1984.
- Jones, L.M., Wang, B., Xu, S. and Fitch, T., The foreshock sequence of the February 4, 1975, Haicheng Earthquake ($M = 7.3$), *J. Geophys. Res.*, **87**, 4575-4584, 1982.
- Jones, L.M., Han, W., Hauksson, E., Jin, A., Zhang, Y., Luo, Z., Focal mechanisms and aftershock locations of the Songpan earthquakes of August 1976 in Sichuan, China, *J. Geophys. Res.*, **89**, 7697-7709, 1984.
- Kanamori, H. and Stewart, S.G., Seismological aspects of the Guatemala earthquake of February 4, 1976. *J. Geophys. Res.*, **83**, 3427-3433, 1978.
- Karnik, V., *Seismicity of the European area*, Part I, pp. 365, D. Reidel Pub. Com., Dordrecht, Holland, 1969.
- Karnik, V., *Seismicity of the European area*, Part II, pp. 218, D. Reidel Pub. Com., Dordrecht, Holland, 1971.
- Ketin, I., Über die tektonisch-mechanischen Folgerungen aus den grossen anatolischen Erdbeben des letzten Dezenniums. *Geol. Rdsch.*, **36**, pp. 77-83, 1948.
- Ketin, I., Über die nordanatolische Horizontalverschiebung: *Bull. Mineral Res. Explor. Inst.*, Ankara, v. 72, pp. 1-28, 1989.

- Ketin, I. and Roesli, F., Markoseismische Untersuchungen über das nordwest-anatolische Beben vom 18 März 1953. *Ecolog. Geol. Helv.*, 46, 187-208, 1953.
- King, G.S.P., Speculations on the geometry of the initiation and termination process of earthquake rupture and its relation to morphology and geological structure, preprint, submitted to *Pageoph*, Topical issue on Friction and Faulting, Ed. T.Tullis, 1986.
- King, G. and Nabelek, J., Role of fault bends in the initiation and termination of earthquake rupture. *Science*, 228, pp. 984-987, 1985.
- Kocyigit, A., The Karayasi fault. *Bull. Geol. Soc. Turkey, (in Turkish)*, 28, pp. 67-71, 1985.
- Kocyigit, A., Oztürk, A., Inan, S. and Gürsay, H., Tectonomorphology and mechanistic interpretation of the Kurasu basin (Erzurum) (in Turkish). *Cambr. Uni. Bull. Earth Sciences*, 2, pp. 3-15, 1985.
- Koide, H., Seismotectonic problem of en echelon systems and earthquake source mechanisms (in Japanese). *Jour. Earth Sci.*, 92, pp. 33-52, 1983.
- Lahn, E., Seismic activity in Turkey from 1947 to 1949. *Bull. Seis. Soc. Ame.*, 42, pp. 111-114, 1952.
- Lawson, A.C., et al., The California earthquake of April 18, 1906. Report of state earthquake investigation commission. 2 vols. plus maps. Carnegie Inst., Washington, D.C., 1908.
- Lay, T., H. Kanamori and L. Ruff, The asperity model and the nature of large subduction zone earthquakes. *Earthquake Prediction Research*, 1, pp.

3-71, 1982.

Le Pichon, X., Lyberis, N., and Alvarez, F., Subsidence history of the North Aegean Trough, in *The geological evolution of the eastern Mediterranean*, edited by J.G. Dixon and A.H.F. Robertson, 726-741, Spec. Publ. Geol. Soc., London, 1984.

Liu, L.H. and Helmberger, D.V., The near-source ground motion of the 6 August, 1979 Coyote Lake, California, earthquake, *Bull. Seis. Soc. Am.*, 73, pp. 201-218, 1983.

Lindh, A.G., and Boore, D.M., Control of rupture by fault geometry during the 1966 Parkfield earthquake, *Bull. Seis. Soc. Am.*, 71, pp. 95-116, 1981.

Louderback, G.D., Central California earthquakes of the 1830's. *Bull. Seismol. Soc. Am.*, 37, pp. 33-74, 1947.

Lyberis, N., Tectonic evolution of the north Aegean trough, in *The Geological Evolution of Eastern Mediterranean*, edited by J.G. Dixon and A.H.F. Robertson, pp. 711-125, Spec. Publ. Geol. Soc. London, 1984.

Marathon Oil Comp., Unpublished report on abandoned Marmara I well, 15, 711-725, 1974.

McEvelly, T.V., Bakun, W.H. and Casday, K.B., The Parkfield, California earthquakes of 1966. *Bull. Seismol. Soc. Am.*, 57, pp. 1221-1244, 1967.

McKenzie, D., The relation between fault plane solutions for earthquakes and the direction of the principal stresses, *Bull. Seis. Soc. Am.*, 59, pp. 591-601, 1969.

McKenzie, D.P., Active tectonics of the Mediterranean Region. *Geophys. J.R.*

- Astr. Soc.*, 30, pp. 109-185, 1972.
- McKenzie, D.P., The East Anatolian Fault: a major structure in eastern Turkey. *Earth Planet. Sci. Lett.*, 29, pp. 189-193, 1976.
- McKenzie, D.P., Active tectonics of the Alpine-Himalayan belt: The Aegean Sea and surrounding regions: *Geophys. Jour. Roy. Astr. Soc.*, 55, pp. 217-254, 1978.
- Mocavei, G., Sur le tremblement de terre de la Mer de Marmara le 9 Aout, 1912. *Bull. Sect. Sci. Acad. Rumania*, 1, 1, pp. 9-18, 1912.
- Molnar, P. and Deng, O., Faulting associated with large earthquakes and average rate of deformation in Central and Eastern Asia. *J. Geophys. Res.*, 89, 6203-6228, 1984.
- Nábělek, J., Chen, W.P., and Ye, H., The Tangshan earthquake sequence and its implications for the evolution of the North China Basin, *J. Geophys. Res.*, in press, 1987.
- Naylor, M.A., Mandl, G., and Siypestieyn, C.H.K., Fault geometries in basement-induced wrench faulting under different initial stress states, *J. Struct. Geol.*, 8, pp. 737-752, 1986.
- Nur, A., Ron, H. and Scotti, O., Fault mechanics and kinematics of block rotations, *Geology*, 14, pp. 746-749, 1986.
- Okada, A., Quaternary faulting along the Median Tectonic line of Southwest Japan, *Mem. Geol. Soc. Japan*, 18, pp. 89-108, 1980.
- Okada, A. and Sangawa, A., Fault morphology and Quaternary faulting along the Median Tectonic Line in the southern part of the Izumi range, *Geogr.*

- Rev. Japan*, 51, pp. 385-405, 1978.
- Pamir, H.N., and Akyol, I.H., Gormur and Erban earthquakes, *Bull. Geograph. Turkey*, 2, pp. 1-7, 1943.
- Pamir, H.N. and Ketin, I., Das anatolische Erdbeben ende 1939. *Geol. Rdsch.*, 32, pp. 279-87, 1941.
- Parejas, E., Akyol, I.H. and Altinli, E., Le tremblement de terre d'Erzincan du 27 Decembre, 1939. *Revue Fac. Sci. Univ. Istanbul, B-VI*, pp. 177-222, 1942.
- Pfannenstiel, V.M., Diluviale Geologie des Mittelmeer Gebietes. *Geol. Rundschau*, 34, pp. 342-424, 1944.
- Pinar, N., Geological and macroseismic investigation of the August 13th 1951 earthquake, I Unive. Fen. Fak. Dergisi, Seri A, Cilt XVIII, pp. 131, 1953.
- Research Group for Active Faults, *Active faults in Japan, Todai Shuppan*, pp. 380, 1980.
- Reid, H.F., The California earthquake of April 18, 1906, The mechanics of the earthquake, in *The State Earthquake Investigation Committee Report*, vol. 2, 192 pp., 1910.
- Riad, S. and Meyers, H., Earthquake catalog for the Middle East Countries 1900-1983, World Data Center A. Report, SE-40, 133pp., 1985.
- Rogers, T.H., Fault trace geometry within the San Andreas and Calaveras fault zones. A clue to the evolution of some transcurrent fault zones. In: *Proc. Conf. Tect. Prob. of San Andreas fault system*, edited by R.L. Kovach and A. Nur., v. 13, pp. 251-258, Publ. Stanford U., 1973.

- Rudnicki, J. and Kanamori, H., Effects of fault interaction on moment, stress-drop, and strain energy release, *J. Geophys. Res.*, **86**, pp.1785-1793, 1981.
- Rynn, J.M.W., and Scholz, C.H., Seismotectonics of the Arthur's Pass region, South Island, New Zealand, *Geol. Soc. Am. Bull.*, **89**, pp. 1373-1388, 1978.
- Salomon-Calvi, W., Anadolu'nun tektonik tarzi tesekkülü hakkında kısa izahat. *Bull. Min. Res. Explo. Inst. Turkey*, **1/18**, pp. 35-47, 1940.
- Sandison, D., Notice of the earthquake of Brussa. *Quart. Journ. of the Geol. Soc. of London*, **11**, pp. 543-544, 1855.
- Saroglu, F., Geological and tectonic evolution of Eastern Turkey during Neotectonic period, Ph.D. thesis (in Turkish), University of Istanbul, 242 pp., 1985.
- Saroglu, F., and Güner, Y., The Tutak active fault, its characteristics and relation to the Caldiran fault (in Turkish), *Yeryuvari ve Insan*, **4** pp. 11-14, 1979.
- Saroglu and Güner, Y., Dogu anadolu'nun jeomorfolojik gelismine etki eden ögeler, jeomorfoloji, tektoni, vakanizma iliskileri: *Bull. Geo. Soc. Turkey*, **24**, pp. 39-50, 1981.
- Saroglu, F. and Barka, A.A., The importance of rock type for seismic parameters (in Turkish), *Yeryuvari ve Insan*, **8.4**, 43 pp., 1983.
- Saroglu, F. and Erdogan, R., Observations on postearthquake movement on the Caldiran fault, *Yeryuvari ve Insan*, **8**, pp. 10-12, 1983.

- Saroglu, F. and Yilmaz, Y., Neotectonics of Eastern Anatolia and related igneous activity, in *Ketin Symposium*, edited by T. Ercan and A.M. Caglayan, pp. 149-162, Spec. Publ. Geol. Soc. Turkey, 1985. 149-162.
- Scholz, C., Molnar, P., and Johnson, T., Detailed studies of frictional sliding of granite and implications for the earthquake mechanism, *J. Geophys. Res.*, 77, pp. 6392-6406, 1972.
- Scholz, C.H., Transform fault systems of California and New Zealand: similarities in their tectonic and seismic styles, *J. Geol. Soc. Lond.*, 133, pp. 215-229, 1977.
- Schwartz, D.P. and Coppersmith, K.J., Seismic hazards: New trends in analysis using geologic data, in *Active tectonics*, National Acad. Press, Washington, D.C., pp. 215-230, 1986.
- Segall, P. and Pollard, D.D., Mechanics of discontinuous faults, *J. Geophys. Res.*, 85, pp. 4337-4350, 1980.
- Sengor, A.M.C., Structural classification of the tectonic history of Turkey, in *Ketin symposium*, edited by T. Ercan and A.M. Gaylayan, pp. 37-62, Spec. Publ. Geol. Soc. Turkey, 1985.
- Sengor, A.M.C., Cross faults and differential stretching of hanging walls in regions of low-angle normal faulting: examples from western Turkey, *Journ. Struc. Geol.*, 8, 1986.
- Sengor, A.M.C., Görür, N. and Saroglu, F., Strike-slip faulting and related basin formation in zones of tectonic escape: Turkey as a case study. In *Strike-slip Faulting and Basin Formation*, edited by Biddle, K.T. and Christie-Blick, N., Society of Econ. Paleont. Min. Spec. Pub., 37, 1985.

- Seymen, I., Tectonic characteristics of the North Anatolian fault zone in the Kelkit valley, Ph.D. thesis. Istanbul Tech. Uni., 192, 1975.
- Seymen, I. and Aydin, A., The Bingöl earthquake fault and its relation to the North Anatolian fault zone, *Bull. Mineral Res. Explor. Inst., Ankara*, 79, pp. 1-8, 1972.
- Sharp, R.V. *et al.*, Surface faulting in the Central Imperial valley, *U.S.G.S. Prof. Pap. 1254*, pp. 119-144, 1982.
- Sibson, R.H., Earthquakes and lineament infrastructure, *Phil. Trans. R. Soc. Lond.*, 317, pp. 63-79, 1986.
- Sieberg, A., Untersuchungen über Erdbeben und Bruchschollenbau im oestlichen Mittelmeergebiet, *Denk. d. Midz. Natw. Ges. zu Jena, Bd. 18*, Jena, pp. 159-273, 1932.
- Sieh, K.E., Slip along the San Andreas fault associated with the great 1857 earthquake: *Bulletin of the Seismological Society of America*, 68, pp. 1421-1448, 1978
- Sieh, K.E., Lateral offsets and revised dates of large prehistoric earthquakes at Pallett Creek, southern California: *Jour. Gephys. Res.*, 89, B9, pp. 7641-7670, 1984.
- Sipahioglu, S., Seismo-tectonic features of the North Anatolian fault zone. Ph.D. Thesis, Ist. Univ. Science Fac. Geophys. Dept. 169, 1982.
- Sipahioglu, S., An evaluation of earthquake acitvity of the Horasan-Narman region before the 30 October 1983 earthquake. *Yeryuvari ve Insan*, 8, pp. 12-15, 1983.

- Slade, M.A., Lyzenga, A.G., and Raefksy, A., Modelling of the surface static displacement and fault plane slip for the 1979 Imperial Valley earthquake. *Bull. Seis. Soc. Am.*, 74, pp. 2413-2433, 1984.
- Slemmons, D.B., State-of-the-Art for assessing earthquake hazards in the United States; Report 6, *Fault and earthquake magnitude*, U.S. Army Eng. Waterways Experiment station, Soils and Pavements Lab., S-73-1. 120 pp., 1977.
- Slemmons, D.B. and Deplo, C.M., . Evaluation of active faulting and associated hazards. In: *Active tectonics*, National Acad. Press, Washington, D.C., pp. 45-62, 1986.
- Solomon, S., Sleep, N.H. and Richardson, R.M., On the forces driving plate tectonics: inferences from absolute plate velocities and intraplate stress, *Geophys. Jour. R. Astr. Soc.*, 42, pp. 769-801, 1975.
- Sykes, L.R. and Nishenko, S.P., Probabilities of occurrence of large plate rupturing earthquakes for the San Andreas, San Jacinto and Imperial faults, California, 1983-2003. *Jour. Geophys. Res.*, 89, pp. 5905-5927, 1984.
- Tabban, A., Geology and earthquakes of cities. *Imar Isk. Bak. Afet Isleri Genel. Mu. Ankara*, 343 pp., 1980.
- Tatar, Y., Tectonic investigations on the North Anatolian fault zone between Erzincan and Refahiye. *Yerbilimleri*, 4 Publ. Inst. Earth. Sci., Hacettepe Univ. (in Turkish), pp. 201-136, 1978.
- Tchalenko, J.S., Similarities between shear zones of different magnitudes, *Bull. Geol. Soc., Amer.*, 81, pp. 1625-1640, 1970.
- Tchalenko, J.S., and Berberian, M., The Salmas (Iran) earthquake of May 6, 1930,

Ann. di Geofis., 27, pp. 151-212, 1974.

Tchalenko, J.S., A reconnaissance of the seismicity and tectonics at the northern border of the Arabian Plate (Lake Van region): *Revue de géographie physique et de géologie dynamique*, v. XIX, pp. 189-208, 1977.

Tchalenko, Z.S. and Brand, Z., Seismicity and structure of the Zagros (Iran): The Main recent fault between 33° and 35° N, *Phil. Trans. R. Soc. London*, 277, pp. 1-25, 1974.

Tchalenko, J.S. and Ambraseys, N.N., Structural analysis of the Dasht-e-Bayaz (Iran) earthquake fractures, *Bull. Geol. Soc. Am.*, 81, pp. 11-80, 1970.

Tokay, M., Geological observation on the North Anatolian fault zone between Gerede and Iluz, in: Symposium on the North Anatolian fault zone, A Spec. Publ. Mon. Res. Expl. Institute of Turkey, 1973.

Toksöz, M.N., Arpat, E., and Saroglu, F., East Anatolian earthquake of 24 November 1978: *Nature*, 270, pp. 423-425, 1977.

Toksöz, M.N., A.F. Shakal, and A.J. Michael, Space-time migration of earthquakes along the N. Anatolian fault zone and seismic gaps. *Pure Appl. Geophys.*, 117, pp. 1258-70, 1979.

Toksöz, M.N., Guenette, M., Gülen, L., Keough, G. Pulli, J.J., Sav, H. and Olguner, A., source mechanism of 1983 Horasan-Narman earthquake, *Yeryuvari ve İnsan*, 8, pp. 47-52, 1983.

Ucer, S.B., Crampin, S., Evans, R., Miller, A. and Kafadar, N., The MARNET radiolinked seismometer network spanning the Marmara Sea and the seismicity of Western Turkey, *Geoph. J. Roy. Astron. Soc.*, 83, pp. 17-30, 1985.

- Weaver, C.S., and Hill, D.P., Earthquake swarms and local spreading along major strike-slip faults in California, *Pure App. Geophys.*, 117, pp. 51-64, 1979.
- Wilcox, R.E., Harding, T.P., and Seely, D.R., 1973. Basic wrench tectonics, *Bull. Am. Assoc. Petrol. Geol.*, 57, pp. 74-96, 1973.
- Woodcock, N.H., and Fisher, M., Strike-slip duplexes, *J. Struct. Geol.*, 8, pp. 725-735, 1986.
- Yalcin, N., Characteristics of the East Anatolian fault between Turkoglu and Karagac (K. Maras) in relation to settlement problems. *Bull. Chem. Geol. Eng., Turkey*, 6, pp. 49-55, 1978.
- Yilmaz, Y., Gozûbol, A.M. and Tüysüz, O., Geology in and around the North Anatolian transform fault zone between Bolu and Akyazi, in: *Multidisciplinary approach to earthquake prediction*, edited by A.M. Isikara and A. Vogel, pp. 45-66, Friedr. Vieweg & Sohn, 1982.
- Zhou, H.L., Allen, C.R. and Kanamori, H., Rupture complexity of the 1970 Tonghai and 1973 Luhuo earthquakes, China, from P-wave inversion, and relationship to surface faulting, *Bull. Seis. Soc. Am.*, 73, pp. 1585-1597, 1983.
- Ziony, J.L. and Yerkes, R.F., Evaluating earthquake and surface faulting potential, in *Evaluating earthquake hazards in the Los Angeles Region - an Earth-Science Perspective*, edited by J.I. Ziony, pp. 43-91, U.S. Geol. Surv. Prof. Paper, 1360, 1985.

FIGURE CAPTIONS

- 1) Major tectonic elements of Turkey. Compiled from Arpat and Saroglu (1972, 1975), Sengör *et al.* (1985). Boxes indicate areas shown in Figures 3, 4, 7 and 8. The North and East Anatolian faults intersect at the Karliova triple junction (K, at approximately 39°N, 41°E). Kahraman Maras, also referred to in text, is represented by an M near 37°N, 37°E.
- 2) Geometrical pattern definitions for strike-slip faults, as used in the text. In all map views fault movement is assumed to be right-lateral. The direction of block motion is considered to be east-west. A-Stepovers. These can be of releasing or restraining type depending on the direction of the step. Cases Ab, c, d characterize different amounts of horizontal separation between fault segments as shown on the page. B - Bends. Smooth bends refer to a gradual change in fault orientation. Sharp bends refer to an abrupt change. C - Combinations of bends and stepovers. D - cross-sectional views of stepovers. Whether the two fault segments join at depth or remain as two separate planes depends on the brittle-ductile characteristics of the upper crust. Flower-like structures (fault planes joining at depth) can be either negative or positive depending on whether the stepover is of releasing or restraining type.
- 3) Active fault segments in the Central and Eastern sections of the North Anatolian fault zone. The inset map shows the general location of the main trace. Boxes in the inset map indicate areas which are blown up in the lower part of the figure. Years displayed as smaller numbers refer to large earthquakes that occurred where numbers are shown. Larger numbers (1-8) along fault zone correspond to fault segments. The

interpreted length and position of each segment are described in the text. Thicker dashed lines denote ruptured segments. Thinner plain lines are unruptured faults (e.g., segment 2). For references see text.

- 4) Active fault segments in the Western section of the North Anatolian fault zone, near the Marmara Sea (South of Istanbul). For explanation see Figure 3.
- 5) Interpreted distribution of active fault segments beneath the Marmara Sea. Thin lines are bathymetric contours from Pfannenstiel (1944). Major basins are indicated by A, B, and C. The fault plane solution for the 1963 earthquake is taken from McKenzie (1972). Fault segments in the southern half of the Marmara Sea are interpreted from reflection profiles (Marathon, 1974). Note the pull-apart nature of the northern Marmara Sea.
- 6) Comparison of previous figure with published interpretations. A - interpretation of this study. B - from Pinar (1943). C - from Pfannenstiel (1944). D - from Sengör (1986). E - from Crampin and Evans (1986). See text for discussion.
- 7) Active fault segments, East Anatolian fault. Only one large earthquake (1971, segment 1) has occurred here during this century. For explanation see Figure 3.
- 8) Major block boundaries and internal active faults, Eastern Turkey. Note conjugate character of most of these faults. Compiled from Toksöz *et al.* (1977), Arpat (1977), Saroglu and Guner (1979), Barka *et al.* (1983) and Barka and Bayraktutan (1984).
- 9) Schematized geometry of ruptured fault segments from Turkey and other

areas. Geometric patterns are characterized in each case by reference to Figure 2, as indicated in each diagram. Arrows indicate direction of rupture (thin arrows), fault slip direction (thicker arrows) or direction of block motion (large open arrows). Ruptured segments are indicated by bold letters in the numerical values column. Stars are epicenters. The location of epicenters is mostly interpreted, based on instrumental epicenters that lie close enough to the geometric discontinuities to be probably associated with them (cases a, b, c, d, e, g, i, k, l, m, p, q, r, s, u, v, x, y; see text for details). In some cases the epicenter is assumed (open star) based on comparison with other more recent examples or from fault orientation (case f, h). Information for earthquakes outside Turkey comes from: k, 1976 - Butler *et al.*, 1979; Nabelek *et al.*, 1987; l, 1966 - Brown, 1970; Segall and Pollard, 1980; Lindh and Boore, 1981; Bakun and Lindh, 1985; n, 1857 - Allen, 1988; Sieh, 1978, 1984; Sykes and Nishenko, 1984; Ziony and Yerkes, 1985; o, 1906 - Lawson *et al.*, 1908; Reid, 1908; Louderback, 1947; Allen, 1988; Clark, 1972; Sykes and Nishenko, 1984; Ziony and Yerkes, 1985; p, 1970 - Zhou *et al.*, 1983; Ding, 1985; q, 1979 - Slade *et al.*, 1984; Sharp *et al.*, 1982; Hartzell and Heaton, 1983; Doser and Kanamori, 1986; r, 1979 - Bakun, 1980, Liu and Helmberger, 1983; s, 1984 - Bakun *et al.*, 1984; Hartzell and Heaton, 1986; t: Zagros Main Recent fault - Tchalenko and Brand, 1974; u, 1968 - Clark, 1972; Hamilton, 1972; v, Songpan earthquakes - Jones *et al.*, 1984; w, 1930 - Tchalenko and Berberian, 1974; The Horasan-Narman and Songpan earthquakes (9i, v) actually occurred on left-lateral faults. Here they have been flipped around (viewed from underside of page in map view) for comparison purposes.

- 10) Schematized geometry of unruptured fault segments. Rupture characteristics are assumed for future earthquakes, with the open star denoting suggested approximate locations for future epicenters. Left-lateral faults are inverted to give equivalent right-lateral fault geometry for comparison purposes (cases l, n, o, p, and t). Geometries for the Median Tectonic Line (MTL), Japan (cases g, r, s) are taken from Research Group for active faults (1980), Okada and Sangawa (1978), Barka and Kato (1985). The Mission Creek segment of the southern San Andreas fault (case 10 q) has a geometry taken from the Clark *et al.*, 1985, 1/1,000,000 scale USGS active fault map of California.
- 11) Relationship between bend angle (α) and slip vector direction (β). These values are defined in the upper diagram. Variations in α relative to β and the effect of these variations on earthquake rupture are shown for single and double restraining bend cases. Stars are assumed epicenters; thin arrows are rupture propagation or direction of fault displacement; thick arrows are direction of block motion. See text for discussion.
- 12) Relationships between single bends, ruptured fault segments and location of epicenters. Solid stars are interpreted epicentral locations. Dashed arrows show distance from interpreted epicenters to the ends of the earthquake surface breaks. A - 1939/12/26 Erzincan earthquake. Dewey's (1976) relocated epicenter is shown as an open star. It is constrained to within about 20 km. Given the rupture length of the event, an epicentral location at the bend is a reasonable assumption. B- 1942/12/20 Erbaa-Niksar earthquake. A well-constrained instrumental epicenter is not available for this event. Maximum intensities were concentrated in the bend area, between Tepekisla and Zilhor (Pamir

and Akyol, 1943) C - 1943/11/26 Tosya earthquake. A well-constrained instrumental epicenter is not available for this event either. Maximum intensities were concentrated between Tosya and Ilgaz (see Figure 3; Barka, 1981). D - 1976/11/24 Caldiran earthquake. The International Seismological Centre bulletin epicenter is indicated by the open star. The inversion of seismic waves generated by this event (King and Nabelek, 1986) confirms that rupture took place bilaterally, away from the bend area.

- 13) Relationship between (a) $\log (\alpha L_2)$ and M_s , (b) $\log L$ and M_s , (c) $\log (\alpha L_2)$ and $\log L$, (d) $\log (\alpha L_2)$ and $\log (uL)$. Parameters α and L_2 are as defined in Figure 11. M_s is surface wave magnitude; L is total ruptured fault length; u is fault displacement. Numerical values are tabulated in Table 2. For interpretation see text.

TABLE 1:**Categorization of ruptured and unruptured fault segments**

Figure 2 type	Examples from Figures 9, 10 *
----------------------	--------------------------------------

Stepovers

2-Ab	9u, 9v
2-Ad	10c

Bends

2-Bb	9b, 9g, 9h, 9i, 9l, 10d, 10m, 10n
-------------	-----------------------------------

Combinations

2-Ca	9b, 9c, 10b
2-Cb	9a, 10k, 10l
2-Cc	9k, 10i
2-Cd **	9b, 9e, 9m, 9n, 9o, 9p, 9q, 9r, 9s, 9t, 10n, 10o, 10p, 10q, 10r, 10s, 10t
2-Ce	9d, 9f, 10e, 10f, 10g, 10h
2-Cf	10j
2-Cg	9j, 10t
2-Ch	9x, 10o
2-Ci	9b, 10a
2-Cj	9w
2-Ck	(Haicheng case, not in Figs. 9,10)*

* Figure 9: already ruptured or partially ruptured; Figure 10: unruptured.
The Haicheng earthquake is discussed in the text.

** Double bends; all restraining double bends except cases 9b and 10o
(these two are releasing double bends).

TABLE 2:**Numerical values corresponding to Figure 13:**

earthquake	M_S	α (°)	L_2 Km	$\log(\alpha L_2)$ (° km)	L Km	$\log L$ Km	u cm	$\log(uL)$ (cm ²)
1) 1857 San Andreas, Calif.	8.5	34	70	3.37	390	2.59	900	10.54
2) 1906 San Andreas, Calif.	8.3	14	70	2.99	450	2.65	500	10.35
3) 1912 NAF, Turkey	7.3	14	30	2.62	80+	1.9	?	----
4) 1939 NAF, Turkey	8.0	20	75	3.17	360	2.55	370-400	10.16
5) 1942 NAF, Turkey	7.0	14	10	2.15	60	1.78	175	9.02
6) 1943 NAF, Turkey	7.3	15	25	2.57	265	2.42	110	9.46
7) 1949 NAF, Turkey	7.0	16	15	2.38	42	1.62	?	?
8) 1953 NAF, Turkey	7.4	17	10	2.23	50	1.7	430	9.33
9) 1967 NAF, Turkey	7.1	20	06	2.08	90	1.95	190	9.23
10) 1970 Tonghai, China	7.5	24	10	2.38	50	1.7	270	9.13
11) 1973 Luhuo, China	7.5	11	45	2.69	90	1.95	360	9.5
12) 1976 Caldiran, Turkey	7.3	18	28	2.70	50	1.7	370	9.26
13) 1976 Tangshan, China	7.8	30	32	2.98	140	2.15	270	9.58
14) 1979 Coyote Lake, Calif.	5.7	10	6	1.78	25	1.4	-----	-----
15) 1979 Imperial Valley, Calif.	6.9	22	5.5	2.08	30	1.48	78	8.37
16) 1984 Morgan Hill, Calif.	6.3	15	6	1.95	28	1.45	42	8.07
17) 1966 Parkfield, Calif. (fore-shock)	5.1*	5	4.5	1.35	?	-----	-----	-----

* M_L value for Parkfield foreshock**RESULTS OF LINEAR REGRESSION FOR DATA PLOTTED IN FIGURE 14:**

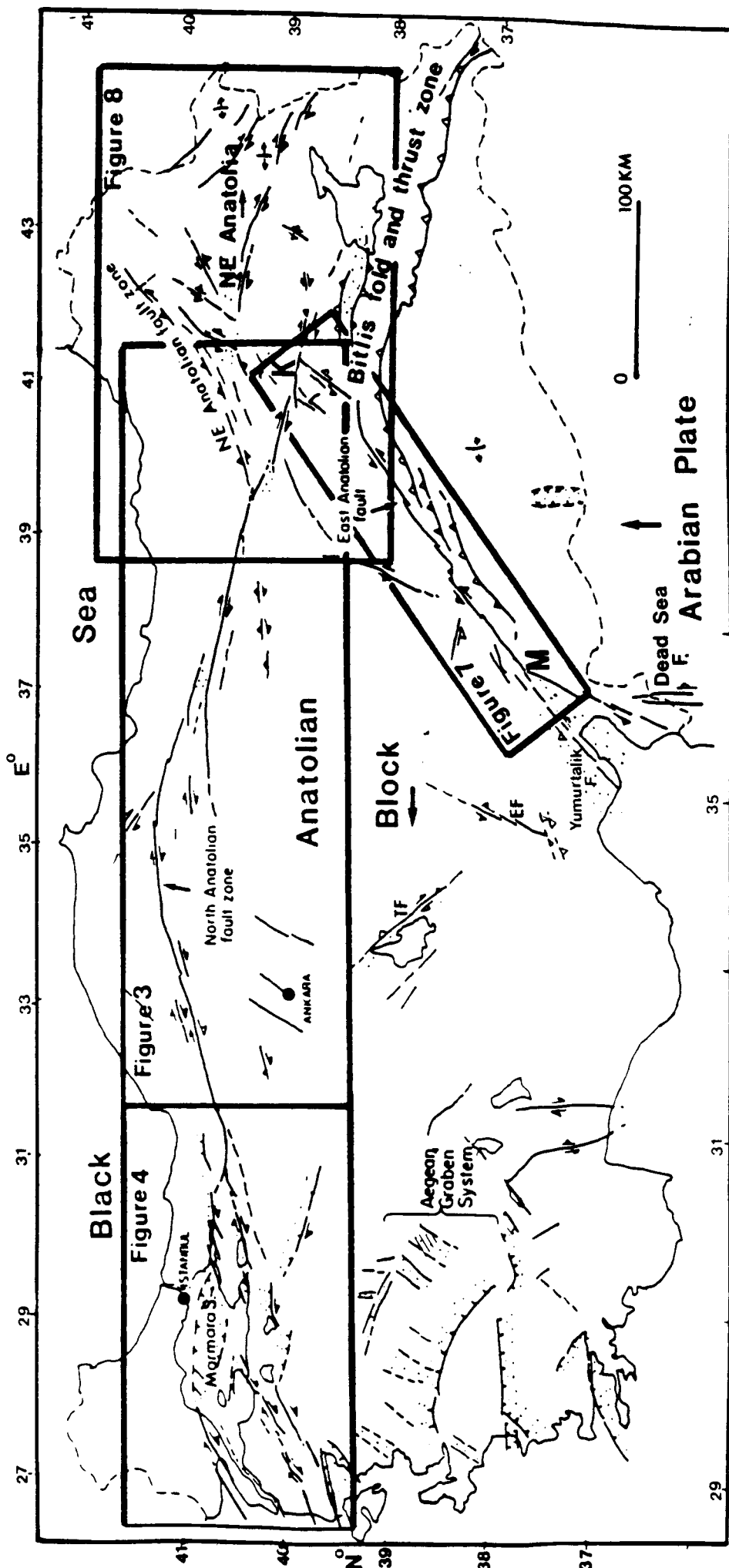
(a) $\log(\alpha L_2) = 0.57 M_S - 1.66$
Correlation coefficient 0.87

(b) $\log(L) = 0.50 M_S - 1.74$
Corr. coef. 0.70

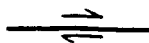
(c) $\log(\alpha L_2) = 0.93 \log L + 0.70$
Corr. coef. 0.72

(d) $\log(\alpha L_2) = 0.59 \log(uL) - 2.95$
Corr. coef. 0.80

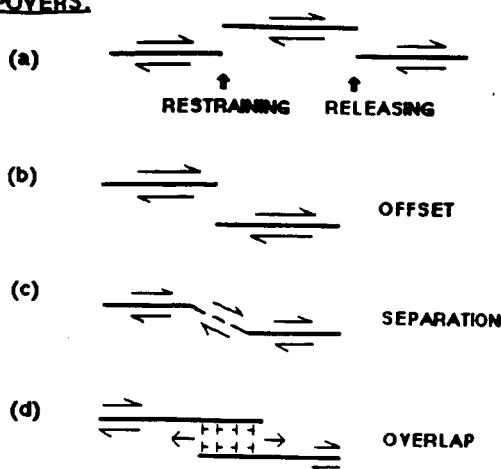
ORIGINAL PAGE IS
OF POOR QUALITY



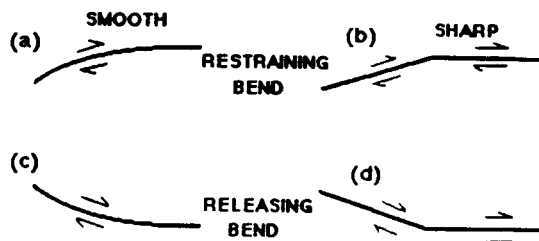
STRAIGHT:



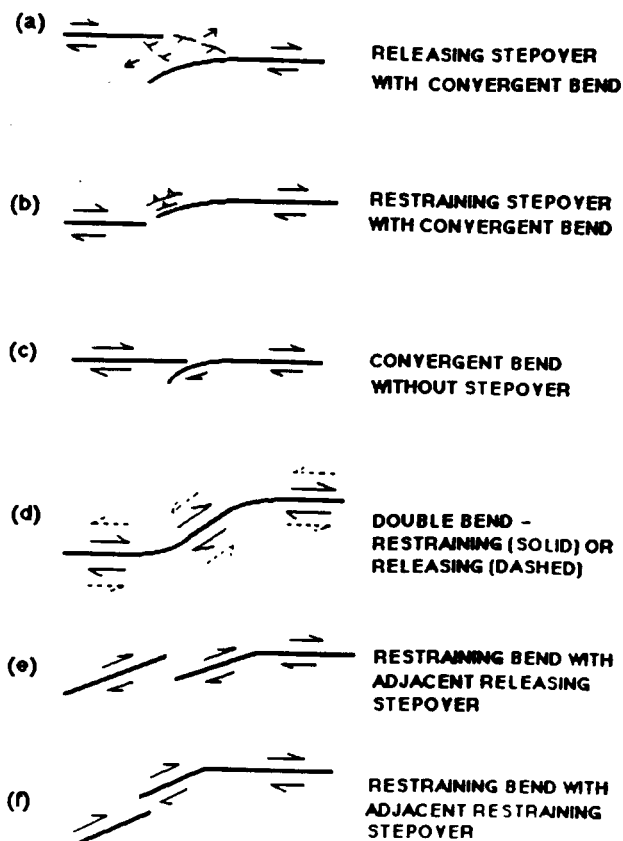
A-STEPOVERS:



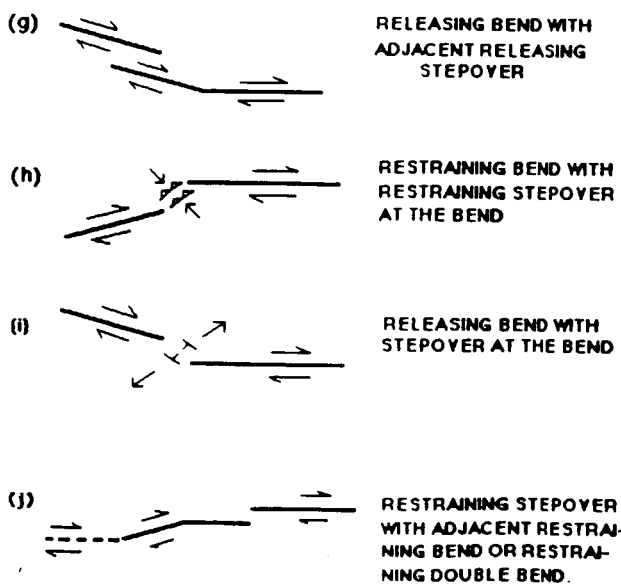
B-BENDS:



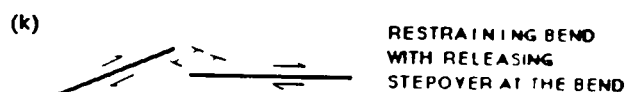
C-COMBINATIONS:



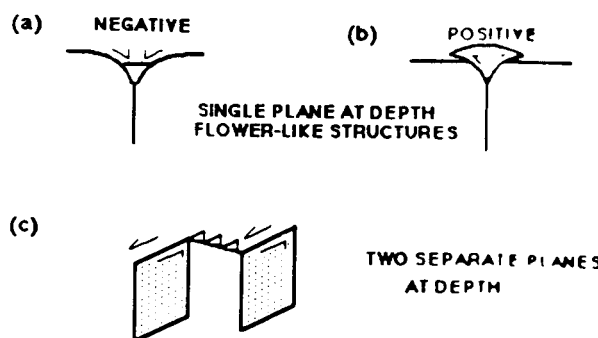
C-COMBINATIONS (continued):

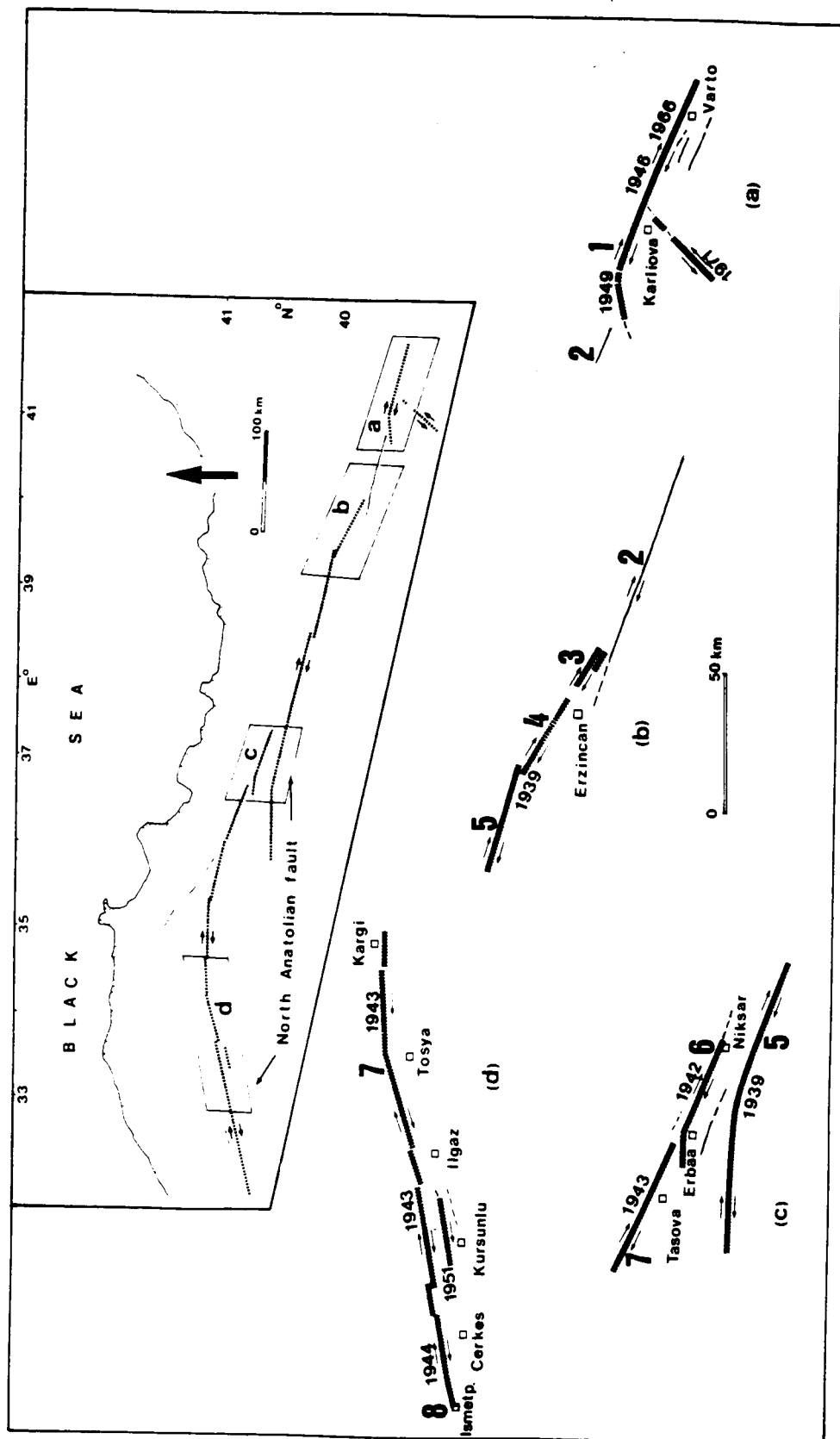


C-COMBINATIONS (continued)

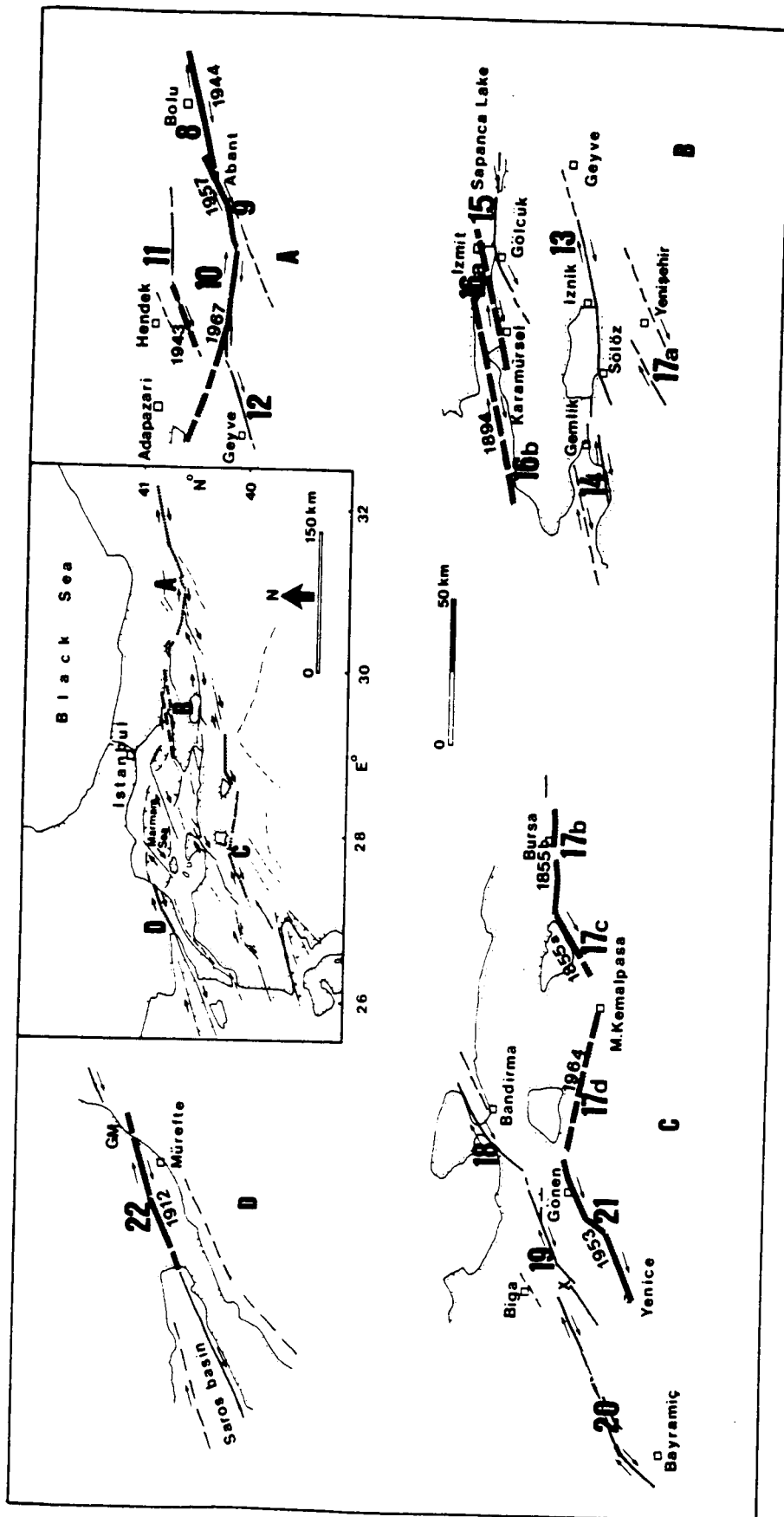


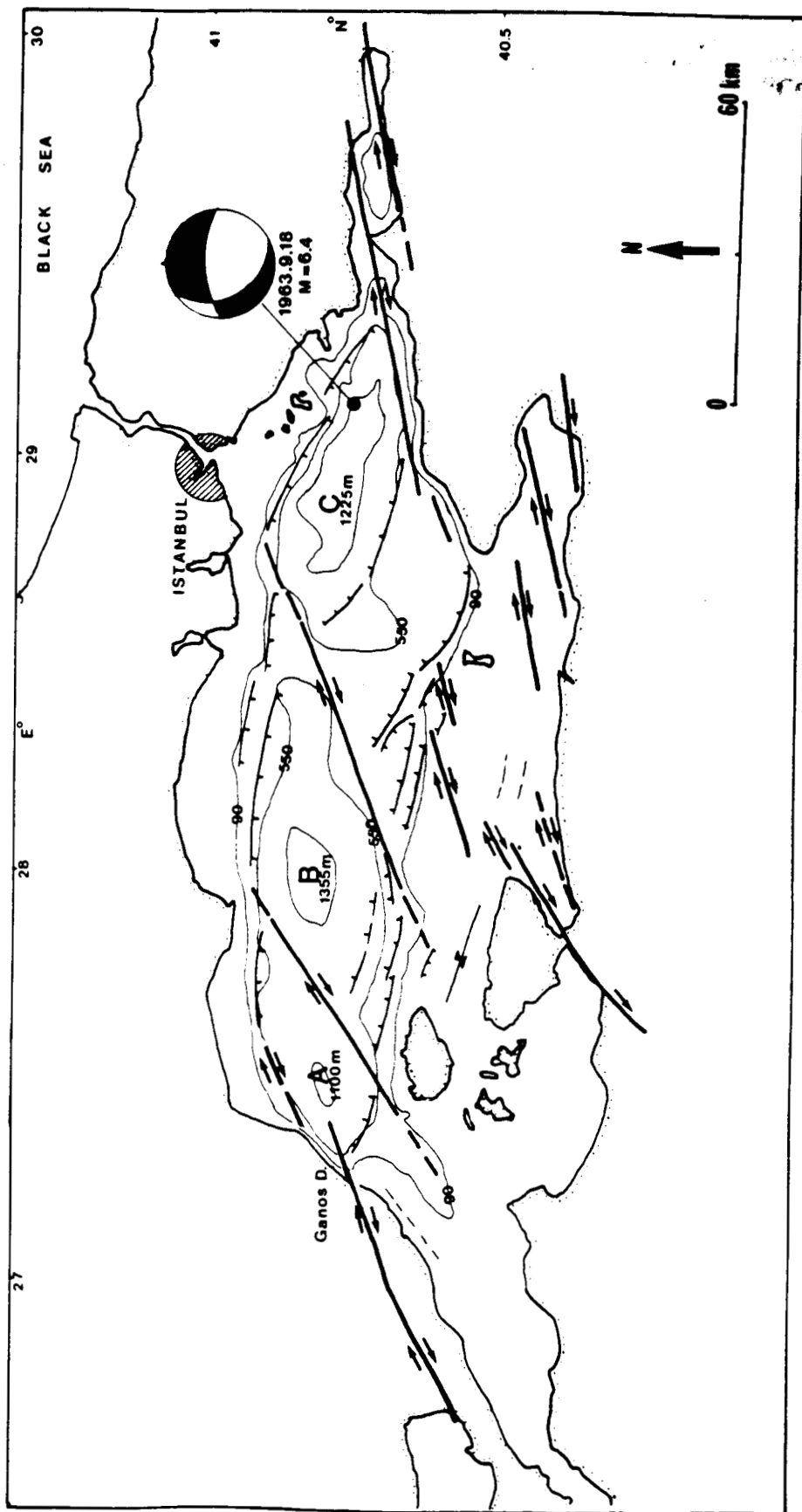
D-CROSS-SECTIONAL VIEWS:

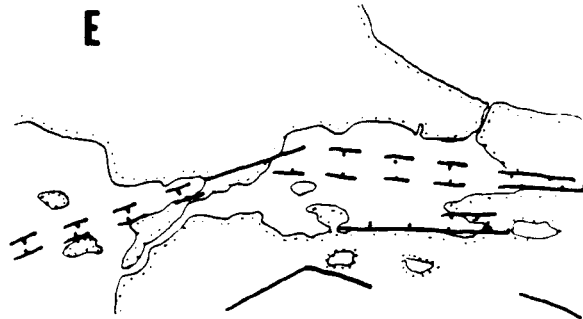
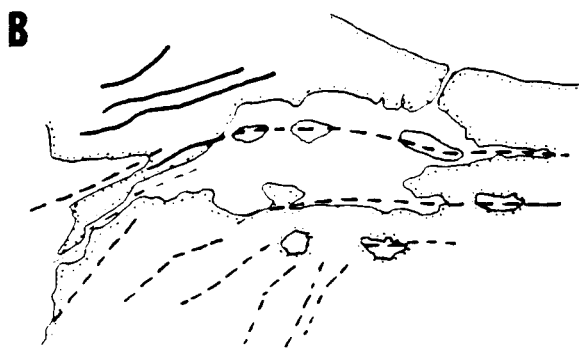
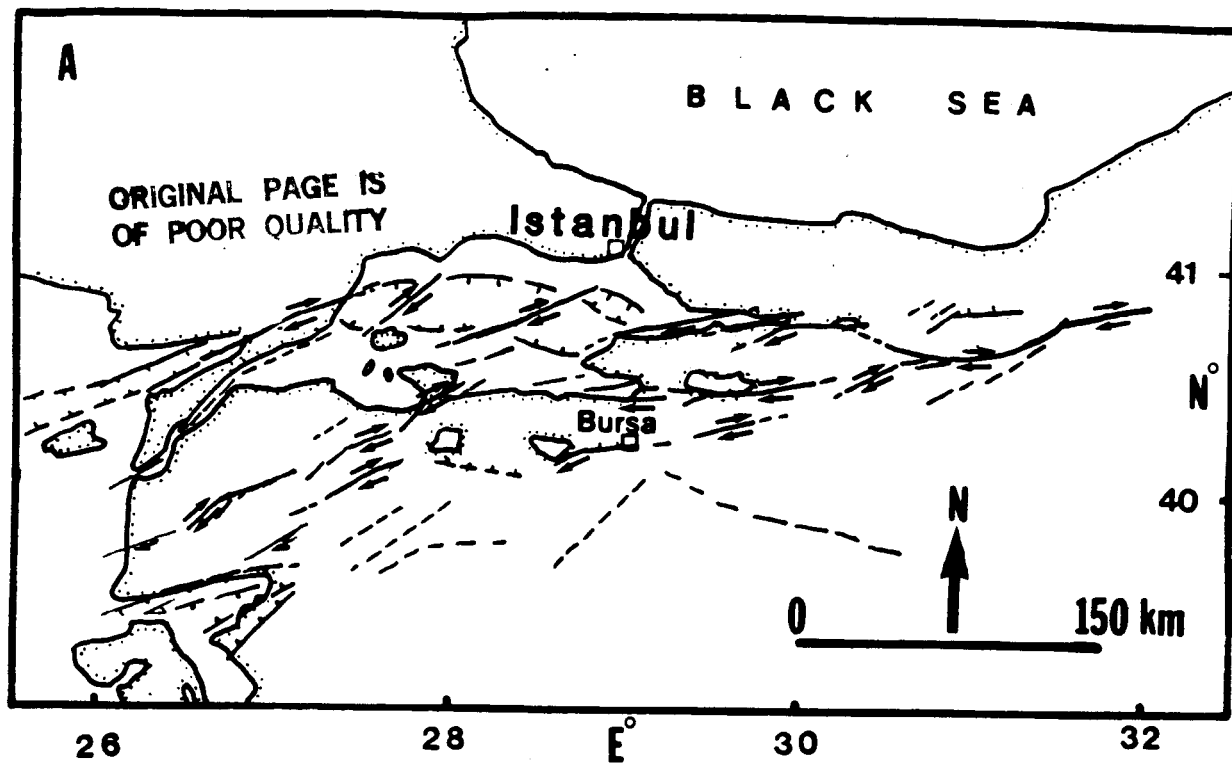


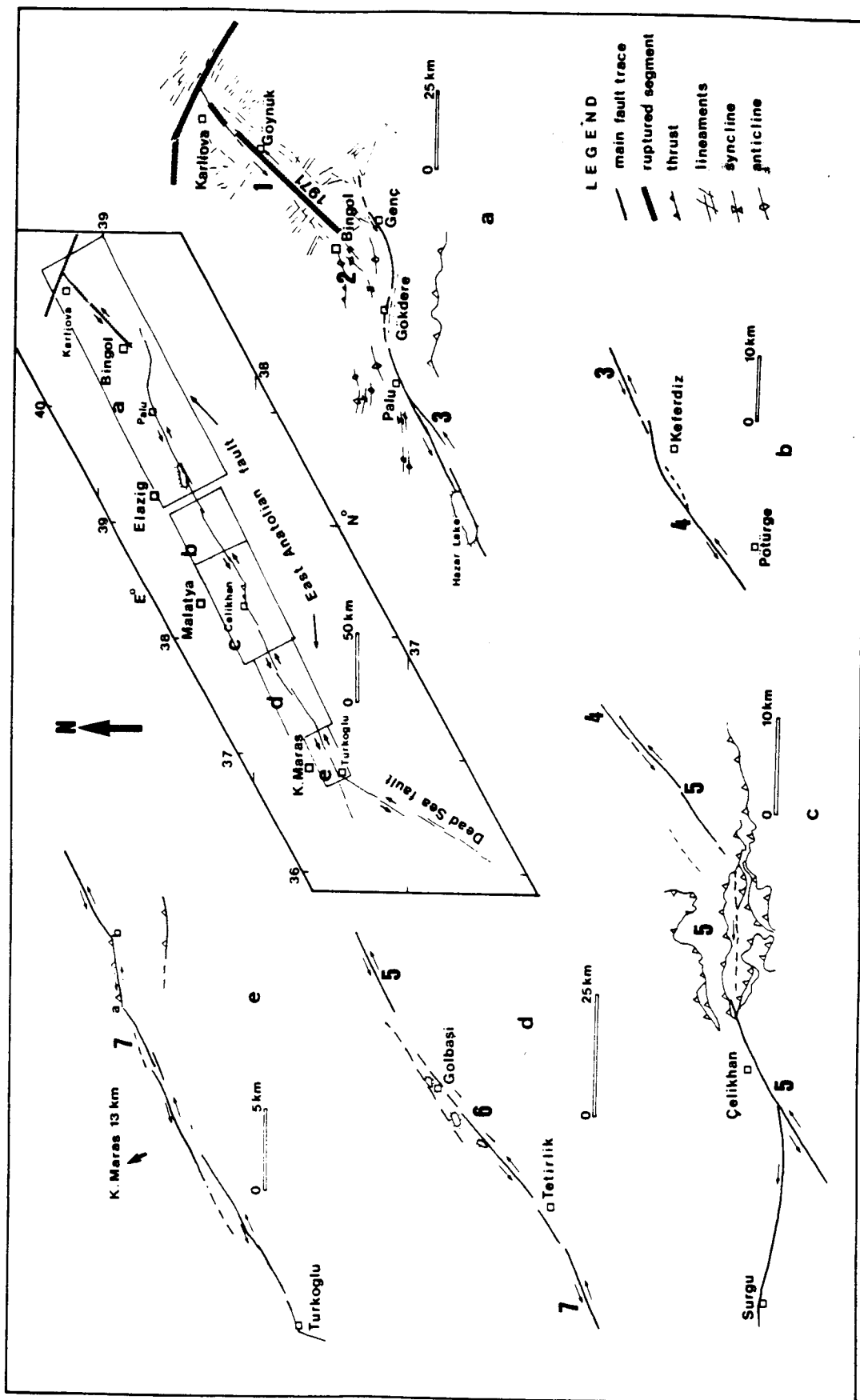


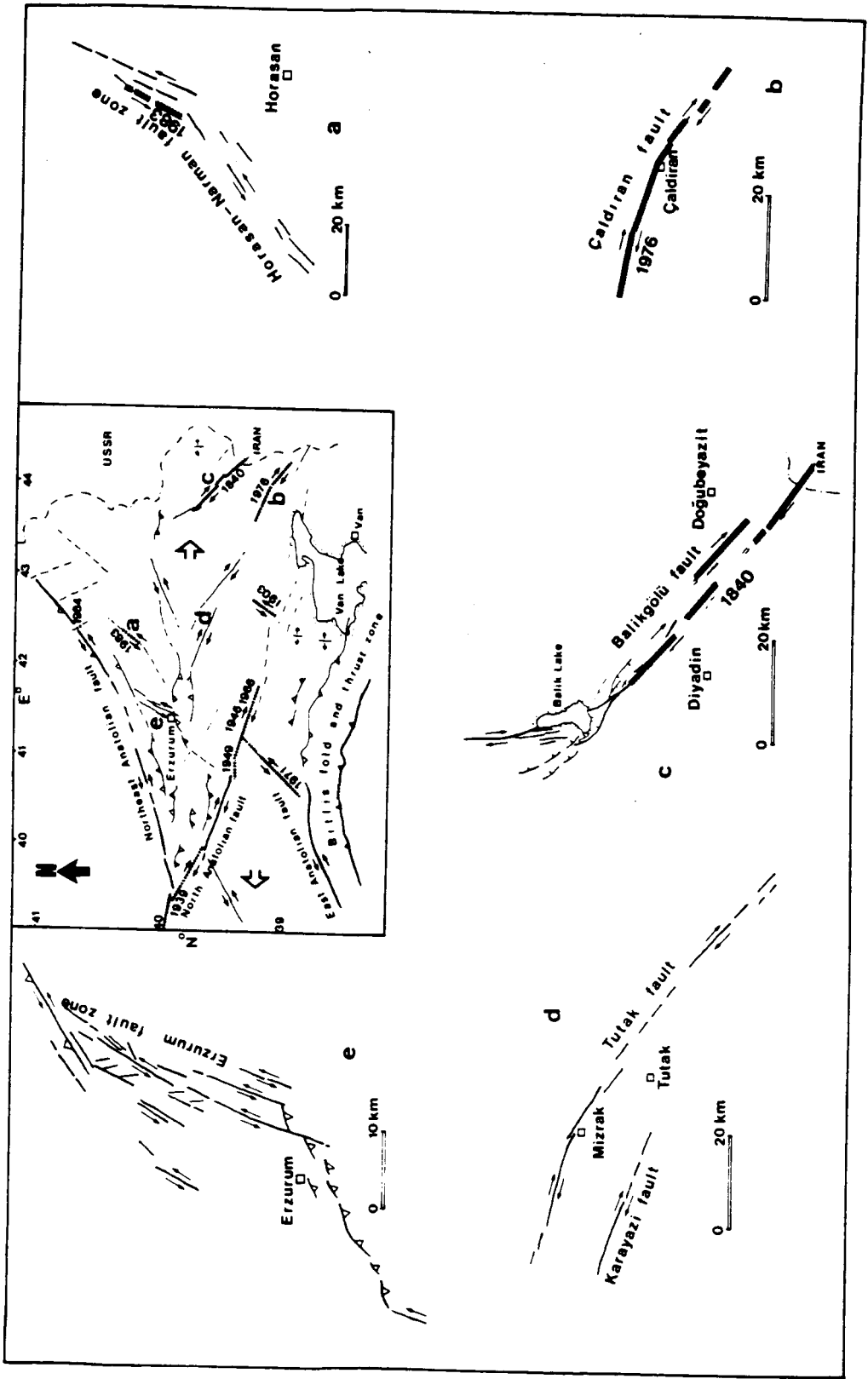
ORIGINAL PAGE IS
OF POOR QUALITY



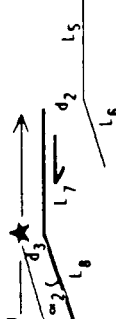
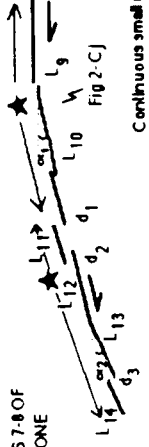




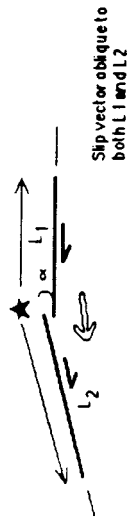


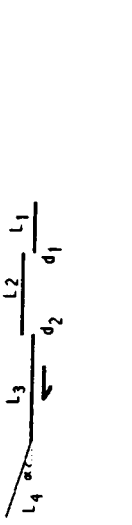





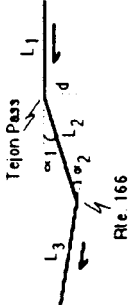
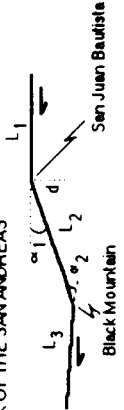

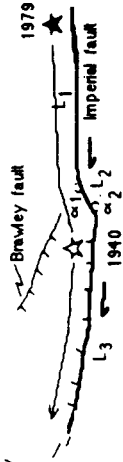




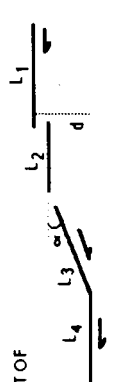









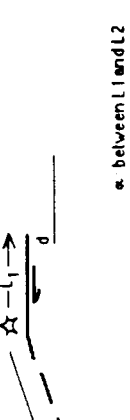




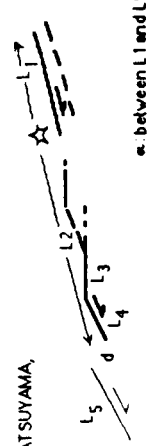
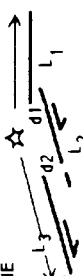



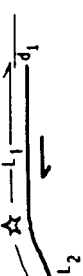
Schematized geometry of ruptured fault segments	Ref. Fig.	Numerical values	Date, Mag.
<p>a SEGMENT 1 OF THE NAF ZONE</p>  <p>Fig 2-Cb</p>	Fig 3a Seg 1 (L1, L2)	$\alpha=16'$ $d=5$ km $L_1=27$ km $L_2=15$ km $L_3=100$ km	1949 M=7
<p>b SEGMENTS 2-5 OF THE NAF ZONE</p>  <p>Fig 2-Ca Fig 2-Ci</p>	Figs 3b, 3c Segs 3, 4, 5 (L4, 5, 6)	$\alpha_1=20'$ $\alpha_2=15'$ $d_1=4.5$ km $d_2=10$ km $L_4=55$ km $L_5=75$ km $L_6=240$ km $L_7=50$ km	1939 M=8
<p>c SEGMENT 6 OF THE NAF ZONE</p>  <p>Fig 2-Ca</p>	Fig 3c Seg 6 (L7, 8)	$\alpha=14'$ $d_2=10$ km $d_3=1$ km $L_7=50$ km $L_8=10$ km $L_9=200$ km	1942 M=7
<p>d SEGMENTS 7-8 OF THE NAF ZONE</p>  <p>Fig 2-Ce Fig 2-Cj</p> <p>Continuous small and moderate shocks between d1 and d2</p>	Fig 3d Seg 7 (L9, 10) Seg 8 (L11, 14)	$\alpha_1=15'$ $\alpha_2=7'$ $d_1=2$ km $d_2=1$ km $d_3=1$ km $L_9=200$ km $L_{10}=65$ km $L_{11}=12$ km $L_{12}=28$ km $L_{13}=10$ km $L_{14}=105$ km	1943 M=7.3 1944 M=7.3
<p>e SEGMENTS 9-10 OF THE NAF ZONE</p>  <p>Figure 2-Cd</p>	Fig 4a Seg 9 (L15) Seg 10 (L16)	$\alpha_1=11'$ $\alpha_2=10'$ $\alpha_3=20'$ $L_{15}=45$ km $L_{16}=6$ km $L_{17}=65$ km * zone of overlap	1957 M=7 1967 M=7.1
<p>f SEGMENT 22 OF THE NAF ZONE</p>  <p>FIG 2-Ce</p>	Fig 4d Seg 22 (Lac)	$\alpha=14'$ $d=5$ km $L_a=20$ km $L_b=30$ km $L_c=30+4$ km (Lc extends offshore)	1912 M=7.3

Schematized geometry of ruptured fault segments (continued)		Ref. Fig.	Numerical values	Date, Mag.
g	ÇALDIRAN FAULT Fig 2- Bb 	Fig 8b (L1,2)	$\alpha=17-19^\circ$ $L_1=22 \text{ km}$ $L_2=28 \text{ km}$	1976 M=7.3
h	SEGMENTS 17B AND C OF THE NAF ZONE Fig 2- Bb 	Fig 4c Seg 17b (L1) Seg 17c (L2)	$\alpha=25^\circ$ $L_1=40 \text{ km}$ $L_2=25 \text{ km}$	1855b 1855a
i	HORASAN-NARMAN FAULT Fig 2- Bb 	Fig 8a	$\alpha=16^\circ$ $L_1=40 \text{ km}$ $L_2=40 \text{ km}$	1983 M=6.9
j	THE BALIKGÖLU FAULT, EASTERN TURKEY Fig 2- Cg 	Fig 8c	$\alpha=35^\circ$ $d_1=3 \text{ km}$ $d_2=3.5 \text{ km}$ $L_1=15 \text{ km}$ $L_2=12 \text{ km}$ $L_3=35 \text{ km}$ $L_4=25 \text{ km}$	1840 M=7.4
k	TANGSHAN, CHINA Fig 2- Cc 	---	$\alpha=30^\circ$ $L_1=26 \text{ km}$ $L_2=32 \text{ km}$	1976 M=7.8
l	PARKFIELD Fig 2- Bb 	---	$\alpha=5^\circ$ $d=3 \text{ km}$ $L_1=10 \text{ km}$ $L_2=18 \text{ km}$ $L_3=4.5 \text{ km}$	1966 M=6.0

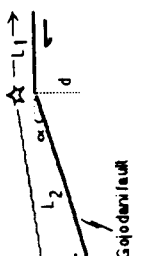
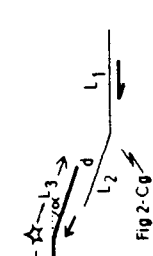
Schematized geometry of ruptured fault segments (continued)		Ref. Fig.	Numerical values	Date, Mag.
m	SEGMENT 21 OF THE NAF ZONE (YENICE-GONEN)  Fig 2-Cd	Fig 4c Seg 21	$\alpha=17^\circ$ $d=3 \text{ km}$ $L_1=15 \text{ km}$ $L_2=10 \text{ km}$ $L_3=26 \text{ km}$	1953 M=7.4
n	1857 BREAK OF THE SAN ANDREAS FAULT  Fig 2-Cd	----	$\alpha_1=12^\circ$ $\alpha_2=34^\circ$ $d=17 \text{ km}$ $L_1=120 \text{ km}$ $L_2=70 \text{ km}$ $L_3=200 \text{ km}$	1857 M=8.5
o	1838-1906 BREAK OF THE SAN ANDREAS  Fig 2-Cd	----	$\alpha_1=10^\circ$ $\alpha_2=14^\circ$ $d=12 \text{ km}$ $L_1=20 \text{ km}$ $L_2=70 \text{ km}$ $L_3=360 \text{ km}$	1906 M=8.3
p	QIUJIANG FAULT, CHINA (TONGHAI EARTHQUAKE)  Fig 2-Cd	----	$\alpha=24^\circ$ $d=4 \text{ km}$ $L_1=10 \text{ km}$ $L_2=10 \text{ km}$ $L_3=30 \text{ km}$	1970 M=7.7
q	IMPERIAL VALLEY  Fig 2-Cd	----	$\alpha_1=12^\circ$ $\alpha_2=22^\circ$ $L_1=12 \text{ km}$ $L_2=5.5 \text{ km}$ $L_3=13 \text{ km}$	1979 M=6.9
r	COYOTE LAKE  Fig 2-Cd	----	$\alpha=10^\circ$ $L_1=13 \text{ km}$ $L_2=6 \text{ km}$ $L_3=6 \text{ km}$	1979 M=5.7

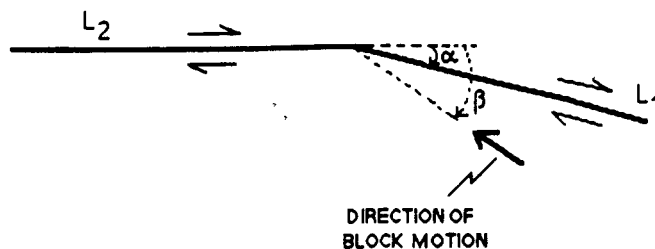
Schematized geometry of ruptured fault segments (continued)	Ref. Fig.	Numerical values	Date, Mag.
<p>s MORGANHILL</p>  <p>Fig 2-Cd</p>	---	$\alpha=15^\circ$ $L_1=2 \text{ km}$ $L_2=6 \text{ km}$ $L_3=12 \text{ km}$	1984 M=6.3
<p>t NORTHWESTERN PART OF MAIN RECENT FAULT, ZAGROS</p>  <p>Fig 2-Cd</p>	---	$\alpha=20^\circ$ $d=46 \text{ km}$ $L_1=100 + \text{ km}$ $L_2=28 \text{ km}$ $L_3=100 \text{ km}$ $L_4=50 + \text{ km}$	1909 M=7.4 1958 M=6.6 1957 M=7
<p>u BORREGO MOUNTAIN, COYOTE CREEK</p>  <p>Fig 2-Aa</p>	---	$d=15 \text{ km}$ $L_1=19 \text{ km}$ $L_2=12 \text{ km}$	1968 M=6.4
<p>v SONGPAN, CHINA</p>  <p>Fig 2-Aa</p>	---	$\alpha=50^\circ$ $L_1=30 \text{ km}$ $L_2=12 \text{ km}$ $L_3=22 \text{ km}$	1976 M=7.2 M=6.7 M=7.2
<p>w SALMAS, IRAN</p>  <p>Fig 2-Ci</p>	---	$\alpha_1=18^\circ$ $\alpha_2=14^\circ$ $d=15 \text{ km}$ $L_1=5 \text{ km}$ $L_2=2 \text{ km}$ $L_3=3 \text{ km}$ $L_4=6.4 \text{ km}$	1930 M=7.2
<p>x SEGMENTS 1-3 OF THE EAF ZONE (PALU)</p>  <p>Fig 2-Ch</p>	Fig 7a Segs. 1-3 (L1,2)	$\alpha=19^\circ$ $d=10 \text{ km}$ $L_1=60 \text{ km}$ $L_2=100 \text{ km}$	1971 M=6.7

Schematized geometry of unruptured fault segments	Ref. Fig.	Numerical values	Analog & remarks
<p>a</p> <p>SEGMENTS 2-3 OF THE NAF ZONE (EAST OF ERZINCAN)</p>  <p>Fig 2-Ca</p>	Fig 3b Seg 2 (L ₁)	$\alpha=15^\circ$ $L_1=100$ km $L_2=10$ km $L_3=15$ km $d=4$ km	Similar to Naksar area, NAF zone
<p>b</p> <p>SEGMENTS 15 AND 16A, B OF THE NAF ZONE</p>  <p>Fig 2-Ca</p>	Fig 4b Seg 15 (L ₁ , L ₂)	$\alpha=20^\circ$ $d_1=4.5$ km $L_1=35$ km $L_2=15$ km $d_2=7$ km $L_3=42$ km $L_4=75$ km $L_3, 4=1894$ (?)	3 separate earthquakes: (L ₁ + L ₂) : L ₃ : L ₄
<p>c</p> <p>MARMARA SEA, NAF ZONE</p>  <p>Fig 2-Ad</p>	Fig 5	$d_1=7$ km $L_1=42$ km $d_2=30$ km $L_2=75$ km $d_3=20$ km $L_3=90$ km $d_4=15$ km $L_4=60$ km $L_5=130$ km	Continuous activity in the pull-apart areas and separate earthquakes on strike slip segments
<p>d</p> <p>SEGMENT 20 OF THE NAF ZONE (BAYRAMCI)</p>  <p>Fig 2-Bb</p>	Fig 4c Seg 20 (L ₁ , L ₂)	$\alpha=22^\circ$ $L_1=40$ km $L_2=40$ km $d=5$ km	
<p>e</p> <p>SEGMENT 12 OF THE NAF ZONE (GEYVE)</p>  <p>Fig 2-Ce</p>	Fig 4a Seg 12 (L ₁ , L ₂)	$\alpha=17^\circ$ $L_1=10$ km $L_2=35$ km $d=2.5$ km	Similar to Tosya - Çekirge area (segs 7-8 of the NAF zone; epicenter near bend
<p>f</p> <p>SEGMENT 19 OF THE NAF ZONE</p>  <p>Fig 2-Ce</p>	Fig 4c Seg 19 (L ₁ , L ₂)	$\alpha=19^\circ$ $L_1=30$ km $L_2=9$ km $d_1=1.5$ km $d_2=3.5$ km $L_3=9$ km $L_4=40$ km	same as above

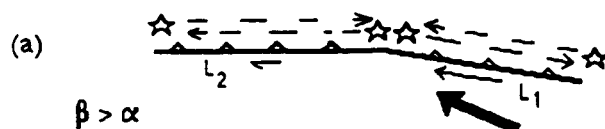
Schematized geometry of unruptured fault segments (continued)	Ref. Fig.	Numerical values	Analog & remarks
<p>g MTL, KAMATSU-MAT SUYAMA, JAPAN</p>  <p>Fig 2-Ce</p> <p>a. between L1 and L5</p>	----	$\alpha=21^\circ$ $L_1=25$ km $d=2.5$ km $L_2=1.5$ km $L_3=1$ km $L_4=2.2$ km $L_5=5+$ km	one single earthquake L1-4 with epicenter near bend area. pull apart = site of aftershocks
<p>h SEGMENT 14 OF THE NAF ZONE (GEMLIK)</p>  <p>Fig 2-Ce</p> <p>a. between L1 and L3</p>	Fig 4b Seg 14 (L1,3)	$\alpha=13^\circ$ $L_1=20$ km $d_1=4$ km $L_2=20$ km $d_2=7$ km $L_3=35$ km	one single earthquake; continuous pull apart activity
<p>i SEGMENT 13 OF THE NAF ZONE</p>  <p>Fig 2-Cc</p>	Fig 4b Seg 13 (L1,2)	$\alpha=20^\circ$ $L_1=65$ km $d=2.5$ km $L_2=5$ km	Similar to Nksar Erbaa (segs 5,8 of the NAF zone)
<p>j TUTAK-KARAYAZI FAULTS, EASTERN TURKEY</p>  <p>Fig 2-Ci</p>	Fig 8d	$\alpha=19^\circ$ $L_1=75$ km $d=16$ km $L_2=20$ km $L_3=80$ km	Two earthquakes L1,2; epicenter at the bend
<p>k SEGMENT 18 OF THE NAF ZONE (BANDIRMA)</p>  <p>Fig 2-Cb</p> <p>a. between L2 and L3</p>	Fig 4c Seg 18 (L1,3)	$\alpha=10^\circ$ $L_1=20$ km $d=4$ km $L_2=15$ km $L_3=12$ km	Similar to Karlova Elmali (seg 1 of the NAF zone)
<p>l SEGMENT 4 OF THE EAF ZONE</p>  <p>Fig 2-Cb</p>	Fig 7b Seg. 4 (L1,2)	$\alpha=17^\circ$ $L_1=35$ km $d_1=2$ km $L_2=7$ km $d_2=2$ km	same as above

Schematized geometry of unruptured fault segments (continued)		Ref. Fig.	Numerical values	Analogs & remarks
m	SEGMENT 11 OF THE NAF ZONE (DÜZCE-HENDEK) Fig 2-Bb Slip vector parallel to L ₁	Fig 4a Seg 11	$\alpha=17^\circ$ $L_1=30$ km $L_2=25$ km	1943 (M=6.6) on L ₂ ?
n	ERZURUM Fig 2-Cd, Fig 2-Bd	Fig 8e (L _{2,4})	$\alpha=35^\circ$ $L_1=40+$ km $d=10$ km $L_2=17$ km $L_3=12$ km $L_4=15$ km	
o	SEGMENT 5 OF THE EAF ZONE (CELIKHAN) Fig 2-Ch or 2-Cd	Fig 7c Seg 5 (L _{1,2})	$\alpha=9^\circ$ $L_1=25$ km $d=7.5$ km $L_2=45$ km	Complex, either single earthquake or separate events on L ₁ , L ₂ and / or in stepover area
p	SEGMENT 7 OF THE EAF ZONE (MARIŞ) Fig 2-Cd	Fig 7e Seg 7 (L _{1,3})	$\alpha=18^\circ$ $L_1=20$ km $d=1.5$ km $L_2=4.5$ km $L_3=25$ km	Similar to Segment 21 (Yenice-Gönen) of the NAF
q	MISSION CREEK, SAN ANDREAS FAULT, USA Fig 2-Cd	---	$\alpha_1=24^\circ$ $L_1=112$ km $\alpha_2=14^\circ$ $L_2=70$ km $d=22$ km $L_3=19$ km	Similar to 1857 break
r	MTL, IYO MISHIMO CENTRAL SHIKOKU, JAPAN Fig 2-Cd	---	$\alpha=15^\circ$ $L_1=100$ km $L_2=2$ km $L_3=20+$ km	

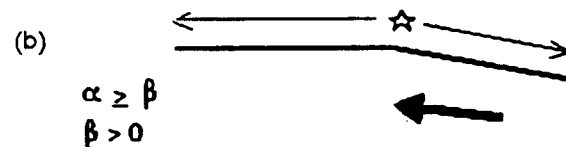
	Schematized geometry of unruptured fault segments (continued)	Ref. Fig.	Numerical values	Analog & remarks
S	 <p>MTL, WAKAYAMA, EASTERN KII, JAPAN</p> <p>Fig 2-Cd</p>	$\alpha=24^\circ$ $L_1=8$ km $L_2=20$ km $L_3=35+$ km $d=8$ km	
I	 <p>SEGMENTS 5-7 OF THE EAF ZONE</p> <p>Fig 2-Cg</p>	Fig 7d Seg. 6 (L2-3)	$\alpha=17^\circ$ $L_1=45$ km $L_2=25$ km $L_3=40$ km $L_4=20$ km $d=2$ km	L_2, L_3 may rupture during earthquakes on L_1, L_4 . continuous activity in pull- apart area



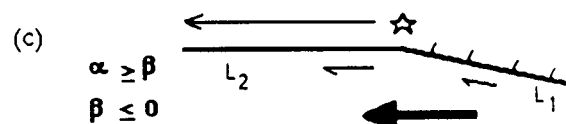
SINGLE BENDS:



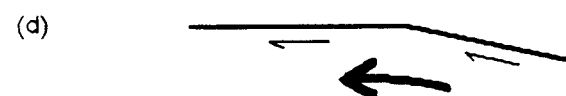
RUPTURE CAN STOP OR
INITIATE NEAR THE BEND.
TWO SEPARATE SEGMENTS.



SINGLE RUPTURE, INITIATES
NEAR THE BEND.

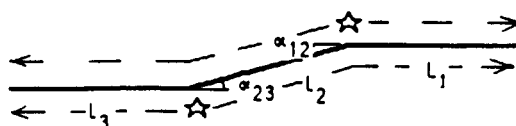


SWARM ACTIVITY ON L_1 .
 L_1 AND L_2 RUPTURE
SEPARATELY.

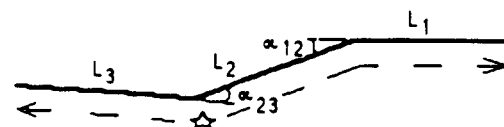


BLOCK ROTATION;
LOCATION OF EPICENTER
NOT WELL CONSTRAINED
MAY BE SIMILAR TO THAT
IN CASE (b).

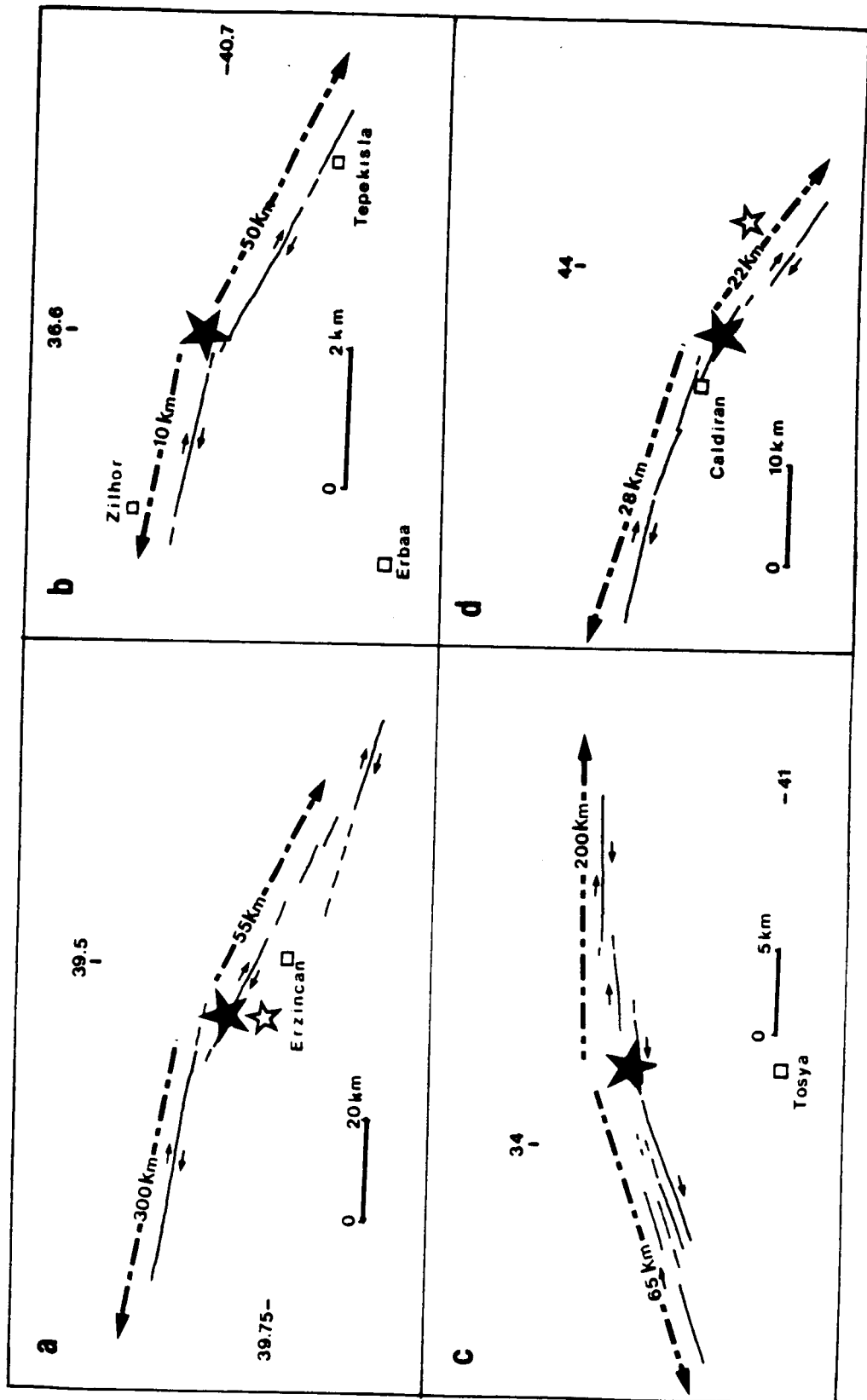
DOUBLE BENDS ($\alpha \geq \beta$):

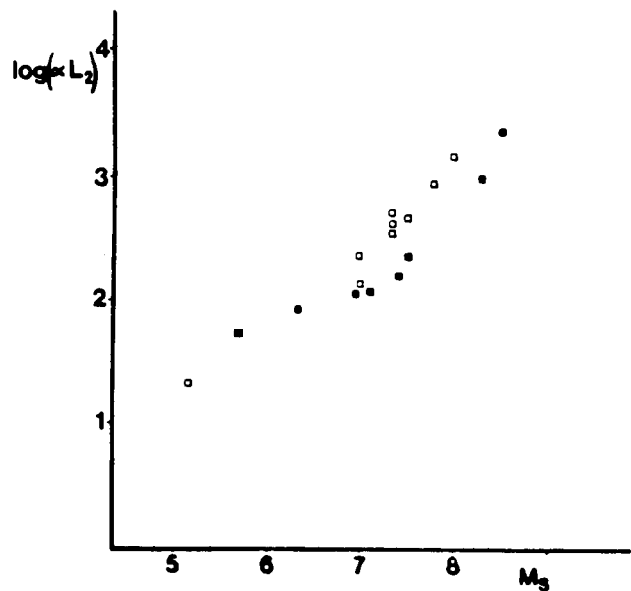
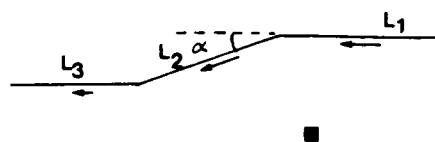
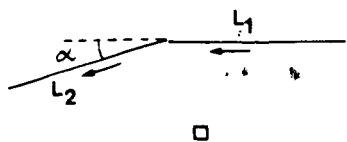


$$\alpha_{12} = \alpha_{23}$$

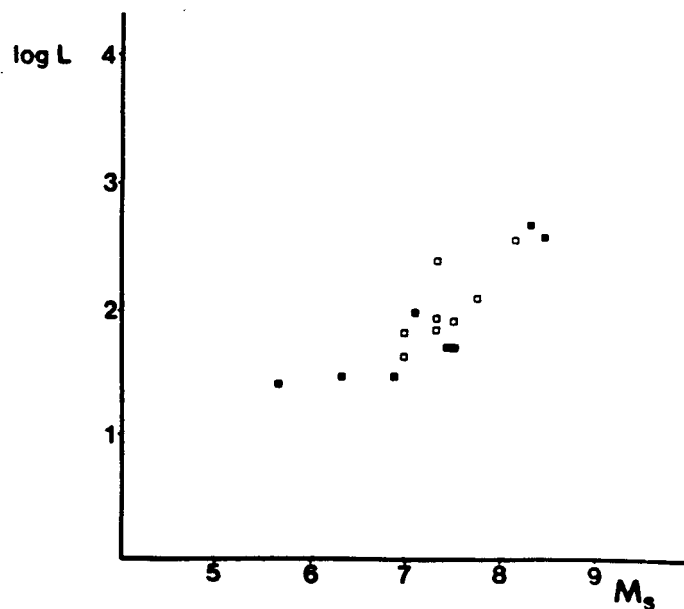


$$\alpha_{12} \leq \alpha_{23}$$

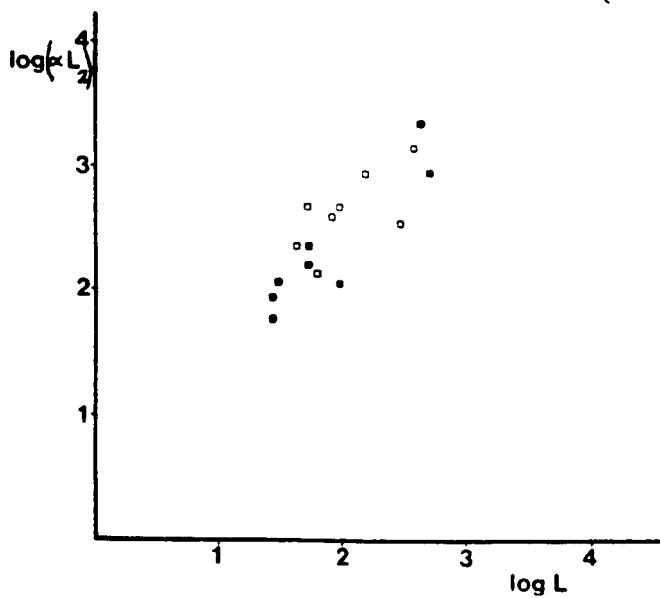




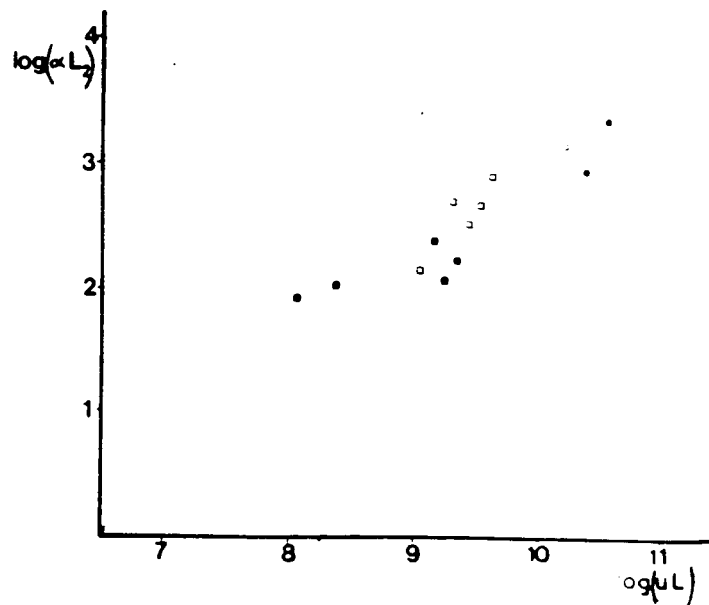
a



b



c



d

NORTH ANATOLIAN FAULT GEOMETRY AND EARTHQUAKE ACTIVITY

BARKA, A.A., KADINSKY-CADE, K. AND TOKSOZ, M.N., Earth Resources Laboratory, Department of Earth, Atmospheric and Planetary Sciences, Mass. Inst. of Technology, Cambridge, MA 02139

A comprehensive examination has been made of strike-slip fault geometry and the known historical and instrumental earthquakes in the North Anatolian fault zone in Turkey. Fault geometry is found to be a critical factor in controlling fault segmentation and hence the distribution of large strike-slip earthquakes. We focus on the eastern end of the North Anatolian fault zone as a means of illustrating these relationships. There are two characteristic magnitudes (about $M=7$ and $M=8$). The epicenter of the 1939 great Erzincan earthquake ($M=8$) occurred near a 20° restraining bend, within the 360 km long segment that ruptured during that earthquake. This segment was terminated at each end by releasing stepovers. Aftershocks mostly occurred in the releasing stepover/releasing bend area located at the eastern end of this segment. Historical records suggest that the 1939 event is characteristic of great earthquakes that occur approximately every 300 years on this segment. The segment to the east of the Erzincan segment is identified as a potential seismic gap. It is 100 km long, and extends from the Erzincan releasing stepover to a restraining stepover-bend combination near Yedisu. This segment last ruptured in 1784. It is the only section of the main part of the North Anatolian fault that did not experience a large earthquake during the well-known 1939-1967 sequence of $M=7-8$ earthquakes that ruptured the fault zone between Varto and the western end of the Mudurnu valley (900 km).

Strike-slip Fault Geometry and Earthquake Activity in Turkey

BARKA, A. and KADINSKY-CADE, K. (Earth Resources Laboratory, Dept. of Earth, Atmospheric and Planetary Sciences, Mass. Inst. of Technology, Cambridge, MA 02139)

A comprehensive examination has been made of strike-slip fault geometry in Turkey. The influence of fault geometry on the behavior of large earthquakes has been compared with that for well-studied strike-slip earthquakes in California and Asia. The two main elements comprising the geometric patterns are stepovers and bends. There are many observed combinations of these two elements. Each combination can be associated with a particular fault behavior. The most commonly encountered patterns are (1) the double bend and (2) the restraining bend with adjacent releasing stepover. Fault segmentation is closely related to fault geometry. The geometric patterns are seen to influence the distribution of maximum dislocation and intensity during large earthquakes. Fault geometry is also a critical factor in providing sites for localized strain accumulation, preferred epicenter locations and aftershock sites. The most important fault geometry parameters are: stepover width (less than about 10 km for a through-going rupture), bend angle α (less than about 30° for a through-going rupture), the length L_2 of the restraining fault segment and the angle b between the direction of block motion and the strike of the main fault. In the case of single and double restraining bends it is observed that $\log(\alpha L_2)$ is roughly proportional to earthquake magnitude, and that the epicenter rarely occurs on L_2 . Aftershocks and swarms of smaller earthquakes cluster in releasing bend and releasing stepover areas. In a few cases foreshocks can be associated with releasing features located adjacent to or within restraining areas.

1. 1987 Spring Meeting
2. 000102749
3. (a) Katharine Kadinsky-Cade
Earth Resources Laboratory
Mass. Inst. of Technology
E34-570
42 Carleton St.
Cambridge, MA 02142

(b) (617) 253-7863
4. S
5. (a) Seismicity

(b) 7230 Seismicity
(or alternatively 7220-
Earthquake prediction)
6. S
7. 0 %
8. \$35 check enclosed
9. C
10. None